UNIVERSITAT DE BARCELONA

# CPEB4-Driven adipocyte reprogramming is required for adipogenesis and pathological inflammation

Núria Pell Vidal

Facultat de Medicina i Ciències de la Salut
Universitat de Barcelona

**Programa de Doctorat en Biomedicina**

# CPEB4-Driven adipocyte reprogramming is required for adipogenesis and pathological inflammation

Tesi presentada per
**Núria Pell Vidal**
per optar al títol de Doctora per la Universitat de Barcelona

Aquesta tesi ha estat realitzada sota la direcció de
**Mercedes Fernandez Lobato**
en el grup d'Angiogènesi en Malalties Hepàtiques ubicat en l'Institut d'Investigacions Biomèdiques August Pi i Sunyer (IDIBAPS)-CEK

Doctoranda
**Núria Pell Vidal**

Directora de la tesi
**Mercedes Fernandez Lobato**

Tutor de la tesi
**Albert Tauler Girona**

Barcelona, Setembre 2020

Als meus estimats pares,

***"La qüestió no és qui no em deixarà, sinó qui m'aturarà"***

Ayn Rand

# Table of contents

# AKNOWLEDGEMENTS

Tenia tantes ganes d'escriure aquestes paraules, que ara ja no se ben bé ni per on començar, el que tinc clar es que aquests 5 anys no haurien estat possibles sense tots els que vindreu a continuació.

Com tota història, la tesis també te un inici i en el meu cas es diu **Mercedes**. Gràcies per donar-me aquesta grandíssima oportunitat per créixer personal i professionalment. Tot i els molts cops de caps durant el procés marxo plenament contenta i orgullosa del meu pas per aquest grup. Gràcies per la confiança. No em puc oblidar tampoc del **Raul i tot el grup del IRB** sense els quals aquesta tesis, com es en el dia d'avui, no hauria estat possible. També m'agradaria donar les gràcies al **Jaume** que tot i no ser director d'aquesta tesis m'ha permès formar part de la família d'HH de la qual m'enduc molt carinyo i bons records.

**Ester**, tu has estat jefa, mentora, amiga, mare i tantes altres coses que m'han anat fent falta en aquest camí que li diuen tesis. On seria jo a dia d'avui sense tu? Probablement molt lluny d'escriure aquestes paraules. Només tinc paraules d'agraïment per tu i alguna de perdó, per fer sempre el que em dona la gana. Gràcies per ensenyar-me tant, a nivell científic i humà. Vull que sàpigues que no m'he deixat mai de sentir afortunada per haver après de tu, un exemple professional a seguir, intel·ligent i amb rigor (mancances de molts en el nostre camp).. ets sens dubte una de les persones més importants que m'emporto del lab, ojalà t'haguessis pogut quedar més al meu costat.. Ah, i felicitats!, perquè aquesta tesis, amb un títol que no t'agrada també es teva.

**Javi,** mi segundo pilar del grupo. Gracias infinitas, primero y SUPER importante por aguantar mi intensidad, se que no ha sido fácil a veces y te pido perdón por ello. Nuestra historia a fluctuado como la CPEB y como de nada vale arrepentirse del pasado voy a dar gracias por el presente donde nos volvemos a encontrar en una nueva historia juntos, la cual no puedo estar más contenta de compartir contigo. Termino con el peloteo que te mereces y que tanto me cuesta a veces decir. Gracias por enseñarme tanto y apoyarme cuando Ester ya no estaba. Eres no solo una excelente persona sino también un gran científico. No dudes de ti porqué los que te rodeamos nunca lo hemos hecho. Me llevo a un buen amigo.

Gràcies també al **Marc Mejias** per compartir costat per costat els primers mesos del meu pas pel labo, per tenir paciència i sobretot per fer-me riure tant. Des de que vas marxar al grup hi ha hagut un buit. Et desitjo el millor.

**Marta,** gràcies per tots els bons moments que hem tingut, que van ser tants els primers anys, i per la teva calma. Molta sort amb la recta final. Gràcies al **Salva**, a pesar de tener una relación de amor odio me he reido mucho a tu lado y te aprecio mucho

como científico. **Alex,** pequeño paduan, tot i haver coincidit poc en el temps desprens una felicitat que contagia. No perdis el teu esperit " I love the science", que t'anirà molt bé. Tampoc puc oblidar-me de la **Júlia**, que tot i passar fugaçment pel laboratori, em va despertar la faceta de mentora.

No puc deixar-me tampoc a l'**Anabel**, per les nostres estones al tren, per els beures, esmorzars, pel viatge a Nova York i en general per ser-hi sempre. No perdis mai el caràcter ni l'energia vital que desprens. Prometo que amb aquesta tesis acaben també els transport de mercaderies Tgn-Bcna! La **Montse**, sempre recordaré amb alegria i nostàlgia els nostres esmorzars a l'office. Ets pura vitalitat i energia. Allà on vagis, tindran sort de tenir-te aprop.

Gràcies també a la resta del laboratori, **Hector,** pessimista però imprescindible, **Sergi Guixé,** gràcies per no "engegar-me" cada cop que et demanava una figura xula, **Peyo i Maria,** gracias por la ayuda y sobretodo por amenitzar tantos ratos en la sala de ratas**, Zoe, Nico**, **Erica, Maria, Genís, David**, així com els que ja no hi son, **Marina, Sergi Vila, Raquel, Maria.**.. perquè tots formeu part de la Núria del present i per tant d'aquesta tesi. **Jordi,** gràcies a tu també per la confiança i per a tractar-me tantes vegades com una JGS més.

Gràcies a la PhD Community per acostar-me a grans persones que d'altra manera no hagués tingut la oportunitat de conèixer. Warriors: **Martí,** gràcies per tantíssims riures i cotilleos. Per cuidar-me en les èpoques més baixes i per tot el que hem compartit tant dins com fora d'aquestes parets. Espero que tot i la distància puguem seguir fen-t'ho. T'enyoraré. **Marcos,** compañero de running, de risas y de viaje. Nunca olvidaré nuestro tiempo en San Diego. Gracias por cuidar-me tanto. **Mire**, sin ti no habría citometria en esta tesis. Me quedo con tu alegría, locura y vitalidad. Tu y yo somos rocas, que como tales a veces chocan, pero te quiero y aprecio muchísimo.

**Laia**, tu vas arribar tard en aquesta historia però t'has convertit en un imprescindible en la meva vida dins i fora del lab, moltíssima sort i força pel que ha de venir.

**Iñi,** mi querido Iñigo, no puedo imaginarme este final de tesis sin ti. Gracias por tantos momentos fuera del lab, que han hecho que dentro todo fuera mas ameno.

**Sangrador,** el regal que em va donar el màster. Des de que vas marxar la meva vida al CEK no ha estat per a res el mateix. Gràcies per ensenyar-me tant quan vaig arribar com un polluelo i per seguir estant al meu costat amb aquesta llum interior tant espectacular que tens.

No puc deixar tampoc de nombrar tots els que m'han acompanyat durant tants anys fora d'aquestes quatre parets. **Turi,** pilar d'aquesta tesis i sens dubte de la meva vida. Gràcies per ser amiga, companya de pis i germana. A les **amigues de Tarragona,** en especial a **l'Andrea** que exemplifiques a la perfecció el que es una gran amiga i bona persona. També als papus, en especial a l'**Héctor**. Tampoc poden faltar en aquesta història els **Donosti runners** i sobretot les Txikis; **Amaia, Maddi i Clau**, quina sort haver-nos creuat, sou les millors amigues que podria demanar.

A les **matriarques de Prades**, des dels inicis dels meus dies i espero que fins el final sou les amigues mes incondicionals que tinc. Gràcies per estimar-me i deixar-me ser sempre jo mateixa; i en especial a tu **Montse**, germana gran, no concebo la Núria del present sense tu.

Gràcies també a la meva família, del primer a l'últim però en especial als meus pares que sempre m'han acompanyat en totes les metes que m'he marcat. A la meva **mama**, tu sempre has confiat en mi fins i tot quan jo no era capaç de fer-ho. Sense el teu suport incondicional aquesta historia mai hagués arribat al final. Gràcies infinites. Ets el referent de la meva vida. **Papa**, gràcies, se que potser d'una manera no tant evident però sempre has confiat amb mi, t'admiro per la teva serenitat, força i intel·ligència. Us testimo. **Iaia**, forta i valenta. Ja saps que jo de gran vull ser com tu, espero estar en el bon camí per a que així sigui.

I a tu **Marc**, per arribar a la meva vida en el moment més crític, i quedar-te acompanyant-me en aquesta muntanya russa que es la tesis i la vida. Gràcies per allunyar-me del laboratori tantes vegades com ho he necessitat i sobretot per ensenyar-me a relativitzar. T'estimo incondicionalment.

# ABBREVIATIONS

# 1 Abbreviations

| | |
|---|---|
| 4E-BPs | Binding protein to 4E |
| AJ | adherent junction |
| AJC | apical junction complex |
| AP1 | activating protein 1 |
| Apo-B | apolipoprotein B-100 |
| ATM | adipose tissue macrophages |
| AUG | initiation codon |
| BAT | brown adipose tissue |
| BMI | body mass index |
| BMDM | bone marrow derived macrophages |
| CLD | chronic liver disease |
| CLS | crown-like structure |
| CO | carbon dioxide |
| COX | cyclooxygenase |
| CPE | cytoplasmic polyadenylation element |
| CPEB | cytoplasmic polyadenylation element binding protein |
| CREB | cAMP-response element-binding protein |
| CTD | C-terminal domain |
| DGF | dispersed gene family 1 |
| EC | endothelial cells |
| eEF2K | eukaryotic elongation factor 2 kinase |
| eIF4F | eukaryotic elongation factor 4F |
| eIF2 | eukaryotic initiation factor 2 |
| Enos | endothelial nitric oxide synthase |
| eRF1 | eukaryotic translation termination factor 1 |

| | |
|---|---|
| eRF3 | eukaryotic translation termination factor 3 |
| FA | fatty acid |
| FFA | free fatty acid |
| FTO | fat mass obesity-associated locus |
| Gld2 | cytoplasmic poly(A) polymerase |
| GLUT4 | glucose transporter protein 4 |
| GNPDA2 | glucosamine-6-phosphatedeaminase2 |
| GR | glucocorticoid receptor |
| HSC | hepatic stellate cells |
| IEC | intestinal epithelial cells |
| IRES | internal ribosome-entry sequences |
| KC | kupffer cells |
| KCTD15 | potassium channel tetramerization domain containing 15 |
| LD | lipid droplets |
| LPS | lipopolysaccharide |
| LSEC | sinusoidal endothelial cells |
| MMPs | metalloproteases |
| Mme | metabolic activated adipose tissue macrophages |
| MTCH2 | mitochondrial carrier2 |
| NAFLD | non-alcoholic fatty liver disease |
| NASH | non-alcoholic steatohepatitis |
| NO | nitric oxide |
| PABP | poly(A) tail-binding protein (PABP) |
| PAP | poly(A) polymerases proteins |
| PBF | percentage body fat |
| PDGF | platelet derived growth factor |

| | |
|---|---|
| PHT | portal hypertension |
| PRRs | patterns recognition receptor |
| RRM | RNA recognition motif |
| SH2B1 | SH2B adaptor protein 1 |
| SREBP-1 | sterol response element-binding protein-1 |
| STAT5A | signal transducer and activator of transcription 5A |
| SVF | stromal vascular fraction |
| TC | ternary complex |
| TG | triglycerides |
| TGF-β1 | transforming growth factor b1 |
| TJ | tight junction |
| TLR4 | tall like receptor 4 |
| TMEM18 | transmembrane protein 18 |
| UCP-1 | uncoupling protein 1 |
| uORFs | upstream open reading frame |
| UPR | unfolded protein response |
| VEGF | vascular endothelial growth factor |
| VLDL | very-low-density lipoproteins |
| WAT | white adipose tissue |
| WHO | world health organization |
| ZZ domain | zinc binding domain |

# INTRODUCTION

# 2 Introduction

## 2.1 Chronic liver diseases

Chronic liver diseases (CLDs) constitute an important, and certainly underestimated, global public health problem affecting 1.5 billion people worldwide, accounting for 2 million of deaths each year and imposing a high burden of morbidity[1,2]. The most common causes of CLDs in the developed countries are chronic viral hepatitis (due to hepatitis B and C viruses), alcohol abuse, and non-alcoholic steatohepatitis (NASH). Cirrhosis represents the common event for the majority of chronic liver diseases.

The liver is the largest organ of the body, which plays a crucial role in host defence against invading microorganisms. Structurally and histologically, the liver can be divided into five tissue systems: vascular system, hepatocytes and hepatic lobule, hepatic sinusoid, biliary system, and stroma[3]. Regarding cell composition, it is formed by many different cell types, divided into parenchymal cells (hepatocytes) and non-parenchymal cells (sinusoidal endothelial cells (LSEC), kupffer cells (KC) and hepatic stellate cells (HSC)) **(Figure 1).** Understanding the liver architecture is basic to be able to understand the disease development. Hepatocytes occupy the 60-70% of liver volume. They are involved in metabolism, detoxification, and in protein synthesis processes of the liver as well as in the activation of the innate immunity. The non-parenchymal cells account for the 30-40% of the total liver population and include; hepatic stellate cells, situated in space of Disse between hepatocytes and the sinusoids. In a healthy state, they are responsible for the storage of vitamin A; kupffer cells are intravascular tissue macrophages that reside within the lumen of the liver sinusoids. They perform scavenger and phagocytic functions, remove protein complexes, senescent red blood cells, and cell debris from portal blood flow through pattern recognition receptors (PRRs)[4]; finally, sinusoidal endothelial cells which form the walls of the hepatic sinusoids. LSEC form a permeable membrane thanks to the absence of basement membrane and the presence of fenestrations or pores through which solutes can apparently move freely into the perisinusoidal space of Disse.

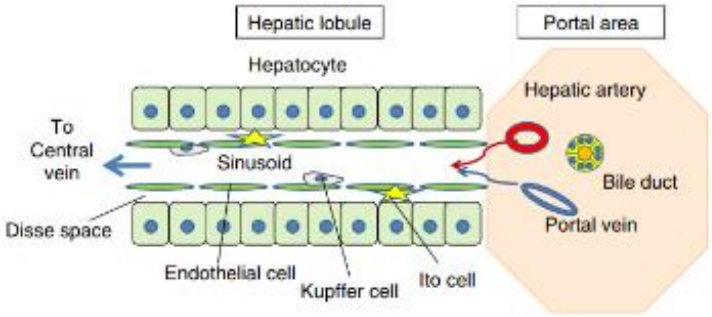


**Figure 1. Liver structure (review Springuer. Liver arquitecture, 2009)**

Knowing the liver architecture in normal conditions, we can define chronic liver disease as a process of progressive destruction and regeneration of the above mentioned parenchyma. As a consequence of the damage and dysfunction of the parenchymal and non-parenchymal cells, there is a nodule formation that lead to fibrosis and eventually, if the injury persists, to cirrhosis. Once cirrhosis is established, patients progress from a frequently asymptomatic compensated stage to a decompensated stage, marked by the development of clinical complications.[5] This progression, from liver injury to cirrhosis may occur over weeks to years. Thus, cirrhosis represents a late-stage liver disease, result of various long-term challenges suffered by the liver. Once more, it is noteworthy that the common feature of almost all chronic liver diseases previous to cirrhosis, is liver fibrosis which remains a key determinant of clinical prognosis.[6]

Chronic liver disease symptomatology is diverse. Progressive condition causes symptoms such as loss of appetite, tiredness, nausea, weight loss, abdominal pain, spider-like blood vessels, severe itching and various complications as impaired metabolic and endocrine functions, splenomegaly due to portal hypertension, haematological derangements, gastrointestinal varices, ascites and hepatocellular carcinoma.

### 2.1.1 Portal hypertension

The most devastating complication for CLD patients among the mentioned above is portal hypertension (PHT). It plays a key role in the transition from a preclinical to a clinic phase in cirrhotic patients thereby representing a potential target in the field in order to control the disease.

Portal hypertension syndrome is defined by, as its name suggest, an increment of blood pressure in the portal vein as well as an increase of splanchnic blood flow **(Figure 2)**. Both determinants are conceptualized, as all dynamic systems, using the derivation of the Ohm's law AP= Q x R, where portal pressure is proportional to the vein blood flow and the resistance against this same flow. So, theoretically speaking, the final portal pressure increase could be due to an increase of the resistance, an increase of the blood flow or a combination of both. From a clinical point of view, portal hypertension critical threshold is defined by values >10 mmHg; in this stage appear the most severe complications for the patient such as variceal bleeding, ascites or encephalopathy.

Portal hypertension can arise from whatever condition that interferes with the blood flow in any level of the portal system. Factors leading to the development of PHT include hypoxia, oxidative stress, inflammation and shear stress, which can also in turn contribute to a pathogenic angiogenic response. Angiogenesis is described as the formation of new vessels from pre-existing ones. The angiogenic process is a hallmark of portal hypertension and cirrhosis being a pivotal feature in the splanchnic vasculature, worsening both the hyperdynamic circulation and portosystemic collateralization.[7,8,9,10]. Thus, portal hypertension associated angiogenesis (pathological angiogenesis) is found both inside the liver and at extrahepatic level.

Moreover, it is important to highlight that angiogenesis does not occur only in pathologic phenomena. Angiogenesis is found as a physiologic process during embryonic development but also in adults, during the female reproductive cycle as well as in wound-healing processes.

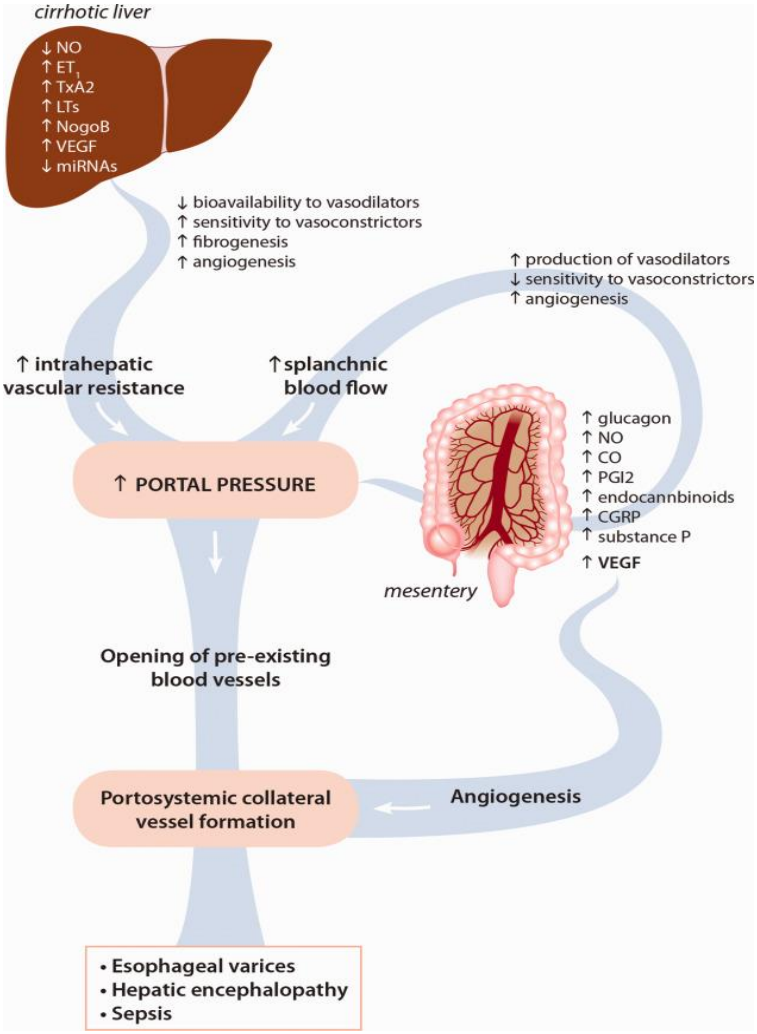


**Figure 2. Molecular physiology of portal hypertension, (Fernandez, M. Hepatology, 2015)**

### 2.1.1.1 Intrahepatic mechanisms

During liver damage, the liver tissue suffers a chain of changes that lead to the above mentioned increased resistance to outflow of portal venous blood. During many years, the increased vascular resistance has been attributed to the liver mechanic/structural obstruction to flow because of fibrotic disruption of the liver architecture and nodule formation. Nevertheless, apart from this mechanic component there is also an important dynamic component contributing to the increased liver vascular resistance.

The mechanic component accounts for the 70% of the increase intrahepatic resistance and it is due to the loss of normal tissue architecture by fibrosis, cicatrisation and nodule formation. Fibrosis is initiated by activation of the stellate cells and Kupffer cells. [11,5,6] Injury to hepatocytes results in the recruitment and stimulation of inflammatory cells, as well as the stimulation of resident Kuppfer cells. Factors released by these inflammatory cells (cytokines and their receptors, reactive oxygen intermediates, autocrine signals and paracrine signals) lead to activation of HSCs. They become highly proliferative, fibrogenic and contractile. In the early stage of activation, stellate cells lose their retinoids with up-regulation of receptors for fibrogenic and proliferative cytokines, like transforming growth factor β1 (TGF-β1) and platelet derived growth factor (PDGF). In this hepatic injury scenario, stellate cells change their phenotype and morphology starting to produce large amounts of collagen (type I and III) and fibronectin that would replace the normal matrix in the space of Disse**.** They acquire myofibroblast features and express a smooth muscle actin being contractile and producing high amount of matrix proteins[12,13] **(Figure 3)**.

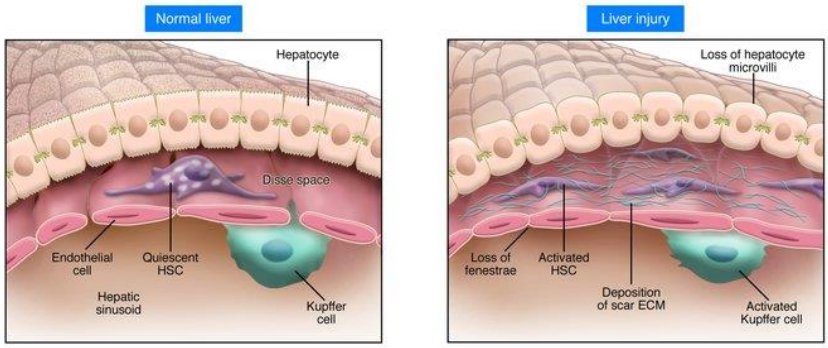


**Figure 3. Sinusoidal events in the development of liver fibrosis. Models of liver fibrosis: exploring the dynamic nature of inflammation and repair in a solid organ (J, Clin Invest. 2007)**

The dynamic component contributes in a 30% of the total resistance increment of the cirrhotic liver[14] , and it is due to, an increment of the vascular tone which affects mainly the hepatic sinusoid. This increase of vascular tone comes from an imbalance between vasodilators and vasoconstrictor agents. The most described molecular components responsible for the increased hepatic vascular resistance are the following:

Nitric oxide (NO), one of the key players in the vasodilation process. It is an important endothelium-derived relaxing factor that has been observed to decrease within cirrhotic livers. The source of NO in the hepatic vasculature are the LSECs and endothelial cells of blood vessels, which express the endothelial nitric oxide synthase (eNOS) and produce a baseline level of NO. Increased IHVR has also been attributed to the exaggerated production of the powerful vasoconstrictors endothelin-1 by HSC and angiotensin II due to the renin-angiotensin system activation. Eicosanoids are additional contributor factors to increase sinusoidal tone in the cirrhotic liver, which include cyclooxygenase (COX)-derived prostaglandins and thromboxane A2, as well as lipoxygenase-derived leukotriene. Moreover, recent evidence indicates that Nogo-B (also known as reticulon-4B) could partially regulate hepatic fibrosis in stellate cells regulating TGF-β/Smad2 signalling pathway[15]. Finally, microRNAs act as finetuning regulators of HSC and endothelial cell functions and their dysregulation might have a role in the pathogenesis of liver fibrogenesis and angiogenesis[16,17].

Moreover, angiogenesis and other cellular alterations at sinusoidal level promote the establishment and maintenance of the abnormal architecture of the liver triggering also the above mentioned dysregulation between vasodilators and vasoconstrictors.

Hepatic angiogenesis could cause irregular intrahepatic circulatory routes and thus increase intrahepatic resistance. Excessive blood vessel growth is also crucially involved in the development of the abnormal hepatic angioarchitecture, distinctive of the cirrhotic liver, which is intimately linked to fibrogenesis. Hepatic angiogenesis differs greatly from extra hepatic angiogenesis because of three components; firstly, because of the presence of hepatic stellate cells that exert a proangiogenic role when are activated. Secondly, because of the presence of the liver's unique microvasculature structures as it is the fenestrated sinusoid. Finally, because of the existence of angiogenic factors liver specific such as ANGPTL3.

### 2.1.1.2 Extrahepatic mechanisms

In the last decades it has been widely reported how alterations occurring during CLDs and so during portal hypertension do not affect only the liver itself but different surrounding organs. It has been well described how portal hypertension is associated with an hyperdynamic syndrome in the circulatory system [8,18]. PH is accompanied by an increase of the blood flow in the splanchnic organs as well as by the formation of portosystemic collateral veins **(Figure 4)**.

The first one comprises a complex and multifactorial process that includes vasodilation of mesenteric blood vessels and a decrease response of endogenous vasoconstrictors. The second represents a major consequence of the increased portal pressure derived from a chronically injured liver. Basically, nature decompresses the hypertensive portal vein by diverting up to 90% of the portal flow through portosystemic collaterals bypassing the liver, resulting in flow mediated remodelling and enlargement of these vessels. Portosystemic collaterals are fragile and can leak causing important complications for the patient as the previously mentioned variceal bleeding. These collaterals are formed by mainly two mechanisms. The first one, establish that collaterals are formed by the opening and remodeling of preexisting vessels, as it has been classically thought. Nevertheless, in the last years, angiogenesis has come into the picture.

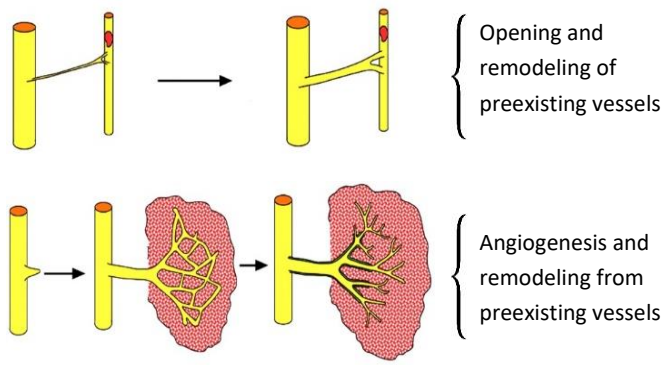


**Figure 4. Portosystemic collateral formation**

Pathological angiogenesis in the splanchnic circulation has been thought to maintain and worsen portal hypertension because an increase in the pathological vasculature could enhance blood flow to the portal venous system, thereby increasing portal pressure [19]. Splanchnic angiogenesis occurs mainly in the spleen, gut and the mesenteric

organ, being this last one the main player. The mesentery is formed by a double fold of peritoneal tissue that suspends the small intestine and large intestine from the posterior abdominal wall. It has been seen for many years as a collection of structures, thus not being considered an organ. Few years ago researchers found the mesentery to be a continuous structure and so started to classify it as an organ[20]. Apart from suspending the intestines, the mesentery provides a conduit for blood and lymphatic vessels and play a role in inflammatory diseases **(Figure 5)**.

Regulation of angiogenesis is classically understood as a dynamic balance between activators and inhibitors. It requires the combined activities of numbers of growth factors such as VEGF, PDGF and angiopoietins. VEGF has been extensively demonstrated by our group and others to be the principal factor implicated in angiogenesis in chronic liver disease, being overexpressed in splanchnic organs of animals with portal hypertension together with VEGF receptor 2[21,9,22,23]. Indeed several factors such as hypoxia, cytokines and mechanical stress have been shown to promote the expression of VEGF [7].

**Figure 5. Macroscopically view of a mesentery with pathologic angiogenesis after 20 days of a partial portal vein ligation**

## 2.2 Obesity

### 2.2.1 Epidemiology

The World Health Organization (WHO) defines obesity as “a condition in which percentage body fat (PBF) is increased to an extent in which health and well-being are impaired".

Over the past years, obesity has reached epidemic worldwide proportions becoming a major public health concern since its major contribution to worsen many pathologies and chronic diseases including insulin resistance and type 2 diabetes, atherosclerosis, non-alcohol fatty liver disease, arthritis, immune system dysfunction, cardiovascular disorders and some cancers[24]. Recent estimates show that 2 billion adults were overweight in 2016 of which 640 million were obese[25] **(Figure 6)**. Regarding children, prevalence of obesity raised to 5% in 2014[26]. These numbers state that, despite the efforts to slow the progress of the epidemic, at the present time, 39% of the world population is overweight or obese and the burden of the disease is not expected to decrease in the coming years.

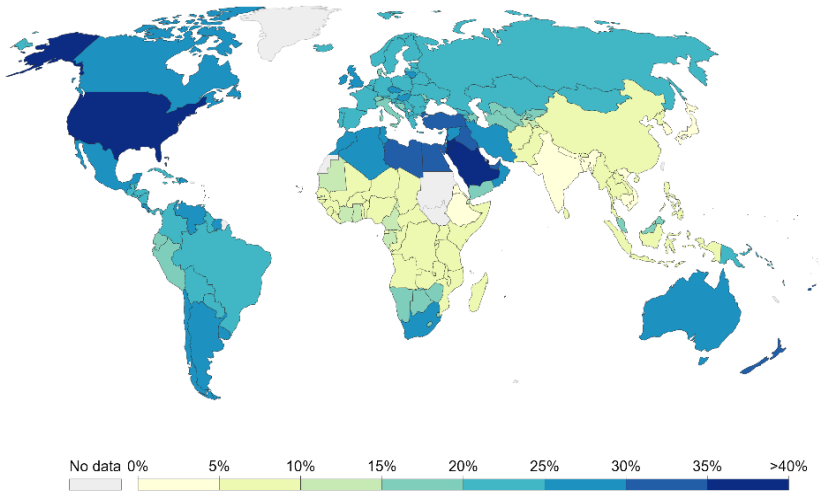


**Figure 6. Obese adult rate 2016 (Our world in data)**

In order to classify obesity, different tools have been used over the past years. Body mass index (BMI) is the most common one, even though considered sometimes imprecise since does not take body composition into account. It is an anthropometric index based on the weight of the individual expressed in kilograms (kg) and divided by the square

height in meters ($m^2$). Generally speaking, below 18.5 kg/$m^2$ defines undernutrition, between 18.5-24.9 kg/$m^2$ defines normal weight, from 25 to 29.9 kg/$m^2$ overweight and over 30 obese **(Table 1)**. Obesity can also be classified based on the distribution of the adipose tissue all over the body thus, in subcutaneous or visceral adipose tissue.

**Table 1: International Classification of weight according to body mass index (Adapted from WHO 1995, 2000 and 2004)**

| Classification | BMI(kg/$m^2$) | |
|---|---|---|
| | Principal cut-off points | Additional cut-off points |
| Underweight | <18.50 | <18.50 |
| Severe thinness | <16.00 | <16.00 |
| Moderate thinness | 16.00 - 16.99 | 16.00 - 16.99 |
| Mild thinness | 17.00 - 18.49 | 17.00 - 18.49 |
| Normal range | 18.50 - 24.99 | 18.50 - 22.99 |
| | | 23.00 - 24.99 |
| Overweight | ≥25.00 | ≥25.00 |
| Pre-obese | 25.00 - 29.99 | 25.00 - 27.49 |
| | | 27.50 - 29.99 |
| Obese | ≥30.00 | ≥30.00 |
| Obese class I | 30.00 - 34.99 | 30.00 - 32.49 |
| | | 32.50 - 34.99 |
| Obese class II | 35.00 - 39.99 | 35.00 - 37.49 |
| | | 37.50 - 39.99 |
| Obese class III | ≥40.00 | ≥40.00 |

Nevertheless, obesity classification as well as its general epidemiology description encounters another difficulty, the marked heterogeneity of individuals that suffer the disease. As with other chronic diseases, obesity, results from an interaction between an individual's genetic predisposition to weight gain and environmental influences (overeating and sedentary lifestyle mainly).

Accumulating evidence has strongly implicated a genetic component playing an important role in the risk of becoming obese[27]. Nevertheless, it has proved challenging as well to identify the specific underlying genetic cause of obesity due to the complex interactions involved in the regulation of adiposity. For instance, genome wide association analysis has identified more than 300 genetic loci for obesity traits since GWAS analysis came into the scene in 2005. Moreover, these associations are considered robust within the field. The major success was the finding of the fat mass and obesity-associated locus (FTO)[28,29] that regulate appetite, thermogenesis, browning and epigenetic mechanisms related to obesity. Even though being large (increasing each allele the risk of obesity by a 1.20-1.32 fold)[30]) was still small within the whole gene

population potentially implicated in obesity. After the finding of the FTO, another genes were subsequently discovered with larger meta-analysis such as transmembrane protein 18 (TMEM18), potassium channel tetramerization domain containing 15 (KCTD15), glucosamine-6-phosphatedeaminase2(GNPDA2), SH2B adaptor protein 1 (SH2B1) or mitochondrial carrier2(MTCH2)[31]. Recently an expanded GIAnt metanalysis has uncovered 32 new BMI associated loci. By now, the current challenge is to understand the underlying biologic mechanisms of these loci and how they confer risk for obesity.

Currently therapeutically approaches to target obesity disease focus mainly on changes in the lifestyle although these modifications are often met with limited long-term success. Moreover, patients with BMIs >30kg/$m^2$ need additional use of pharmaceutical agents in order to lose weight. Unfortunately, medical options to manage obesity are plagued with unacceptable side effects[32,33]. Thus, there is a huge need to understand the mechanisms underlying weight regulation in order to prevent obesity as well as to find new effective and safe anti-obese medications.

### 2.2.2 Adipose tissue

Adipose tissue is the most prevalent tissue in the whole body, found surrounding internal organs as well as in the subcutaneous loose. It is composed mainly by mature adipocytes in a 20-40% and by the inter-adipocyte stromal vascular fraction (SVF) for the remaining percentage. SVF is mainly composed by extracellular matrix with dispersed stem cells (2-10%), endothelial cells (7-30%), fibroblasts (50%), pre-adipocytes and different types of immune cells. These elements are involved in the tissue expansion and cell turnover, ensure tissue integrity, and orchestrate recruitment and activation of immune cells involved in adipocyte control metabolism.

Since adipocytes represent the principal cell type in the overall adipose tissue it is important to review their subtypes **(Figure 7)**. There are two major classical types of adipocytes, white adipose tissue/adipocytes (WAT) and brown adipose tissue/adipocytes (BAT). Brown adipose tissue has been negatively correlated with the BMI. Among its characteristics we found that contributes to energy expenditure via thermogenesis to maintain body temperature. It's formed by brown adipocytes innervated by the sympathetic nervous system. Brown adipocytes are typically ellipsoid in shape and range from 15–50 μm in size. These cells are characterized for having the mitochondria densely packed, with the cytoplasm containing several lipid droplets and a roundish nucleus. They accomplish their function through the actions of uncoupling protein 1 (UCP1) and BAT specific proteins, located within the mitochondria.

On the contrary, white adipose tissue shows fewer nerves and a lower number of blood vessels. In morphology, white adipocytes contain a single large lipid droplet occupying about 90% of the cell volume. The nucleus is squeezed to the cell periphery and the cytoplasm forms a very thin rim. The organelles are poorly developed; in particular mitochondria are small, elongated and have short, randomly organised cristae compared to brown adipocytes. White adipocytes are the most abundant in humans and are strongly associated with insulin resistance and the so called metabolic syndrome.

A novel type of adipose tissue called beige/brite adipose tissue has recently been included in the classification. Their main characteristics as beige adipocytes are their capacity to be recruited in the white adipose tissue to dissipate heat as an adaptive thermogenesis. These cells appear as UCP1+ clusters within white fat depots hence, sharing a brown fat-like morphology. They are uniquely programmed to be an energy storage when there is no thermogenic stimuli but at the same time are capable of turning on heat production when they receive the appropriate signals. It has been demonstrated how in a compensatory way, beige fat is induced when there is a selective loss of classic brown fat restoring body temperature and resistance to diet-induced obesity.[34]

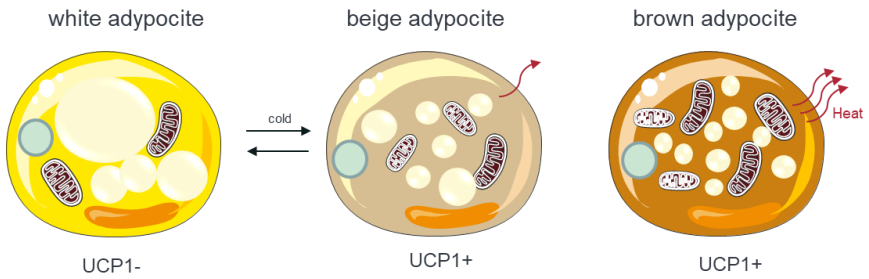


**Figure 7. Types of adipocytes**

### 2.2.2.1 Adipose tissue localization

Adipose tissue deposits in multiple locations around the body; in some in a discreet manner and in others as a large accumulation of fat. The classical classification of the adipose tissue according to localization distinguishes subcutaneous from visceral fat. Subcutaneous adipose tissue located under the skin constitutes 80% of the total body fat. Visceral adipose tissue is located surrounding digestive organs and accounts for the rest 20% of the body fat. It includes mesenteric adipose tissue, perirenal and pericardial adipose tissue. Going back to adipose tissue subtypes, BAT is found in vascularized deposits as are the shoulder blades, perirenal surrounding the kidneys, in the neck and along the spinal cord. Consequently, WAT is found in the remaining localizations of the above mentioned **(Figure 8)**. It should be pointed out that visceral adipose tissue shows depot-specific effects as well as disease-specific effects which have to be considered in the study of this tissue. For instance, preadipocytes express gene signatures specific of their depot origin while adipocytes behave differently when secreting adipokines as well as depending on the lipolysis rate and triglycerides synthesis.

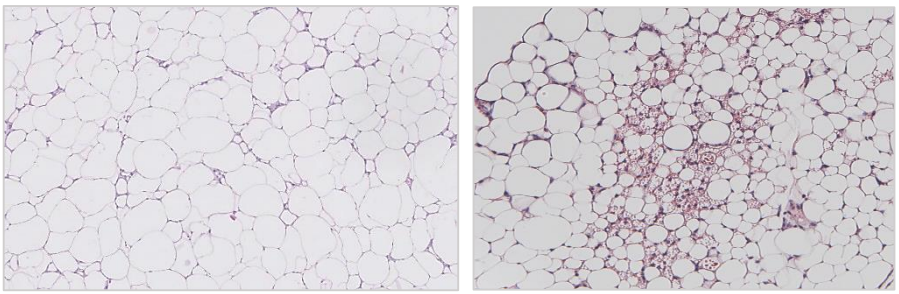

**Figure 8. Haematoxylin and eosin staining showing a WAT section of the epididymal depot on the left and a BAT section from the retroperitoneal on the right**

### 2.2.2.2 White adipose tissue

White adipose tissue has been seen for many years as a simple connective tissue that stores fat. However, the metabolic role of white fat is far more complex. Thus, it has been found that this tissue plays a key role in nutrient homeostasis serving as a source of circulating free fatty acids during fasting[35,36]. Finally, It was in the early 90s by Friedman's group with the discovery of the serum factors secreted by the adipose tissue when it was no longer considered as a passive storehouse of excess energy but as an active endocrine organ with a profound effect on physiology and pathophysiology [37,38,39]

. So, the most common functions of the WAT could be divided in storage of lipid, maintenance of insulin sensitivity and endocrine signalling.

The traditional function attributed to white adipose tissue comprises both lipogenesis and lipolysis depending on the fatty acids demand. Thus, lipolysis is the process by which TG are broken down to FFA and glycerol in times of energy need**.** In periods of excess energy intake, dietary lipids are taken up by fat cells (adipocytes) and esterified into triglycerides (TGs), which are stored in cytosolic lipid droplets (LDs). In conditions like fasting and exercise, when mobilization of endogenous energy stores is required, TG are hydrolysed through the process of lipolysis and released to the circulation as free fatty acids (FFAs) **(Figure 9).**

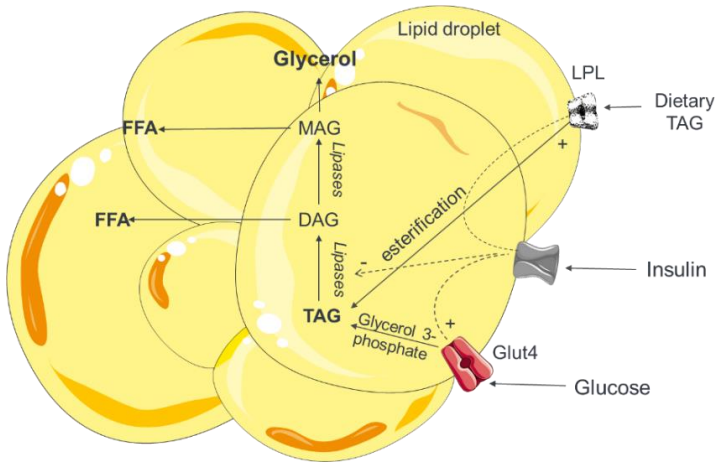


**Figure 9. Schematic representation of the Lipolysis pathway in adipose tissue**

In addition to regulating lipid release and storage, adipose tissue functions as a large endocrine organ. Its role as an endocrine organ started with the discovery of leptin in 1994 [40]. Leptin is a hormone secreted mainly by adipose cells but also by enterocytes in the small intestine. Its serum levels correlate with fat mass and it also exerts a role in the central nervous system and in the periphery through specific receptors. Data demonstrated the high expression of leptin receptor (LEPR) in lymphocytes activated by mature adipocytes while they upregulate proinflammatory cytokines**.** Another determinant adipocyte factor is adiponectin. Its expression is adipose specific and it is constitutively secreted[41]. Contrary to leptin, adiponectin inhibits the transformation of

macrophages into foam cells and endothelial cell activation. Its expression and secretion decreases in visceral obesity despite the increased fat mass. Even though much of the research in this area has been focused on leptin and adiponectin, these findings have opened a new scope of research where many new adipokines have been identified every year on (resistin, visfatin, plasminogen activator inhibitor 1, IL6, angiotensin).

Finally, adipose tissue is also needed for normal glucose homeostasis being the responsible of insulin resistance when hypertrophies. Adipose tissue secretes molecules that are associated with enhanced insulin sensitivity[42] such as FFA itself or the novel discovered type of anti-diabetic FFA, FAHFAs [43]. They are present in the highest levels in white and brown adipose tissue. Some of these novel lipids enhance the effect of insulin on glucose uptake in adipocytes and augment glucose-stimulated GLP1 secretion from entero-endocrine cells and insulin secretion by pancreatic beta cells. Moreover, levels of the insulin-regulated glucose transporter protein (GLUT4) are reduced in adipose cells in insulin-resistant obesity and in prediabetes, as well as in type-2 diabetes mellitus itself[44].

#### 2.2.2.3 Adipogenesis

Adipogenesis is defined as the process by which preadipocytes get differentiated into adipocytes. Adipocytes develop from mesenchyme generally called pre-adipocytes, even though the specific precursors differ for different types of adipocytes.[45] The development of differentiated adipocytes from their mesenchyme precursor cells it's a complex process that progress sequentially, activating several transcription factors **(Figure 10)**. Briefly, in white adipocytes this sequence starts with the activation of members of the activating protein-1 (AP-1) family of transcription factors, and continues with the induction and expression of PPARγ. Other transcription factors facilitate adipocyte maturation, including STATs, members of the KLF family of proteins, sterol response element– binding protein-1 (SREBP-1), and members of the C/EBP family. So, based on *in vitro* studies adipogenesis would proceed through the activation of at least two waves of TFs. The first includes TFs such as the CCAAT-enhancer-binding proteins C/EBPβ and -δ as well as the glucocorticoid receptor (GR), signal transducer and activator of transcription 5A (STAT5A), and the cAMP-response element-binding protein (CREB). These factors in turn activate TFs of the second wave, which initiate the adipocyte gene program. PPARγ and C/EBPα appear to play the most prominent roles in this second wave [46,47]. There are many other proadipogenic transcription factors that have been characterized, but none of them are as critical as PPARγ, the master regulator of adipocyte differentiation and gene expression. Of note, the majority of the identified

repressors and activators of adipogenesis have been shown to modulate PPARγ expression and/or activity [48,49]. Apart from the above mentioned positive and negative effectors of the adipogenesis it exists also an endocrine control through a large variety of peptide hormones.

During adult life, adipose tissue has to expand to accommodate chronic excess caloric intake. In the same line, during obesity, the further growth of the white adipose tissue comes determined mainly by an increase of the adipocyte size (hypertrophy) and/or an increase in adipocyte number (hyperplasia). It is important to consider that adipose tissue expansion through adipogenesis not only distributes excess calories among the newly formed small adipocytes, but also, reduces the number of hypertrophic adipocytes secreting pro-inflammatory factors. By contrast, large hypertrophic adipocytes experience hypoxic stress, increase inflammatory infiltration and overall exacerbate obesity-associated metabolic decline [50,51].

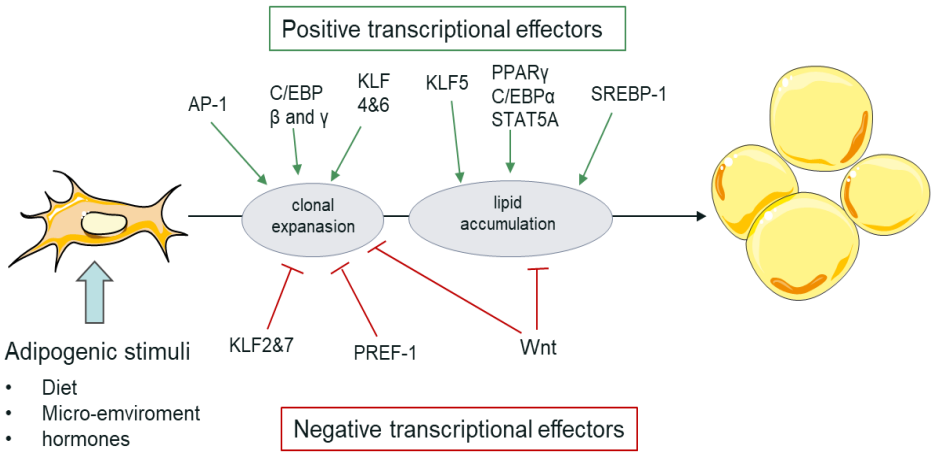


**Figure 10. Transcriptional regulation of adipocyte differentiation. (Adapted from Stephens JM. PLoS Biol, 2012)**

### 2.2.1 Adipose tissue angiogenesis

Adipose tissue is the most vascularized tissue in the body[52]. In this regard, its vascularization capacity exerts an underappreciated influence on adipose tissue physiology. In the early stage of the adipose tissue development, adipogenesis is found to be tightly associated with angiogenesis[53]. Some studies revealed that differentiating adipocytes trigger blood vessel formation and that, in turn, adipose tissue endothelial cells (ECs) promote preadipocyte differentiation[54,55]. The angiogenic process is regulated by the WAT production and secretion of different types of proangiogenic factors such as vascular endothelial growth factor (VEGF)-A and hepatocyte growth factor (HGF), the two key angiogenic factors produced by adipocytes.

Nonetheless, expansion of adipose tissue must be also accompanied by its vascularisation, through processes of angiogenesis. Therefore, during first stages of obesity, adipogenesis is coordinated with vascularization of the adipose depot allowing to preserve the function of white adipose tissue [56]. At this point, obesity has been described as metabolically healthy. But what happens if the overnutrition persists? the adipose depot expands beyond the tissue's capacity leading to local and unresolved hypoxia, associated with a metabolically unhealthy obesity. At this point, the adipose tissue angiogenic potential results to be insufficient, leading to adipose tissue dysfunction. Although the mechanism of obesity-induced endothelial dysfunction is multifactorial, the adipokines released by the AT are the main contributors, leading to elevated blood pressure, formation of atherosclerotic plaques, oxidative stress, prothrombotic state and alterations in glucose and lipid metabolism[57,24] **(Figure 11)**.

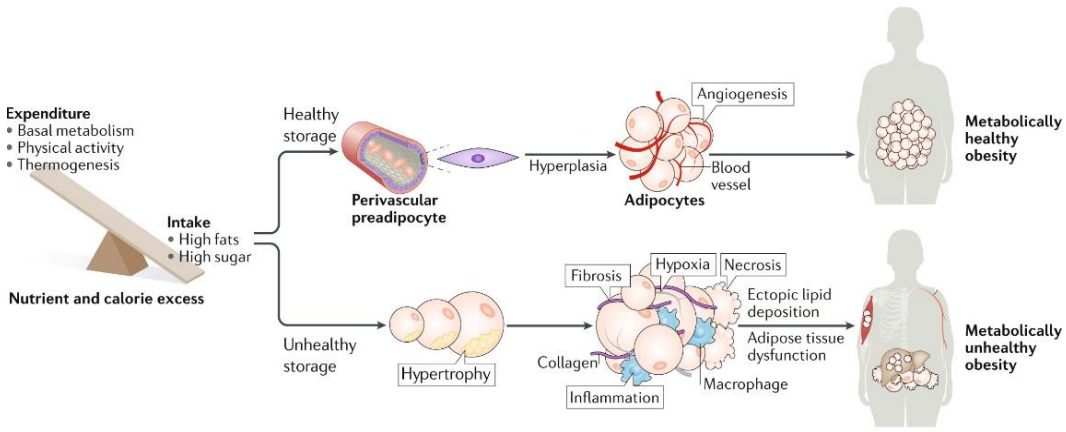


**Figure 11. Mechanisms of adipose tissue expansion, Alexandra L et al. (Nature Reviews Molecular Cell Biology, 2019)**

### 2.2.2 Obesity: a low grade inflammation state

Another important contributor to the adipose tissue dysfunction during obesity is its state of low-grade chronic systemic inflammation when undergoes expansion[58] **(Figure 12)**. In recent years, immune cells populating the fat pat have gained a huge importance in playing a central role in adipose biology. Thus, the immune cell imbalance has been likely described to be the core of the obesity development[59].

Inflammation occurs to maintain tissue homeostasis and as a protective response to an injury. There are mainly two types of inflammation; the first one is an acute inflammation, characterized by edema and migration of leukocytes, and the second one is chronic inflammation, which is characterized by the infiltration of lymphocytes and macrophages and the proliferation of blood vessels and connective tissue. This one is considered a characteristic feature of metabolic syndrome in an attempt to restore the homeostasis of the tissue[60] with clinical consequences.

Moreover, adipose tissue represents an important source of adipokines and cytokines being their main producers the macrophages that reside in the fat pad, called adipose tissue macrophages (ATM). Macrophages are key players in tissue homeostasis although other immune cells such as neutrophils, mast cells, B lymphocytes and T lymphocytes play also a significant role in the inflammatory tone of the obese fat pad.

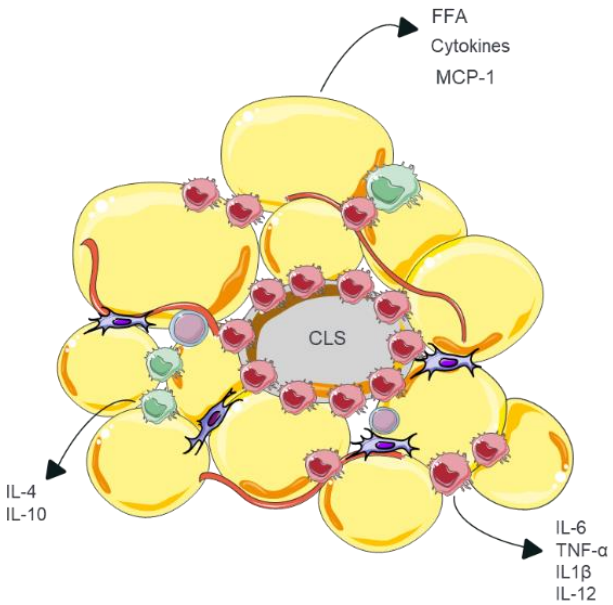


**Figure 12. Hypertrophic adipose tissue**

#### 2.2.2.1 Adipose tissue macrophages

ATM reside in the adipose tissue as the most abundant class of leukocytes. They carry out different regulatory functions such as tissue remodelling and insulin sensitivity. They produce inflammatory cytokines and clear dead adipocytes that accumulate during prolonged obesity; when adipose tissue expands enough to produce hypoxia ATM form crown-like structures (CLS) surrounding dead or dying adipocytes. Nevertheless, they also perform beneficial functions, internalizing excess free fatty acids released by insulin resistant adipocytes.

The vast majority of macrophages are not resident but recruited in the adipose tissue. They are recruited through pathogenic mechanisms that have been under extensive investigation lately. The adipocyte increased production and release of some chemokines has been the major implicated[61,62]. Once the adipocyte has sent the recruitment signals, ATM secrete interleukins that likewise would recruit more macrophages. The most common proinflammatory cytokines are IL6, Il1β, TNFα and IL12. On the contrary, resolutive interleukins comprise IL10, IL4, IL13 among others.

But, which type of macrophages is responsible for each duty? Phenotypically there is a lot of controversy when describing macrophage classification. The classical M1/M2 model was introduced in 2000 by Mills et al [63]. M1 has always been associated to a pro-inflammatory phenotype caused by Th1 mediators while M2 macrophages were described to have anti-inflammatory functions, clearing dead cells and maintaining tissue integrity and remodelling. However, recent studies revealed a new more complex range of macrophage activation than the previous M1/M2 model which did not reflect the inflammation situation in vivo where a spectrum of mixed markers is found[64]. They exist usually between M1 and M2 as the polarization process is dynamic. Thus, in 2014, under the need of adequately describe the functions of ATM during obesity, it was described the so called metabolically activated adipose tissue macrophages (Mme)[65,66]. Metabolically activated macrophages are both mechanistically and functionally distinct from M1 phenotype. Although expressing M2 surface markers, they use both pro and anti-inflammatory pathways to perform functions of cytokine production and lipid metabolism. Moreover, it has been demonstrated how over two different time points during diet-induced obesity, macrophages can exhibit contradictory phenotypes[65,67] **(Figure 13)**.

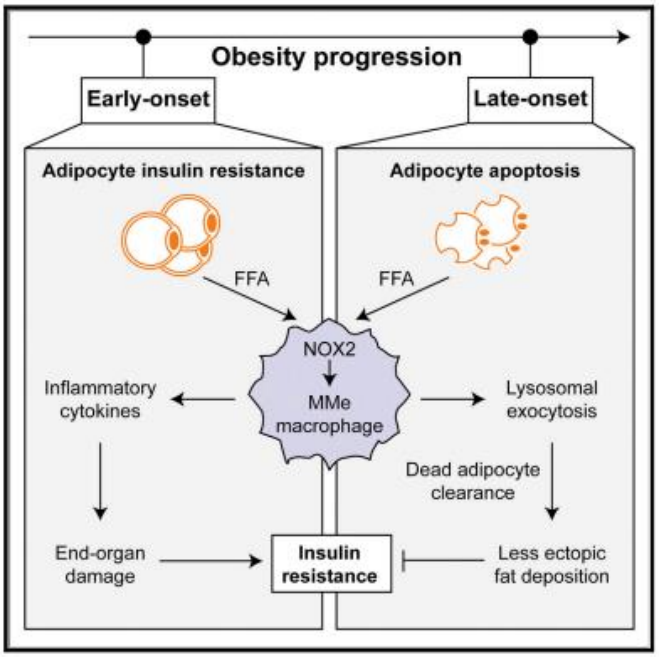


**Figure 13. MMe macrophages detrimental and beneficial functions. (Brittney R. Coats, Cell Rep. 2017)**

### 2.2.3 Adipocyte cross-talk

As previously described, adipocytes are surrounded by a wide variety of cell types apart from macrophages, including immune cells, fibroblasts, preadipocytes and stem cells. Adipocytes exert an important influence on all these neighbouring cells and tissues establishing what is called a cross-talk (reciprocal signals) **(Figure 14)**. This cross-talk is typically mediated in three different ways: through nutritional mechanisms, neural pathways and via elaboration of autocrine, paracrine and endocrine agents commonly named adipokines.

The nutritional mechanisms involve the store excess of calories and release thought lipolysis when there is nutritional deprivation, all in form of free fatty acids. Neuronal signals play a crucial role regulating adipose tissue growth and cellularity. Adipocytes can communicate to the brain via nerves to communicate information about nutritional status. However, the most complex and so where more efforts have been made to understand the adipocyte biology is in understanding the adipokine biology. Finally, as described before, white adipose tissue represents the largest endocrine tissue in the

human body. Adipocytes produce a wide range of factors called adipokines which regulate different physiological processes [35,68] as well as factors implicated in the main processes of the adipose tissue: food intake, energy expenditure, metabolism homeostasis, immunity and blood pressure[69,70].

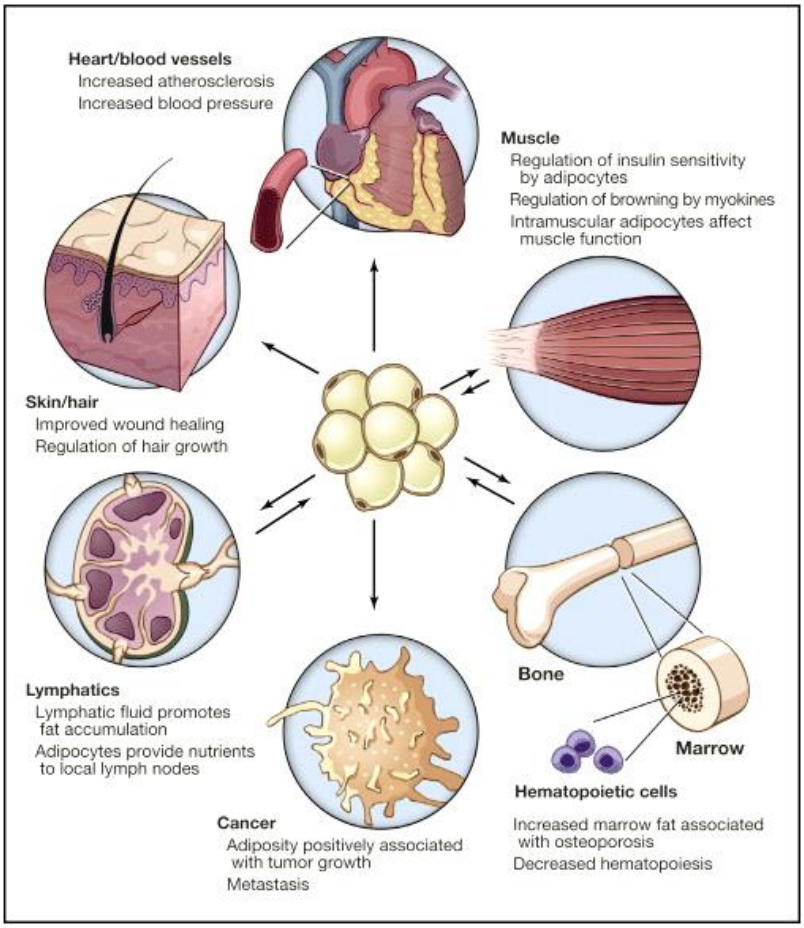


**Figure 14. What we talk when we talk about fat. (Cell, 2016)**

### 2.2.4 Obesity related diseases

#### 2.2.4.1 Metabolic syndrome

Obesity is closely related to the so called metabolic syndrome that was introduced at the early 50s [71,72]. It described the risk factors associated with obesity being a clustering of at least 3 to 5 of the following medical conditions: visceral adiposity, hypertriglyceridemia, low levels of HDL, elevated blood pressure and increased glucose levels. In general terms metabolic syndrome is associated with obesity and consequently with visceral adipose tissue, contributing to the burden of chronic diseases including insulin resistance, hyperinsulinemia, impaired glucose tolerance, hypercoagulability, hypertension and overall fat accumulation in different organs.

#### 2.2.4.2 NAFLD

Among all the chronic diseases worsened by obesity, non-alcoholic fatty liver disease (NAFLD) is increasingly recognized as the liver disease component of the metabolic syndrome even though there is still controversy in which one is the precursor[73,74,75]. It represents the most prevalent liver disease worldwide (25%)[76] whose levels rise, not surprisingly, in parallel to obesity pandemia.
NAFLD is defined by its hallmark feature, steatosis described as abnormal retention of fat in the liver.

##### 2.2.4.2.1 Intrahepatic NAFLD

The liver is considered fatty when the presence of hepatic steatosis or intrahepatic triglycerides is more than 5%, in the absence of competing liver disease etiologies[77].
Thus, steatosis develops when the rate of fatty acids (FA) input is greater than the output. Fatty acids input come determined by the uptake derived from the hydrolysis of adipose tissue triglycerides plus the novo fatty acid synthesis lipogenesis as described before. Fatty acids output is the result of fatty acid oxidation and export through cholesterol **(Figure 15).**

Fatty acid uptake depends on two factors; First the delivery of FFA that the liver receives and second, the liver's capacity to transport FFA[78,79]. Regarding delivery, FFA arrive to the liver from the hepatic artery and the portal vein and derive, originally, from three different sources; visceral and subcutaneous fat, being this last one the main contributor, plus from the lipolysis of circulating TG in NAFLD patients[80,81].

Liver is also able to synthesize fatty acids *de novo*. This lipogenesis is accomplished through the complex cytosolic polymerization in which acetyl-CoA is converted to malonyl-CoA by the enzyme acetyl-CoA carboxylase. After several cycles, a palmitate molecule is formed[82,81]. *De novo* lipogenesis in NAFLD patients is associated with increased hepatic expression of the genes involved in this process. From both mentioned sources, *de novo* lipogenesis accounts for a 20% of the total incorporated in NAFLD patients while fatty acids uptake would account for the rest.

Moving to free fatty acids output, fatty acid oxidation (FAO) is one of the major contributors. Intrahepatic beta-oxidation occurs primarily in the mitochondria in response to lipid accumulation to prevent lipotoxicity and to support gluconeogenesis[79,83]. Mitochondrial β-oxidation shortens the fatty acyl-CoA to acetyl-CoA, through a series of dehydrogenation, hydration, and cleavage reactions that involve a membrane-bound and soluble enzymes, which are transcriptionally regulated by PPAR-α[84]. Finally, acetylCoA product of the FAO can either enter the tricarboxylic acid cycle for complete oxidation and energy production for the liver, or can be condensed to form ketone bodies, which are exported to provide energy for other tissues.

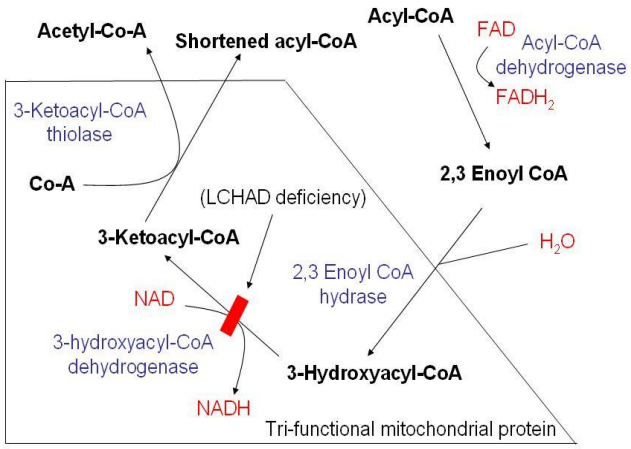


**Figure 15. Beta oxidation process, (4 February 2017. Wikipedia)**

The final contributor to fatty acid output is their exportation through very-low-density lipoproteins (VLDL). Hepatocytes distribute lipids into peripheral tissues by the export of VLDLs produced by the liver into the systemic circulation. VLDLs are necessary in order to convert TG in a soluble form, able to be exported[79]. This mature soluble form is the result of the fusion of an apolipoprotein B-100 (Apo-B) molecule with a TG droplet

through a triglyceride transfer protein. Thus, impaired VLDL export limits hepatic disposal of triglycerides and induces hepatic steatosis[85]. Altogether, non-alcoholic fatty liver disease is typified by increased hepatic lipid uptake, synthesis, oxidation and export **(Figure 16)**.

But who is orchestrating all these processes in the liver? Hormones are responsible for all these events to happen[84]. The typical hormonal environment in fatty liver disease is characterized by hyperinsulinemia, hyperglucagonemia, elevated sympathetic tone, hypercortisolemia and growth hormone deficiency. Insulin and catecholamines are the inhibitory and stimulatory regulators of adipose lipolysis[86,87]. During fasting and exercise, insulin levels are low, allowing norepinephrine, cortisol and growth hormone to synergistically stimulate lipolysis and increase systemic fatty acid[88]. Similarly, hepatic lipid accumulation induces endocrine changes that dysregulate adipose tissue lipolysis, including insulin resistance.

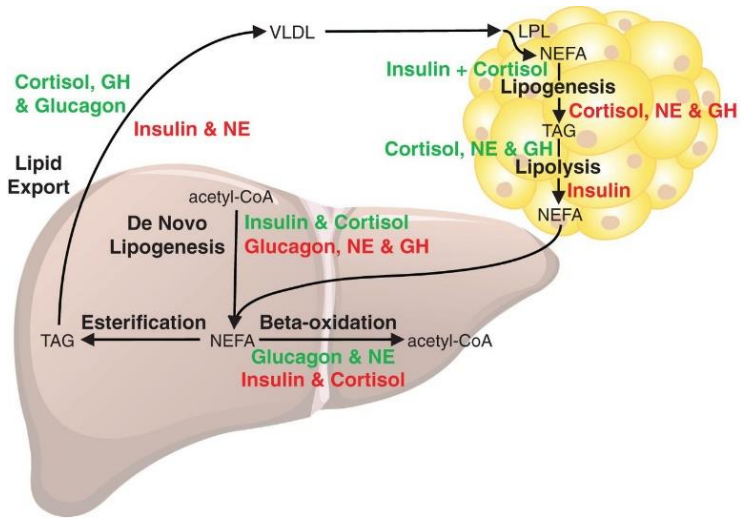


**Figure 16. Hepatic Lipid Metabolism (Caroline E Geisler, Journal of Endocrinology, 2017)**

As mentioned before, NAFLD has been described for many years as a consequence of the metabolic syndrome[89,58]. Although its severity is directly related to classic components of the metabolic syndrome, NAFLD can also precede the development of other components of the metabolic syndrome like type 2 diabetes mellitus or coronary heart disease[90,91], leaving the temporal sequence still open.

#### 2.2.4.2.2 Extrahepatic NAFLD

Even though most of the effort in understanding NAFLD disease has been focused on the study of the liver, this complex metabolic disease presents an extensive multi-organ involvement[92], which extends far beyond the liver.

In the last years a "multiple-hit" hypothesis has emerged to explain its pathogenesis. Such hits include insulin resistance, hormones secreted from the adipose tissue, nutritional factors, gut microbiota and genetic and epigenetic factors. Among them, the gut–liver axis (GLA) seems to play a central role. Liver is the initial site of filtration of gut-derived products, being susceptible to the exposure to microbial products from the gut[93]. The relationship between the two has been called the "gut–liver axis," and involves many organs in between them. Thus, it is not surprising the huge evidence that has been published in the last years supporting a link between the gut barrier integrity and NAFLD.

The gut barrier is the first key component of the system. In a healthy gut, the intestinal epithelium forms a dynamic and semipermeable barrier that allows in one side the absorption of nutrients and antigens necessary for immune regulation but, on the other side, protects the host from the direct microbiota as well as from toxic molecules to translocate outside the gut. However, numerous factors such as pathogen infections or intake of excess dietary fat can alter components of this system, compromising the barrier[94].

It is well known how a high fat diet alters the internal homeostasis, disrupting the intestinal barrier integrity by numerous mechanisms (bacterial overgrowth, physical disruption of the gut mucosal barrier, impaired host defense…) that would lead eventually to chronic liver disease[95,96]. One of the first mechanisms by which dietary fat modulates the permeability of the intestinal barrier is by modulating the microbial composition producing an imbalance of the bacteria found in the gut, known as dysbiosis[97]. These microbial imbalance has been reported to result in increased bacterial products, such as lipopolysaccharide (LPS), that would translocate from the gut to the blood stream [98,99,100,101]. LPS is able to translocate from the lumen into the lamina propia and blood and produce what is known as endotoxemia.

Taking together all the above mentioned mechanisms, we can picture the sequence of events that take place in the NAFLD development at gut level. Dysbiosis produced by a high fat diet results in a shift in species abundance, breakdown of the intestinal barrier, intestinal inflammation, and translocation of microbial products such as LPS and endotoxins. They enter into the blood stream and activate inflammatory cascades at different levels. In adipose tissue it causes hypertrophy of the adipocytes increasing the

release of FFA that would travel to the liver. Besides the effect of LPS in the adipose tissue, LPS would also activate macrophages through receptor TLR4 signaling. These macrophages can infiltrate both in adipose tissue and in the liver, secreting proinflammatory cytokines, which would in turn promote hepatic inflammation and fibrogenesis by Kupffer cells and stellate cells in the liver. TLR4 mediated proinflammatory signaling in adipocytes and macrophages creates a feed-forward mechanism in promoting systemic and hepatic inflammation **(Figure 17)**.

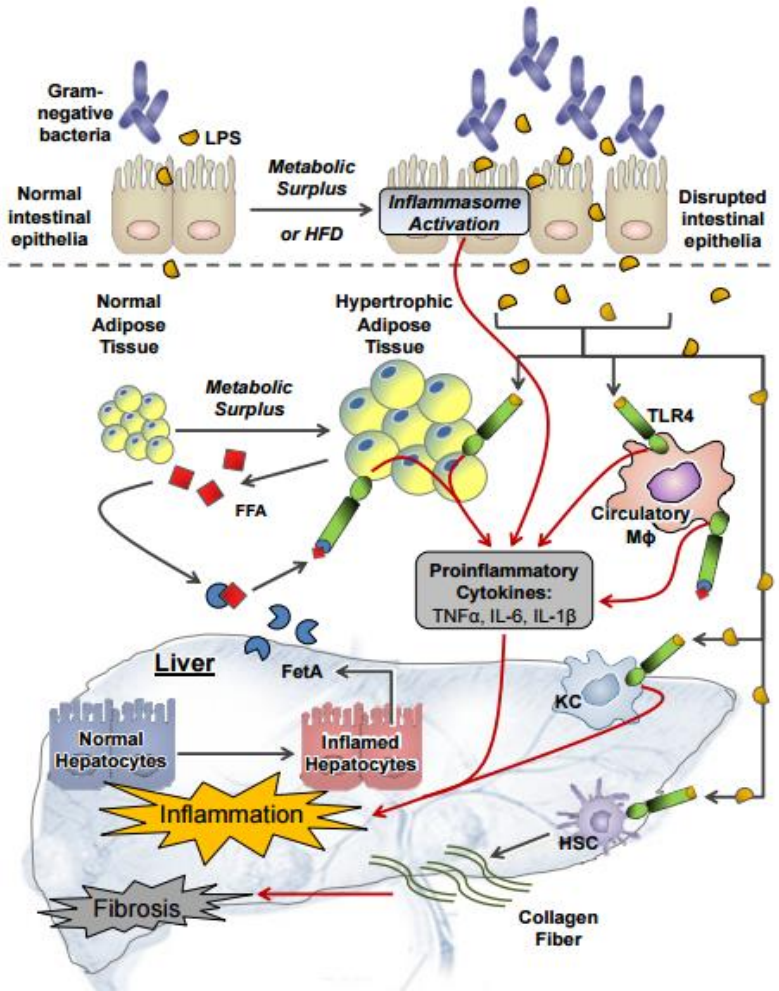


**Figure 17. Mechanisms of extra-hepatic perturbations in non-alcoholic fatty liver disease (NAFLD) progression. (Blanche. C et al, Nutrients, 2014)**

### 2.2.4.2.1 NASH

Non-alcoholic steatohepatitis (NASH) identify a histologically specific pattern of NAFLD. Most patients with NAFLD have increased steatosis alone, but others, develop as a more advanced stage, increasing hepatic inflammation known as NASH, and chronologically, up to 20% develop progressive hepatic fibrosis, cirrhosis and may eventually develop hepatocellular carcinoma **(Figure 18)**.

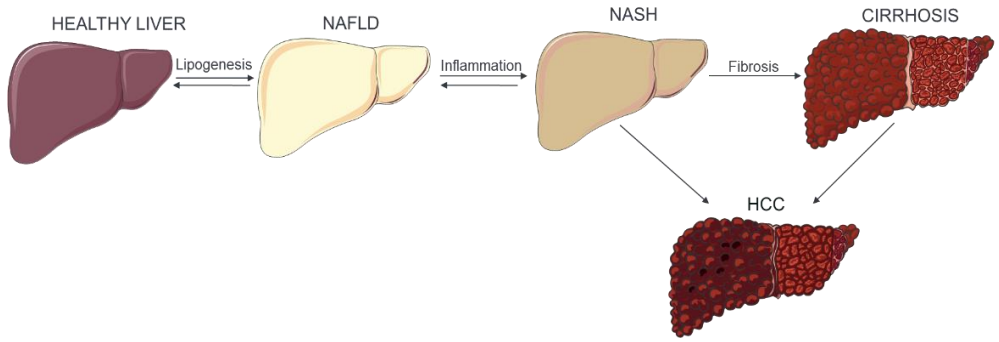


**Figure 18. Natural history of NASH/NAFLD-related cirrhosis and HCC**

Thus, NASH is considered the inflammatory form of NAFLD. It is characterized by steatosis, hepatocellular damage, known as ballooning, lobular inflammation and almost always fibrosis[102]. Initially, NASH disease was based in a two-hit hypothesis; based on the appearance of steatosis as a first hit and followed by inflammation, hepatocyte damage, and fibrosis as a second hit[103]. More recently, a multiparallel hypothesis was proposed [104]; it suggests that NASH is the result of numerous conditions acting in parallel, including genetic predisposition, abnormal lipid metabolism, oxidative stress, lipotoxicity, mitochondrial dysfunction, altered production of cytokines and adipokines, gut dysbiosis and endoplasmic reticulum stress [105],[106].

Although it seems clearly stepwise, NAFLD progression in humans is more dynamic than previously thought. Some patients appear to skip over the stage of cirrhosis and go straight from NASH to liver cancer, while others progress to liver cancer without developing notable fibrosis. Moreover, it is not clear why many individuals with 'benign' fatty liver disease never develop NASH. Thus, as more contributing factors are continuously identified, a more complex picture of NAFLD pathogenesis is emerging[107].

## 2.3 mRNA Translation

As the central dogma of molecular biology states, the expression of a protein is accomplished by the transcription of a gene into an intermediary messenger RNA (mRNA), which is then translated into the sequence of amino acids that will form the protein [108,109].

Translation of mRNA into a protein represents the last step in the expression pathway. As a general process, translation of mRNA occurs in the cytoplasm and contains the initiation, elongation and termination steps.

Translation initiation is the more complex of the three steps and involves no less than 25 proteins. It is commonly divided in the standard cap-dependent translation and in a cap-independent translation initiation. Cap specific sequence is region of all nuclear transcribed eukaryotic mRNAs present in the 5' mRNA that allows the binding of the factors responsible for the translation initiation. The other end is characterized by the presence of adenine residues (poly(A) tail).

Cap-dependent translation is based, in general terms, on the binding of the factor eukaryotic translation initiation factor-4F (eIF4F) in the cap region. eIF4F consists of the members eIF4A, eIF4E and eIF4G. This binding is the responsible of recruiting the 43S pre-initiation complex to the mRNA.
Translation starts when the eukaryotic ribosome, known as 80S complex, is formed and placed on the initiation codon (AUG)[110]. The small ribosomal subunit 40S forms a 43S pre-initiation complex that binds to the mRNA when recruits the ternary complex (TC). The TC is formed by the eukaryotic initiation factor 2 (eIF2, a heterotrymer of α, β and γ subunits) bound to GTP and a methionine-charged initiator tRNA (Met-tRNAi). Once recruited, this complex binds the mRNA and scans it until the initiation codon. At the initiation codon, the 43S complex is able to bind the mRNA through the interaction with eIF4E, which, at the same time is bound to the poly A tail in the 5'end. Following this recognition, hydrolysis of the eIF2-GTP takes place and most initiation factors are released. Subsequently, the large 60S ribosomal subunit joins and the catalytic competent 80S ribosome can start the elongation process. For the formation of the final complex is essential the interaction between the factor eIF4G and eIF4E and the 3' poly(A) tail-binding protein (PABP) at the poly(A) tail bringing both ends of the mRNA together in a closed-loop conformation[111,112] **(Figure 19)**.

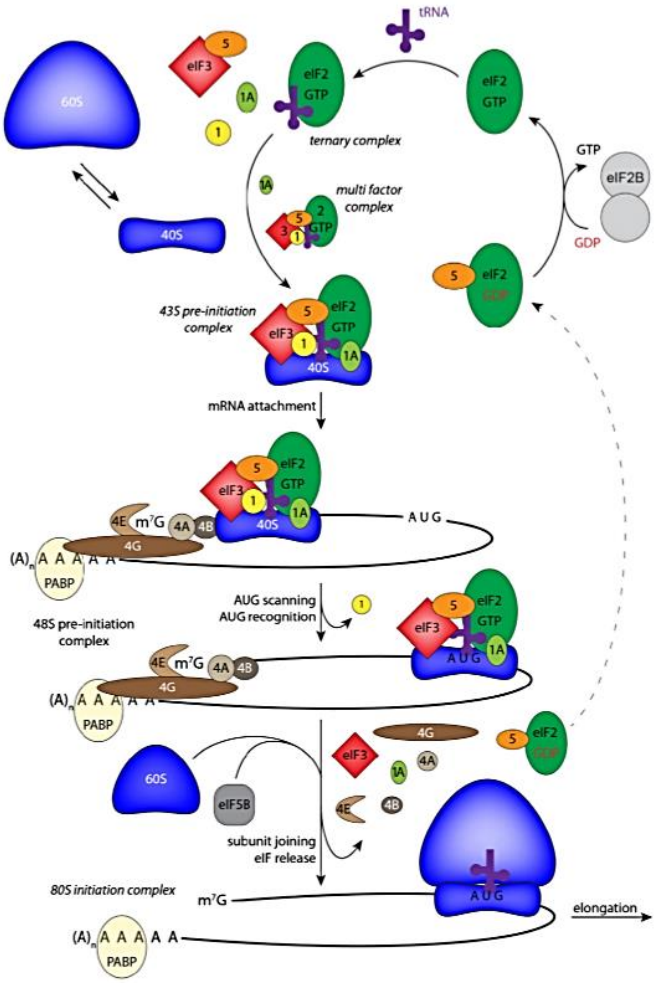


**Figure 19. Scheme of the different steps during cap-dependent translation initiation. (Leppek et al. 2018)**

However, one should not lose sight on the poorly studied alternative cap- independent way of recruiting mRNA to ribosomes. Some cellular transcripts rely on other elements such as internal ribosomal entry sites (IRES) to initiate their translation. IRES are RNA elements that, through their secondary structure or primary sequence, recruit the 40S ribosomal subunit independently of the cap-binding factor eIF4E[113].

Translation elongation involves the aminoacid addition in order to produce a protein chain. The ribosome selects the amino acid that must enter from a pool of 40 different

aminoacyl-tRNAs and the correct codon-anticodon pairing induces changes in the ribosomal structure, which contribute to its subsequent displacement on the mRNA. This process is performed by the 80S ribosome together with the elongation factors eEF1A and eEF2 and, of course, the cellular pool of charged tRNAs.

Translation termination is triggered when the ribosome arrives to a stop codon. Termination is mediated by two release factors (eRF1 and eRF3), which mediate the release of the synthesized peptide and the establishment of the post-termination complex. This complex facilitates the ribosome recycling by which the 80S ribosome splits into its 40S and 60S subunits to prepare for another round of translation. Ribosome recycling can also happen upon failure on the polypeptide synthesis, when damaged mRNA is encountered, or following the assembly of empty ribosomes. Moreover, the closed-loop structure of mRNAs can also favour the direct re-entry of ribosomes to the translation initiation point, enhancing mRNAs translation efficiency[114].

### 2.3.1 Translational regulation of mRNAs

Regulation of gene expression has long been believed to happen generally during transcription. Nevertheless, over the last decades translation regulation has risen in importance since there has been enormous progress in dissecting the molecular mechanisms of eukaryotic translation.

The regulation of translation is used to modulate gene expression in different biological situations and allows for more rapid changes in the concentration of the encoded proteins. Translational regulation is exerted mainly in the initiation step when the 40S subunit binds the ARNm. There are two general modes to control de translation at this point, a global and a specific control.

Global or general control is due to modifications of translation-initiation factors and regulates most mRNA of the cell. The eIF4E availability is used to regulate the general tax of translation since eIF4e needs to interact to eIF4G in order to ensemble the ribosome. eIF4E availability is regulated by 4E binding proteins (4E-BPs) phosphorilation **(Figure 20).** When 4E-BPs are hipo phosphorylated they bind eIF4E preventing in this way its interaction with eIF4G and consequently the union of the 40S with the mRNA and repressing the translation. On the contrary, when 4E-BPs are hyper phosphorylated by extracellular signals coming from mTOR pathway (a known regulator of 4EBP), 4E-BPs release eIF4 allowing the translation initiation.

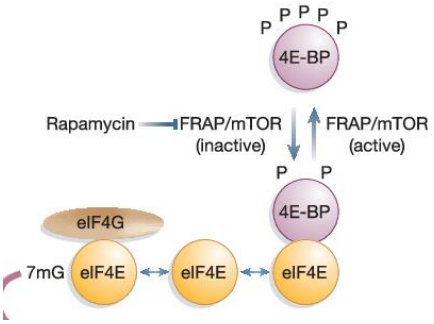


**Figure 20. General control of translation, (Richter J et al. Nature, 2005)**

The specific control is driven by complexes of proteins that recognize specific elements of the mRNA presents in the 5' or 3' UTRs of their target mRNAs without affecting the general synthesis of the protein in the cell. These proteins bind specific elements of the mRNA inhibiting eIF4E function therefore, regulating translation. These specific elements of the mRNA, which are responsible of its translational fate, include: canonical end modifications, internal ribosome-entry sequences, upstream open reading frames (uORFs), secondary and tertiary RNA structures and specific binding sites for regulatory complexes. Maskin represents an example of proteins that inhibit eIF4E through specific binding sites of the mRNA. Maskin interacts with cytoplasmic polyadenylation element binding protein (CPEB), a protein that binds specific sequences of the mRNA called cytoplasmic polyadenylation elements (CPE), enabling the regulation of translation through cytoplasmic polyadenylation **(Figure 21)**. The complex CPEB-Maskin-eIF4E inhibits specifically the translation of around 20% of the mRNA of the cell.

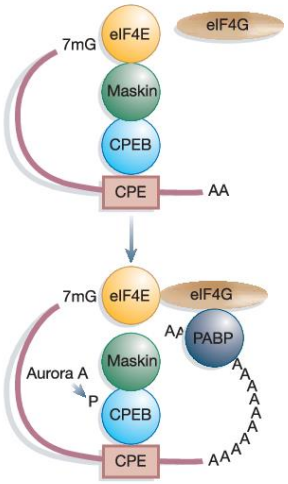


**Figure 21. Specific control of translation (Richter J. et al. Nature, 2005)**

Nevertheless, and although less frequent, translation regulation can also occur at the elongation step. For example, eEF2 phosphorylation by the eukaryotic elongation factor 2 kinase (eEF2K) reduces its affinity for ribosomes and therefore represses translation elongation. Among others, MAPK (mitogen-activated protein kinase) or mTOR signalling pathways can inactivate eEF2K in order to promote eEF2 elongation function[115]. Moreover, in recent years, further elongation-related regulatory mechanisms have emerged as new determinants of protein synthesis. Some examples would be acyl-tRNA availability and modifications, ribosome composition and function, or codon optimality [116,117].

### 2.3.2 CPEB- family of proteins

The family of cytoplasmic polyadenylation element binding proteins (CPEBs) introduced previously, is a key regulator of translation initiation.

CPEB family is formed by 4 different RNA binding proteins (from 1 to 4) with a double function, able to activate or repress the mRNAs they bind[118]. Importantly, bioinformatics analysis predict that 20% of human genome transcripts would be potential CPEBs targets [119,120] being CPEB-mediated translational control a widespread mechanism to regulate protein production.

CPEB paralogs can be classified into two subfamilies based on sequence identity: CPEB1 in one hand and CPEB2 to 4 on the other[111]. Structurally, they all share similarities. They contain a similar RNA-binding C-terminal domain (CTD) comprised of two RNA recognition motifs (RRMs) and a zinc-binding domain (ZZ domain). The N-terminal regulatory domain varies between paralogs [121]. The RRMs of CPEB2–4 share 97% sequence identity between them, while the RRMs of CPEB1 shares 48% pairwise sequence identity with those of CPEB2–4 [122,111]. Moreover, CPEB1 contain a PEST motif which mediate the destruction of the protein trough the proteasome **(Figure 22)**. These differences on their RRMs can confer certain specificities to the two subfamilies.

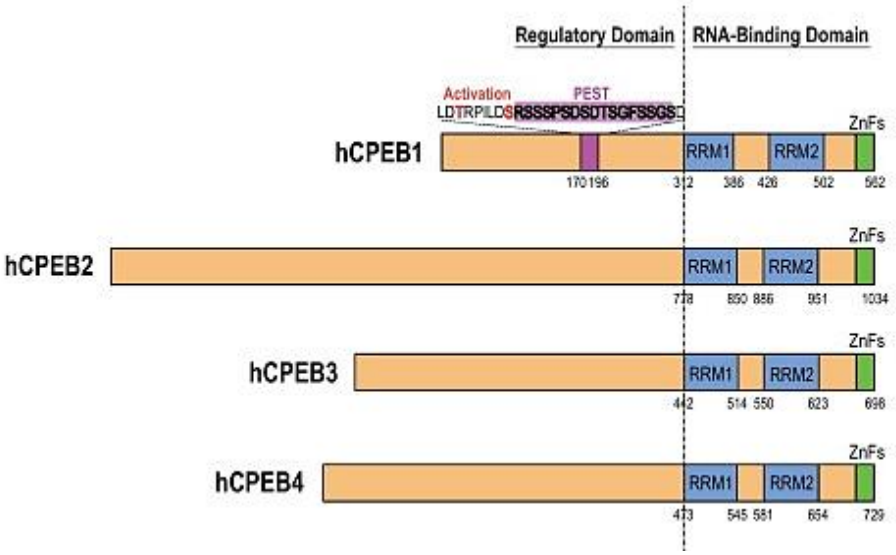


**Figure 22. CPEB family structure (Mendez R et al, Ageing Research Rewiew, 2012)**

#### 2.3.2.1 Translation regulation by CPEB

CPEBs are regulators of the translation in time and space specifically via cytoplasmic deadenylation and polyadenylation events. This binding is carried out through the cytoplasmic polyadenylation elements (CPEs). CPE is the most characterized sequence on mRNAs mediating cytoplasmic polyadenylation, even though few other sequences have been also proposed to mediate this process, but their contribution is still poorly understood[123].

Most of the eukaryote mRNAs leave the nucleus with a polyA tail of around 150-200 nucleotides. After nuclear export, CPEB proteins are able to bind mRNAs that contain sequences CPE and as a result, be translated by polyadenylation or deadenylated and repressed[124].

Importantly, the activation or repression of translation by CPEB is determined by the specific positioning of CPE elements in relation to the cis-acting elements hexanucleotide AAUAAA(Hex) as well as other elements in the target mRNA[118] .

For translation activation, CPEB has to bind the 3'UTR of the mRNA in the CPE element. Consequently, they get activated by different signal pathways discussed further below, such as Aurora A Kinase. Thus, being able to regulate the length of poly(A) tail by the recruitment of poly(A) polymerase proteins (PAP)[111,125]. As in nuclear polyadenylation, cytoplasmic elongation of the poly(A) tail is mediated by PAP, being PAPD4 (Gld2) the best characterized cytoplasmic PAP. Once elongated, it is recognized by the polyA binding protein ePAB, which, bounded to eIF4G stabilizes the union of eIF4F to the 5', enhancing the initiation of the translation by the 43S complex **(Figure 23).**

Regarding translational repression by CPEB the target mRNA must have at least two close CPEs elements[118]. The closeness of these two CPE elements support the formation of a CPEB dimer which would disrupt the complex cap-eIF4E-eIF4G-ePAB-poly(A) at different levels. First, it allows the recruitment of the deadenylase PARN which would shorten the poly(A) tail as well as the binding of ePAB. Subsequently, it represses the mRNA expression through the disruption of the necessary interaction between eIF4E and eIF4G. Many repression models have been described in the last years and many of them appear to be exclusive for each CPEB isoform. This fact leaves open the possibility of being all of them regulating different steps of the cycle.

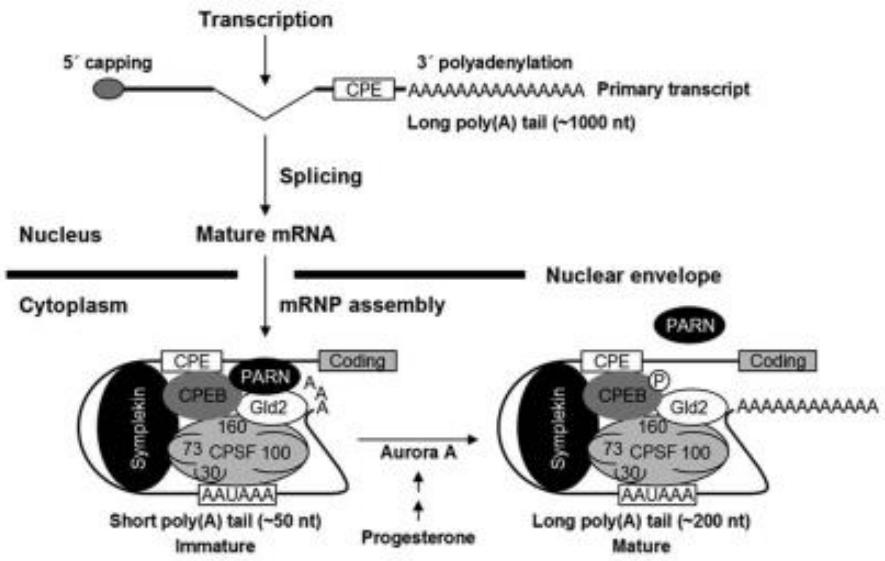


**Figure 23. Adapted from Translational regulation through polyadenylation. (Jong Heon Kim et al Handbook of Cell Signalling (Second Edition), 2010)**

### 2.3.2.2 Regulation mechanisms of CPEB activity

CPEBs are regulated through different mechanisms depending on the context they are found, and even depending on the paralog. Thus, even if their targets partially overlap, each CPEB might be performing opposite functions on them. CPEB functions can be modulated through activation by phosphorylation, by protein-protein interaction or by localization[121].

CPEB1 was the first member of the family whose regulation was discovered in several contexts. Its regulation was first discovered in oocytes of Xenopus where is regulated through two sequential phosphorylations[125]. When unphosphorylated, CPEB1 represses its mRNA target by recruiting PARN or by inhibiting the formation of eIF4F complex[111]. Upon phosphorylation by the aurora A kinase, CPEB1 increases its affinity for CPSF that displaces PARN and allows the polymerase GLD2 to extend the poly(A) tail[126,127]. The other CPEB forms do not have Aurora A union sites nor PEST boxes suggesting a different posttranslational regulation. Furthermore, CPEB1 has been found to control alternative 3'-UTR processing. CPEB1 shuttles to the nucleus, where it co-localizes with splicing factors and mediates shortening of mRNA 3' UTRs[128]. These altered 3'UTRs do not contain certain regulatory elements, thus changing the control of its translation.

CPEB2 was first discovered in mouse germ cells[129]. Although many functions have been attributed to this isoform in the last years, no post-translational modifications have been described so far[130,131,132,133]. Regarding its mechanism of action, it was proposed that CPEB2 repress translation by interacting with eEF2, inhibiting the elongation[134]. Its activity as activator of some target mRNA has also been proposed even though the mechanism of action is still unknown[135].

CPEB3 is generally repressed in normal conditions and its activity is dependent on an N-terminal region. It is activated in neurons by monoubiquitination enhancing GluA1 and GluA2 translation expression, crucial for the maintenance of long-term memory-related synaptic plasticity. Moreover, N-terminal cleavage or deSUMOylation can also switch its function and promote the translation of its targets[136,137,138]. Additionally, this switch on CPEB3 function also needs a change from a soluble to an aggregate CPEB3 state as a key mechanism of regulating this isoform[137,139].

CPEB4 known regulation is coordinated by phosphorylation through a CPEB1 dependent mechanism. As just reviewed, during cell cycle CPEB1 is activated by AuroraK-A leading to the translation of different mRNAs, among them CPEB4. Its activation by CPEB1, in turn, activate the kinases responsible for its hyperphosporylation, ERK2 and Cdk1. CPEB4 in its non-phosphorylated state was found to be stored in liquid-like droplets[140]. Moreover, it has also been proposed a role for CPEB4 during terminal erythroid differentiation where it would act as a repressor of translation[141].

Finally, it has also to be taken into account that CPEBs mRNA contain multiple predicted miRNA binding sites. Thus, miR-122 has been shown to control CPEB1[142] mRNA while miR-92 and miR-26 have been found as regulators of CPEB from2 to 4 mRNA stability[143].

#### 2.3.2.3 CPEB4 functions

During the last years CPEB specific functions have been extensively investigated in somatic tissues as well as in germinal cells. Among them, CPEB1 was the first member identified almost three decades ago, in Xenopus oocytes, as a key regulator of the translation of proteins implicated in the meiosis process[119]. Further on it was also elucidated its role in mitosis[120]. Discovering CPEB1 roles helped also to unveily many CPEB4 essencial functions in somatic cells in the last years.

All members of CPEB family were found to be required for cell cycle progression. CPEB1, 2 and 3 are essential to successful mitotic cell division whereas CPEB4 is necessary for

cytokinesis[144,120]. In addition to its crucial role in development, CPEB4 was also found to be important in pathologic situations.

CPEB4 has been implicated in many cancers as well as in tumorigenesis**.** CPEB4 is overexpressed in gliomas and pancreatic cancer[145]. In these tumours, CPEB4 was not strictly necessary for cell proliferation, but was found to act in a non-cell autonomous manner remodelling the stroma and favouring tumour vascularization and invasion. Interestingly in this context, CPEB4 was demonstrated to exert a role also in melanomas, controlling two lineage-specific melanoma drivers[146]. In breast cancer, CPEB4 promotes cell migration and also invasion upregulating the marker of endothelial-to-mesenchymal transition, vimentin[147].

Moving on from cancer to other pathologic scenarios, CPEB4s is found to be highly expressed in liver pathologies. During non alcoholic fatty liver disease, CPEB4 was found to coordinate hepatic unfolded protein response (UPR) activity[148]. In this same work a role of CPEB4 regulating the lipidic mechanism in the hepatic steatosis was found, suggesting that CPEBs could be involved in the negative effects of obesity in liver disease. Concerning also liver diseases, the translation mediated by CPEB1/CPEB4 was identified as an essencial mechanism for the pathologic angiogenesis in the mesentery and liver during portal hypertension and chronic liver disease [149]. CPEB4 activation through CPEB1 phosphorylation regulates the proangiogenic VEGF overexpression during cirrhosis. Besides the angiogenic process, CPEB4 expression increase upon portal hypertension has been found to correlate spatiotemporally with vascular stem progenitor cells expansion and neovascularization[150]. Moreover, our group recently found another CPEB4 role in activated hepatic stellate cells during liver disease. The driver of glycolisis PFKFB3, was shown to be overexpressed in activated HSC thanks to posttranscriptional regulation by CPEB4[151].

Yet, CPEB4 functions do not end in the liver. Recently, CPEB4 has been related to the autism syndrome, regulating risk genes of the disease. In this scenario, patients suffering autism disorder expressed a high percentage of an specific isoform of CPEB4 mRNA[152]. This specific isoform entails a reduction of the polyA tail and subsequently reduces the expression of those genes of risk.

Concerning neuronal system, CPEB family are widely expressed in the brain, being CPEB4 necessary for hippocampal neuronal cell survival. It likely regulates mRNA processing required for neuroprotection against cellular stress[153].

Thus, it is reflected how CPEB functions are important in many crucial pathologic processes.

# OBJECTIVES

# 3 Objectives

Despite constant progress in the field, the management of patients with chronic liver disease remains an important and frequent clinical problem, for which there are few therapeutic options available. Among the broad range of aetiologies, a very important risk factor for the development of chronic liver disease is the global epidemic of obesity/overweight, which has become a major societal challenge and is alarmingly affecting the world population. Obesity leads to non-alcoholic fatty liver disease (NAFLD) and its more severe form non-alcoholic steatohepatitis (NASH). Both are strong risk factors for liver fibrosis, cirrhosis and ultimately liver cancer.

The pathogenesis of NAFLD is not fully understood, and the factors that contribute to disease progression from steatosis to NASH remain enigmatic. Previous studies on NAFLD have almost exclusively focused on the liver, leaving aside its extrahepatic manifestations, which may play a major role in the evolution and aggravation of the disease.

Indeed, NAFLD is strongly associated with abdominal obesity and may be further complicated by the wide spectrum of splanchnic disturbances characteristics of liver disease. Growing evidence suggests that adipogenesis and inflammation in specific depots of white adipose tissue (WAT) has a key role in NAFLD progression, but experimental evidence for the involvement of WAT and the underlying mechanisms is still lacking. Filling this knowledge gap is imperative to have a deeper understanding on liver disease and improve human health.

Thus, this thesis started with the need to understand more precisely the functional and therapeutic implications of obesity-induced inflammation in WAT on the development and severity of NAFLD. Our hypothesis was that posttranscriptional reprogramming mediated by the RNA-binding protein CPEB4 could regulate common mechanisms involved in the pathogenesis of obesity and chronic liver disease comorbidities, such as inflammation. We therefore, set ourselves two principal objectives with their specific goals.

**1. To characterize the influence of obesity in the progression of chronic liver disease**

1.1 Determine if the obesity-related disturbances create a pathogenic microenvironment in the splanchnic organs that increases the predisposition and severity of chronic liver disease.

1.2 Study specifically the behaviour of adipose fat pads in the presence of obesity driven liver disease.

**2. To unveil the contribution of Cytoplasmic Polyadenylation Element Binding Protein 4 in obesity driven NAFLD**

2.1 Characterize CPEB4 expression in adipose tissue.

2.2 Understand the relevance of CPEB4 in pathologic adipocytes during obesity.

2.3 Determine the contribution of CPEB4-mediated translational control on the adipocyte development.

2.4 Determine the contribution of CPEB4 in the angiogenesis and inflammation processes that take place during adipose tissue expansion.

2.5 Define CPEB4 target mRNAs in adipocyte during obesity-inflammation.

# MATERIALS & METHODS

# 4 Materials & Methods

### Animal studies

Sprague-Dawley rats were purchased from Charles River Laboratories at the age of 6 weeks old. Ubiquitous and constitutive depletion of CPEB4 mice were obtained by crossing CPEB4lox/lox mice with animals expressing DNA recombinase Cre under control of a human cytomegalovirus minimal promoter (B6.C-Tg(CMV-cre)1Cgn/J). Excision of exon-2 of CPEB4 gene leads to a frame shift in the mRNA generating several new premature stop codons, resulting in mice that are deficient in CPEB4 protein (CPEB4KO). Myeloid-specific Cpeb4 KO mice (Cpeb4MKO) were generated in the Raul Mendez Lab crossing conditional Cpeb4 knockout animals (Cpeb4lox/lox) with LysM-CreT/+ transgenic animals obtained from Jackson Laboratory. Both offspring were maintained in a C57BL/6J-129S mixed background.

Both male rat and mice were grouped randomly into a 60% High fat diet (0% fat, 20% protein, and 20% carbohydrate; Research Diets Inc, USA) or Control diet (7.42% fat, 17.49% protein, and 75.09% carbohydrate; Research Diets Inc, USA) group and fed ad libitum for a period of 16 weeks beginning at 6 weeks of age. For the Cpeb4MKO diet was administered for 15 weeks. In the Sprague-Dawley rats case, after these period all animals were randomly subjected to a partial portal vein ligation (n=26) or a sham control operation (n=26).

All animal studies were approved by the Laboratory Animal Care and Use Committees of the University of Barcelona, and were complied with the National Institute of Health (NIH) guidelines on handling of experimental animals.

### Animal model of portal hypertension

Portal hypertension was induced in male BALB/c mice and in Sprague-Dawley rats by partial portal vein ligation (PPVL). Briefly, under isoflurane anaesthesia a midline abdominal incision was made. The portal vein was dissected free of surrounding tissue, and a loose ligature of silk suture (size 3.0 for rats and 5.0 for mice) was guided around it. A blunt-end needle (20G in rats, 27G in mice) was placed alongside the portal vein, and a suture was tied snugly around the portal vein and needle. The needle was subsequently removed to yield a calibrated constriction of portal vein. In Sham control animals the portal vein was similarly manipulated but not ligated. After 7 days post-surgery, animals were sacrificed. All animal studies were approved by the Laboratory

Animal Care and Use Committees of the University of Barcelona, and were completed with the National Institute of Health (NIH) guidelines on handling of experimental animals.

**Hemodynamic studies**

Rat hemodynamic studies were performed under anaesthesia with ketamine (100 mg/kg) and midazolam (5 mg/kg). PE-50 catheters were introduced into the femoral artery and portal vein to measure mean arterial pressure (mmHg), heart rate (beats/min), and portal pressure (PP, mmHg). Perivascular ultrasonic flowprobes (Transonic Systems, New York, NY) were placed around the superior mesenteric artery (SMA) to measure SMA blood flow (SMABF, ml/min21/100g21), and portal vein to measure portal vein blood flow (PVBF, ml/min21/100g21). Portohepatic resistance (mmHg/ml21/min21/100g21) was calculated as: PP/PVBF. Portosystemic shunting was quantified by injection of yellow microspheres (15 lm diameter, Dyetrak, Triton Technologies, San Diego, CA) into the spleen, as collateralization (%)5(lung microspheres)/ (lung microspheres1 liver microspheres)x100.

**Stromal Vascular fraction isolation**

Epididymal fat pads from male C57BL/6 mice fed with normal diet or high-fat diet were excised and minced in Krebs-Ringer (2x) with 1% FAF-BSA and 2mM EDTA. Tissue suspensions were centrifuged at 500*g* for 5 min to remove free erythrocytes and leukocytes. Collagenase A (Sigma-Aldrich) was added to 1 mg/ml before incubation at 37°C for 30 min with continuous shaking. The cell suspension was filtered through a 100-µm nylon filter and spun at 300*g* for 5 min to separate top mature adipocytes from the stromal vascular fraction (SVF) pellet. The SVF pellet was re-suspended and incubated in 4 ml erythrocyte lysis buffer (0.15M NH4CL, 10mM KHCO3, 0.1 mM EDTA) for 5 min. Cell suspension was filtered with a 40um nylon mesh and centrifuged at 500g for 5 minutes, previous final resuspension in sorting buffer (PBS with 1% fetal bovine serum, 1 mmol/l EDTA, and 25 mmol/l HEPES).

**Flow cytometry**

SVF from mice eWAT was isolated as described above. Pellet was counted and incubated with Fc Block (BD biosciences) at a concentration of 1ug/106 cells for 5 minutes at 4ºC before staining with conjugated antibodies or their corresponding IgG controls for 30 minutes at 4ºC. Abs used in these studies included: BV-711 anti-mouse CD11c, eFluor 450 anti-F4/80 (clone BM8), PE- anti CD206 (MMR) (cloneMR6F3), APC- CD11b (clone M1/70). Additionally, fluorescence minus one and single stain controls were carried out for all experiments in order to gate and compensate. After incubation with primary Abs, cell suspensions were washed in 2 ml of sorting buffer and centrifuged at 500 × *g* for 5 min. Cells at a concentration of 250.000/condition were suspended in 0.3 ml sorting buffer and analysed by flow cytometry with a BD FACSDIVA5 cytometer and FACSDiva v6.1.3 software (BD Biosciences, San Jose, CA). Live/Dead Near-IR (Termofisher) was used to exclude dead cells. Each sample was obtained from a pool of 5 to 8 mice (WT or KO).

**Cell Lines**

3T3-L1 preadipocytes were maintained and propagated in DMEM (Gibco) supplemented with 10%(v/v) new born calf serum (Sigma). Two days post-confluent (day 0) cells were induced differentiation with DMEM containing 10% (v/v) FBS (Reactiva) and 0.5mM IBMX, 1uM dexamethasone, 10ug/mL insulin and 2uM rosiglitazone until day 2. Cells were then cultured with DMEM supplemented with 10% FBS(v/v) and insulin (10ug/ml) for 3 days. After the differentiation period cells were cultured with DMEM containing 10%FBS and 1% Penicillin/streptomycin. When indicated cells were treated with FFA 500uM (300uM of Palmitic acid, 100uM Oleic Acid and 100uM Linoleic Acid).

**Preparation and treatment of fatty acid–albumin complexes**

Saturated palmitic acid, linoleic acid and monounsaturated oleic acid were used in this study. Lipid-containing media were prepared by conjugation of FFA with 2% BSA- fatty acid free at a final concentration of 500uM (300uM Palmitic Acid, 100uM Oleic Acid, 100uM Linoleic Acid). The complex of fatty acid and FAF-BSA was prepared by dissolving and heating (70ºC) the different fatty acids with EtOH to a stock solution. The stock solution was sterile filtered and stored in dark at-20ºC. The stock solution was heated before use in the cellular experiment. The day prior to the treatment cells were incubated Overnight with DMEM 0,2% fatty acid free- BSA.

**Adenoviral infection**

To generate 3t3-L1 CPEB4 KD cell lines, short hairpin RNA (shRNA) encoding sequences were delivered to the cell line through lentiviral infection. Lentivirus were produced by transfection of HEK293 packaging cells with the plasmids psPAX2 (Addgene, Watertown, MA), pCMV-VSV-G (Addgene) and pLKOPuro-IPTG-3xLacO (Sigma), using the liposome-based DNA transfection reagent LipoD293 (SignaGen, Rockville, MD). The inducible pLKO-Puro-IPTG-3xLacO vector carried a sequence specific for CPEB4 short hairpin RNA (shRNA) expression (5'-GCTTGTAGGTGGCTTGGGGTG-3') or a scramble control sequence (5'-GCGCGATAGCGCTAATAATTT-3'). This vector contained a LacI (repressor) 1 2 3 4 5 6 7 8 9 10 11 12 13 14 15 16 17 18 19 20 21 22 23 24 25 26 27 28 29 30 31 32 33 34 35 36 37 38 39 40 41 42 43 44 45 46 47 48 49 50 51 52 53 54 55 56 57 58 59 60 61 62 63 64 65 8 and a modified human U6 shRNA promoter with three LacO (operator) sequences, affording both tight regulation and great gene silencing. In the absence of isopropylβ-D-thio-galactoside (IPTG), an analogue of lactose, LacI binds to LacO preventing expression of the shRNA. When IPTG is present, the allosteric LacI repressor changes conformation, releasing itself from LacO-modified human U6 promoter, and subsequently allows expression of the shRNA. Media from transfected HEK293 cells were removed and replaced with fresh media every 24 hours. At 72 hours post-infection, media (containing the lentivirus but not the packaging cells) were harvested, filtered through a 0.22 μm filter and used to infect LX2 cells grown on 6- cm dishes. Efficiently transfected 3T3-L1 cells were selected with 4 μg/ml puromycin to create stable CPEB4 knockdown 3T3-L1 cells inducible with 1 mM IPTG.

**Primary adipocytes isolation from murine visceral adipose tissue**

White adipose tissue was isolated from the mouse epididymal depots. Adipose tissue from 2 to 3 mice were pooled and carefully minced and treated with collagenase (type II; Sigma). Several centrifugations and filtrates were carried out in order to separate the SVF from mature adipocytes. Mature adipocytes were discarded and the SVFs where the preadipocytes were present was plated and induced to undergo in vitro differentiation to adipocytes. Pellets containing the SVFs were suspended in 4 ml DMEM/animal for all tissues and seeded in six-well plates (2 ml cell suspension/10 cm2 /well; Corning). Medium was changed 1 day after seeding and subsequently every second day. Two days after cells reach confluency differentiation was induced by addition of the induction media. Differentiation-inducing medium consisted of Dulbecco modified Eagle medium (DMEM)/F12 (Sigma), 10% FBS, 10mg/ml insulin, 1mM Dexamethasone, 25mM IBMX,

6mM Indomethacin, 5% penicillin-streptomycin. Cells of SVF were cultured at 37°C and 8% CO2. After 48h induction media was replaced with maintenance medium for 7 to 10 days.

**Isolation of BMDM**

BMDM from 10-15 week-old mice were obtained from the femurs and tibias of C57Bl/6 mice as described [154].Briefly, bone marrow is flushed out from the mice femur and the tibia with a 26-gauge needle. Bone marrow cells are harvested and cultured with DMEM containing macrophage colony–stimulating factor (M-CSF, Preprotech, 20ng/mL) in non-treated p150 plates. After 7 days in culture, contaminating non-adherent cells are washed and eliminated while adherent cells are harvested for assays. Adherent bone marrow–derived macrophages are usually better than 90% pure.

**Scratch/ Wound Healing migration assay**

On day 1 isolated BMDMs were seeded in the ibidi Culture-Inserts at a concentration of 80.000cells/insert. Cells were kept in medium without serum OVN. On the next day cells were treated with Mitomycin 10ug/µL for 1h at 37ºC. Inserts were then removed and the conditioned medias from 3T3-L1 cells lines were added to each BMDM condition. Pictures were taken at time 0 and 24h with AXioCAm MRc5 Zeiss. Cell migration was quantified by counting the number of cells that had invaded the scratch at 24 h, considering the reference area at time 0 h. Experiment was performed in triplicate.

**Transwell chamber migration assay**

Chamber migration assays were performed using 0.47 cm2 Transwell inserts with an 8 µm pore size membrane (#140629, Thermo Scientific). Conditioned media from adipocytes treated with FFA for 24 h, medium containing 200 ng/ml MCP-1 (Biolegend, San Diego, CA) as positive control, or low-serum DMEM as negative control were placed in the lower chamber. One hundred thousand bone marrow-derived macrophages were suspended in DMEM medium containing 0.1% serum and seeded in the upper part of the chamber. Cells were incubated at 37°C and 5% CO2 for 3 hours. Cells that had not migrated and remained in the upper chamber were removed by gently swiping the membrane with cotton tips. Cells that migrated were fixed with 2.5% glutaraldehyde, permeabilized with 0.5% Triton-X-100 and stained with 0.1% crystal violet. Images were

taken using a DMR inverted microscope. The amount of cells that migrated was quantified from 6 fields of 10x magnification/condition using fluorescence microscope. The experiment was repeated twice.

**Human samples**

Human liver tissue of patients suffering from NAFLD and NASH (*n* = 62) was obtained during bariatric surgery at the St. Franziskus-Hospital in Cologne. The ethics committees of the North Rhine-Westphalian Chamber of Medicine (no. 2017110) and of the University Hospital Bonn (no. 194/17) approved the study. Experienced liver pathologists analyzed the biopsies, and Kleiner score was calculated based on histopathomorphology. NAFLD patients included in this publication had a Kleiner score of 3–4. Subjects belong to obese NAFLD (n=15), obese without NAFLD (n=12) and NASH (n=14) groups. Adipose tissue samples from vWAT were obtained during bariatric surgical procedures. All subjects gave written informed consent Samples were frizzed at -80ºC and proceed to extract protein and RNA. Control Samples (n=10 /BMI<25) and data from patients included in this study were provided by the FATBANK platform promoted by the CIBEROBN and coordinated by the IDIBGI Biobank (Biobanc IDIBGI, B.0000872), integrated in the Spanish National Biobanks Network and they were processed following standard operating procedures with the appropriate approval of the Ethics, External Scientific and FATBANK Internal Scientific Committees.

RNA was prepared from samples using RNesay Lipid Tissue Mini Kit (quiagen). Concentration was determined using NanoDrop 100 (Thermo Scientific).

**Histologic analysis & Immunohistochemistry**

Liver and Epididymal fat pads were collected and fixed in formalin overnight. After paraffin embedding 5µm thick cuts were obtained and stained on Hematoxylin & Eosin entire epididymal fat pad cross-sections or leave it for immunostainings.

For measuring adipocyte area, magnification was at 10x and a digital slide scanner was used to digitalize the image. Images were then imported for computer-assisted quantitative image analysis using ImageJ software (version 1.34s; National Institute of Health, USA). Pictures were converted into a binary black and white images (8-bit; grey scale). The ‘watershed’ function was used to mark the boundaries of individual fat clumps. The ‘analyze particle’ command was used to measure clump numbers and areas

with 'cellularity' set at 0.70– 1 and 'size' set at 500-infinity. The command 'measure all' was used to automatically generate all measurements.

For immunostainings 5µm paraffin sections were deparaffinised in Xylol and rehydrated in graded alcohol series after the staining. For epitope retrieval, sections were boiled in a streamer for 30min in citrate or EDTA buffer. Endogenous peroxidase was inhibited using 3%$H_2O_2$ and blocked with 5% goat serum for 1h at RT. Slides were incubated OVN with the following primary antibodies (CD68 ab125212 1.100 ,CD31 ab28364 1.50). Washing of the sections was performed with PBS previous to the incubation with the secondary DaKo Real EnVision Detection System for 30min at RT. Antibody binding was revealed using hydrogen peroxide as a substrate and diaminobenzidine as a chromogen. Haematoxylin was used as a counterstain. For negative control, primary antibody was omitted and then sections were incubated with the corresponding secondary antibodies and detection systems. Tissue samples were scanned in the Nanozoomer 2.0HT of the histopathology facility of the IRB. Scanned sections were visualized with the NDP.view2 Viewing software.

**Quantification of circulating triglycerides**

Triglycerides from mice serum were analysed using the automated clinical chemistry analyzer FUJI DRI-CHEM 4000V (Fujifilm, Japan). Triglycerides (TG) between the range of 10 to 500 mg/dl were obtained by using a total sample volume of 10µl of mice serum. The slide is incubated at 37ºC for 6 minutes and the optical density is measured at 650nm, converting the optical density into triglyceride concentration using an already preinstalled reaction.

**Quantification of Liver triglycerides**

Frozen tissue was weighted and suspended in 9X PBS (137 mM NaCl, 10 mM Phosphate, 2.7 mM KCl at pH= 7.4). 300mM Methanol, 700mM Chloroform and 100mM H2O were added to the mixture and centrifuged at 12000rpm for 10 minutes. Supernatant was mixed with premixed 1/5 dilution of Triton-100 and Chloroform. Resulting mix was dried overnight (o/n) with a dry-vacuum and suspended the next day with 100ul H2O. Finally, Triglycerides Reagent Set (Pointe Scientific Inc., USA) was added on each sample and measured using Epoch microplate spectrophotometer (BioTek, USA). Triglyceride content was measured using a standard regression curve.

**ELISA**

MCP-1 levels in epididymal adipose tissue were determined by a specific sandwich ELISA by using capture/biotinylated detection antibodies obtained from Peprotech (London, UK) according to the manufacturer's recommendations. IL-10 was measured using the Multiplex Assays techonolgy (Merck) based on Luminex technology.

**RNA extraction and gene expression analysis**

Total RNA was isolated and purified from mouse tissue and cells using RNAspin Miki Kit (Quiagen). RNA was reverse transcribed with Quantitect Reverse Transcription Kit

The synthesized cDNA was then amplified by real-time TaqMan PCR using mouse CPEB4 (), PPArgamma (Mm00440940_m1), CBEPα Mm00514283_s1) GLUT4Mm00436615_m1), IL-6(Mm00446190_m1), IL-10(Mm01288386_m1), ACTB (Mm02619580_g1), HPRT (Mm00446968_m1) Human CPEB4 (Hs03929097_g1) TaqMan Gene expression assays (Thermo Fisher Scientific), in an ABI PRISM 7900 Sequence Detection System (Applied Biosystems, Foster City, CA). All PCR reactions were performed in duplicate, using nuclease-free water as control. Resulting expression levels of the mRNA of interest gene were normalized to endogenous control βactin and, or HPRT expression, which was unaffected in the different treatment groups.

**Immunoblotting**

Protein extract was obtained from frozen tissue homogenized or cells with cold RIPA lysis buffer (Sigma; R0278) supplemented with a protease and phosphatase inhibitor cocktail (Thermofisher, Waltham, MA; 78440). In the case of cells, lysates were sonicated previous to centrifugation to obtain total protein extract. Protein concentration in the resultant lysates was measured using the Bradford Protein assay (BioRad, Hercules, CA). Equal amounts of protein (10-25 μg) were heated (95ºC, 8 minutes) in sample buffer containing sodium dodecyl sulfate (SDS) and βmercaptoethanol. Samples were resolved in different acrylamide percentage gels for SDS-Page and were subjected to immunoblot analysis in 0,45 μm pore size PVDF membrane (Sigma-Aldrich, USA).

The following monoclonal and polyclonal antibodies were used: CPEB4 (ab83009, Abcam), VEGF (ab1316, Abcam), CD68 (ab125212, Abcam), CD206 (ab64693, Abcam) TNFα (ab66579, Abcam), TLR4 (sc-293072, Santa Cruz), IL1b (sc-1252, Santa Cruz) PCNA ( NA03, Calbiochem), FLK1 (sc-315, Santa Cruz), iNOS (BD610432), CD163 (sc-59865,

Santa Cruz), GLUT4 (novus biological, NBP1-49533SS) C/EBPa (sc-365318, Santa Cruz), PPARγ (sc-7273, Santa Cruz), GLUT4 (Novus Biological, NBP1-49533SS), Perilipin-1 (#9349, Cell signalling), pHSLSer565 (#4137, Cell signalling) pHSLSer660 (PA5-64494, Thermo Fisher), VEGFA (ab46154, Abcam). GAPDH (sc-32233, Santa Cruz), β-actin (A2228, Sigma) and tubulin (T9026, Sigma) were used as loading controls. Proteins were then detected using horseradish peroxidase-conjugated secondary antibodies (Stressgen) at 1:10.000 and the enhanced chemiluminescence detection system ECL (GE Healthcare). Quantification of protein signals was performed using computer-assisted densitometry.

**Immunofluorescence**

Tissue sections (5µm) were deparaffinised, and antigen retrieval and blocking were performed as described in the immunoblotting section. Primary antibody Perilipin 1 (#9349S cell signalling 1.200) was used and incubated overnight 4ºC. For fluorescence visualisation of antibody reactions, Perilipin 1 primary antibody was detected using secondary antibody labelled with the fluorochrom Alexa Fluor (Alexa anti rabbit-488, Invitrogen). To detect Isolectin B4 an already conjugated antibody was used (Isolectin GS-B4 Alexa fluor 646 (132450 life technologies). To detect cell nuclei, tissues were counterstained with DAPI (Vector Laboratories) for 1 minute and mounted with Fluoromont mounting media. Negative controls were run omitting the primary antibody and incubating with secondary antibodies labelled with the fluorochromes Alexa Fluor. Images were obtained from slide scans. Scanned was performed in the Nanozoomer 2.0HT of the histopathology facility of the IRB. Scanned sections were visualized with the NDP.view2 Viewing software and analysed with the QuPath 2.0 software using the positive cell detection command.

**Statistical analysis**

Data are shown as mean±SEM. Results that were normally distributed ($P>0.05$ from Kolmogorov-Smirnov test) were compared with parametric statistical procedures (Student t test and ANOVA followed by Bonferroni´s test for multiple comparisons). Non-normally distributed results were compared with non-parametric tests (Kruskall-Wallis one-way ANOVA and Mann-Whitney-U test). Significance was accepted at $P<0.05$. All cell culture experiments were performed at least 3 times.

# RESULTS

# 5 Results

## 5.1 Obesity impact in liver disease lies not only in the liver but also in the splanchnic territory

To study the extrahepatic impact of obesity on liver disease we generated a model with Sprague Dawley rats of 6 weeks of age fed with high fat diet (60% Kcal of fat) or normal diet (13% kcal of fat) for 16 weeks. After this period, both groups were randomly subjected to a partial portal vein ligation (PPVL) or to a faked surgical operation (Sham). We used the PPVL model to mimic the extrahepatic alterations of chronic liver disease. All groups were studied 7 days after surgery **(Figure 1A)**.

As expected after 16 weeks of diet, high fat diet fed rats exhibited a significantly increased body weight compared to the normal diet fed rats **(Figure 1B)**. This increase correlated with a higher energy intake and a lower food intake in the HFD fed group compared to their normal diet controls **(Figure 1D)**. Moreover, measurement of body weight one week after surgery did show also a significant increase in the HFD-PPVL rats compared to their control ND PPVL rats, suggesting a possible exacerbation of the adiposity by the PPVL hit **(Figure 1C).**

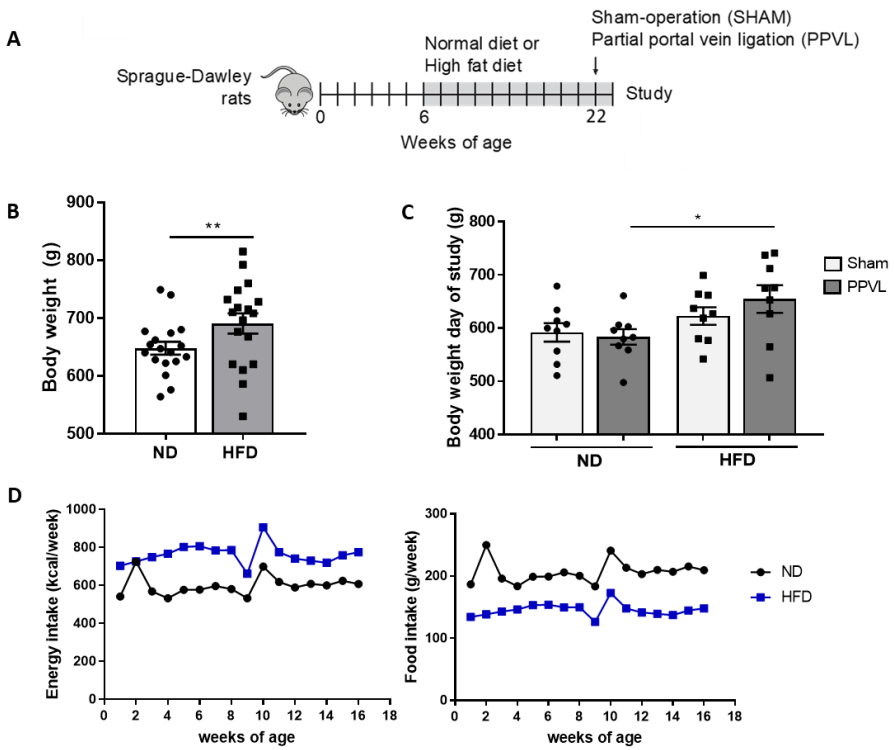

**Figure 1. Phenotypical characterization of the NAFLD model in rats. (A)** Schematic representation of the NAFLD model protocol used in Sprague-Dawley rats. **(B)** Body weight profile on Normal diet (n=18) vs High fat diet fed animals (n=18) after 16 weeks of HFD exposure. *p<0.005 versus Normal Diet. **(C)** Body weight profile on ND vs HFD fed animals after one week of surgery (partial portal vein ligation, PPVL or sham operation, Sham) (n=9/condition/diet). *p<0.05 versus ND-PPVL. **(D)** Energy and food intake profile during the 16 weeks of control diet feeding. All studies were conducted in rats at 22 weeks of age after 16 weeks of diet. Statistical analysis was performed by t-student test. All results are expressed as mean ± SEM.

Since liver disease is highly characterized by hemodynamic disturbances, we first measured the hemodynamic parameter behaviour after a PPVL plus a high fat diet insult. As expected, portal pressure (PP), superior mesenteric artery blood flow (SMBF) and portosystemic shunting were significantly increased in the portal hypertensive rats without relevant effects of the diet on the portal hypertensive group **(Figure 2A and B)**. Moreover, neither PPVL surgery nor the high fat diet produced a systemic effect as reflected by no significant differences in the mean arterial pressure (MAP) values **(Figure 2D).**

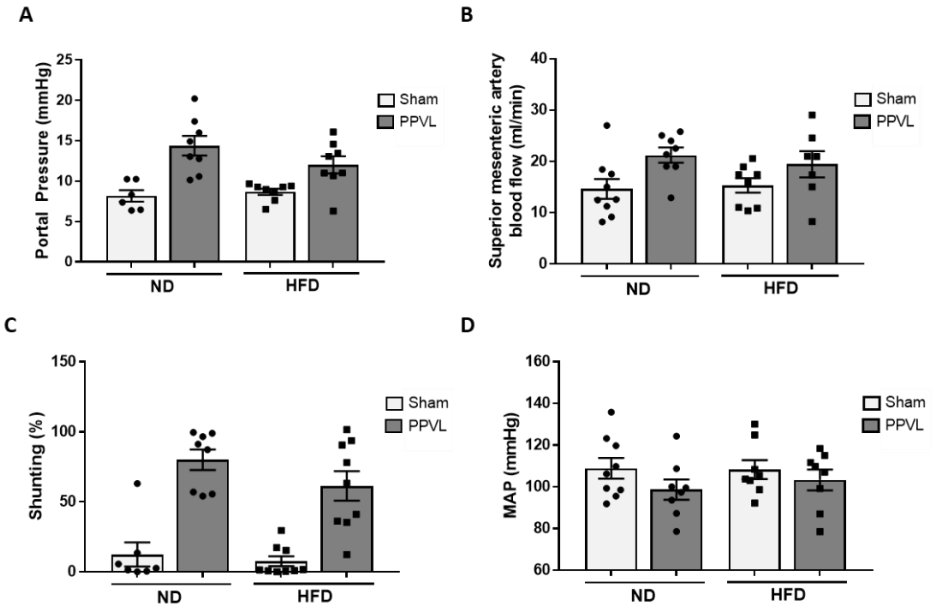


**Figure 2. Hemodynamic effects of the combination of HFD and PPVL in rats. (A and B)** Effects on the portal pressure and the superior mesenteric blood flow of ND-PPVL (n=7-8), HFD Sham (n=8-9) and HFD-PPVL animals (n=8-9). ND fed Sham animals were used as a control grup (n=6-9). **(C)** Portosystemic shunting. **(D)** Effect of both liver disease induction and high fat diet feeding on the mean arterial pressure. All results are expressed as mean ± SEM.

To further characterize the model, we put our focus into the extrahepatic territory, specifically on the adipose tissue. We sought to determine if the fat depot behaviour under a HFD exposure changed after the induction of the liver disease. As expected, HFD fed rats showed more adiposity exhibited by bigger white adipose tissue depots. Total visceral fat pat weight slightly increased in the PPVL obese rats compared to the obese Sham group without reaching significance **(Figure 3A)**. When dissecting the different white fat pads, mesenteric and epididymal fat depots showed a tendency to present heavier fat depots, contributing to the final increase of the WAT **(Figure 3B).**

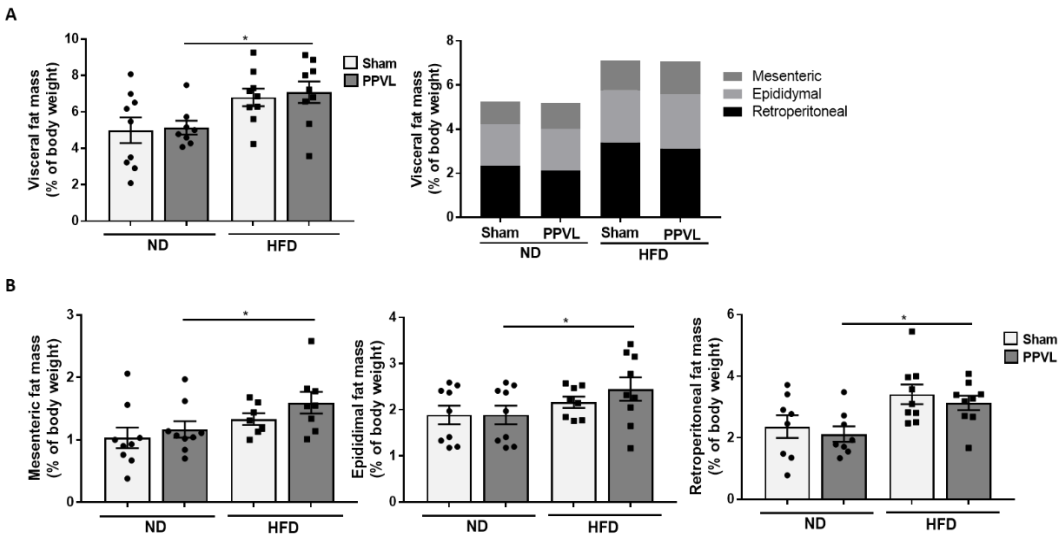


**Figure 3. Increased adiposity of white fat depots on PPVL mice fed with HFD for 16 weeks. (A)** Total WAT weight derived from epididymal, mesenteric and retroperitoneal white adipose tissues from LFD or HFD fed rats under a Sham or PPVL operation. **(B)** Mesenteric, epididymal, and retroperitoneal individual fat pad weight. All results are expressed as mean ± SEM.

## 5.2 The pathogenesis and severity of the extrahepatic manifestations of liver disease is exacerbated in an obesity situation due to an increased proliferation and inflammation of the adipose tissue

To further dissect the adipose tissue phenotype and behaviour in our model, we deeply investigated the mesenteric and epididymal adipose tissues. As extensively reported, adipocyte hypertrophy prevails in obesity. Thus, staining of mesenteric and epididymal adipose tissue on HFD fed rats revealed greater cell size in the HFD fed rats, indicating, as expected, hypertrophy of the adipose tissue in the groups fed with HFD **(Figure 4A).** Interestingly, both groups within the HFD fed rats presented a tendency to have bigger adipocytes. However, when dissecting adipocyte size by range we saw the presence of giant adipocytes (>5000 $\mu m^2$) on the mesenteric adipose tissue from the HFD-PPVL rats, **(Figure 4B)** indicating a more pathologic adipose tissue. A comparable increase was seen in the epididymal adipose tissue **(Figure 4C)** where the majority of the biggest adipocytes (>8000 $\mu m^2$) were also present in the HFD-PPVL group **(Figure 4D).** These findings suggest that obesity exerts an important extrahepatic effect on liver disease development.

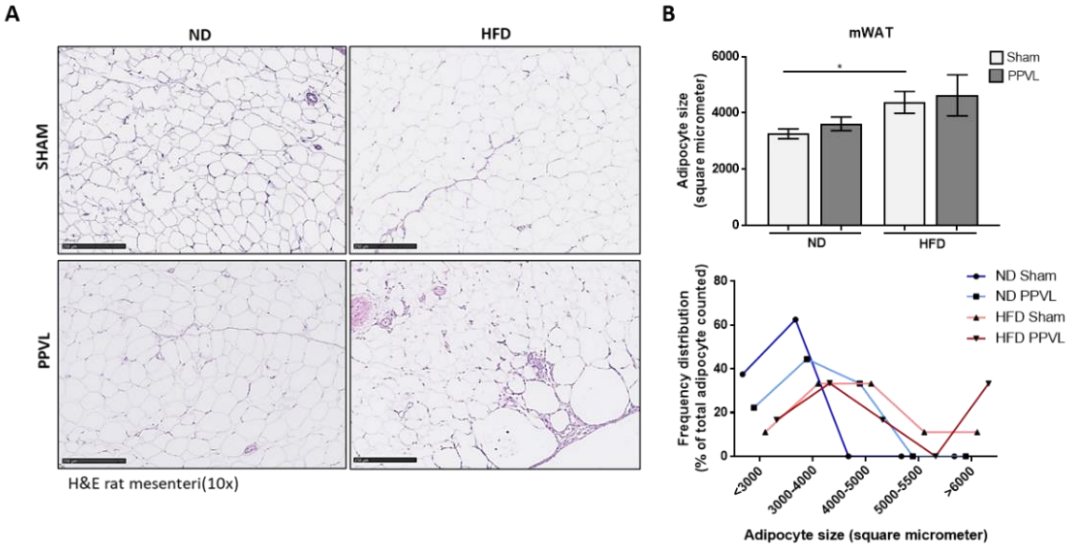

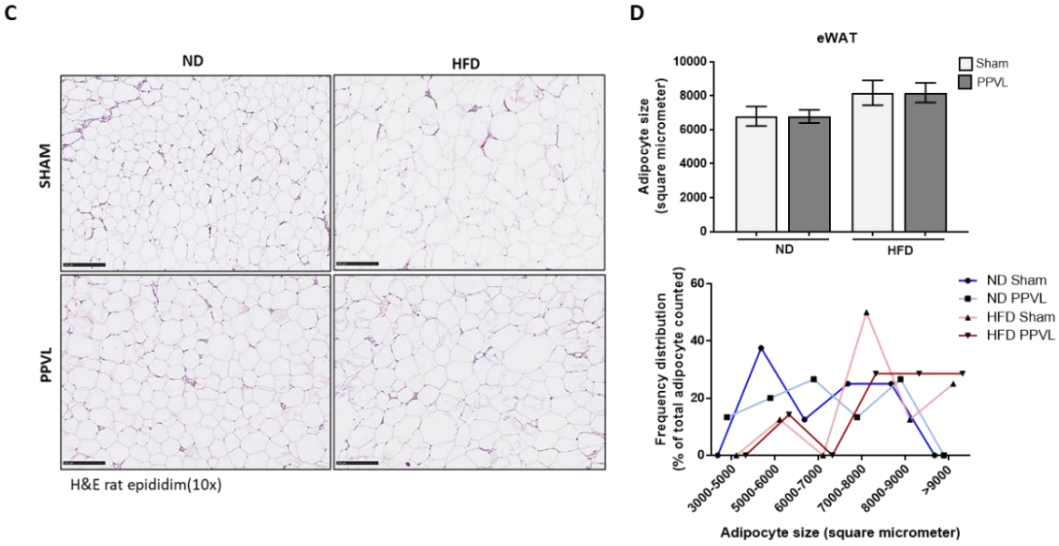


**Figure 4. Effect of a PPVL on the HFD-induced adipocyte hypertrophy. (A)** Representative images of haematoxylin and eosin (H&E) staining in the mesentery of Sham or PPVL rats fed with ND or HFD. **(B)** Quantification of mesenteric adipocyte area (top) and frequency adipocyte distribution per area (bottom). ND Sham (n=8), ND PPVL (n=9), HFD Sham (n=9), HFD PPVL (n=6) *p<0.05 versus ND Sham. **(C)** Representative images of haematoxylin and eosin (H&E) staining in the epididym depot of Sham and PPVL rats fed 16 weeks with ND or HFD. **(D)** Quantification of epididymal adipocyte size (top) and frequency adipocyte distribution per area (bottom). ND Sham (n=5), ND PPVL (n=9) HFD Sham (n=8), HFD PPVL (n=7). All results are expressed as mean ± SEM. Scale bars =250 μm (A, C)

Under pathologic conditions, adipose tissue represents also a great source of inflammation. To investigate the effect of liver disease on adipose tissue inflammation, we measured first the expression of key inflammatory markers on mesenteric WAT. HFD fed animals showed increased CD163 and TNFα **(Figure 5A)** in the mesentery, consistent with an increase inflammatory infiltrate on the adipose tissue in HFD rats. Of note, CD163 macrophage marker increased in the HFD PPVL group compared with the ND PPVL control.

Moreover, the proinflammatory cytokine IL1β and the macrophage marker CD68 were notably overexpressed only in the HFD PPVL rats in the mesenteric tissue **(Figure 5A).** In the same line, we observed a significant increase on the TLR4 expression, a key transmembrane protein of the innate immune system.

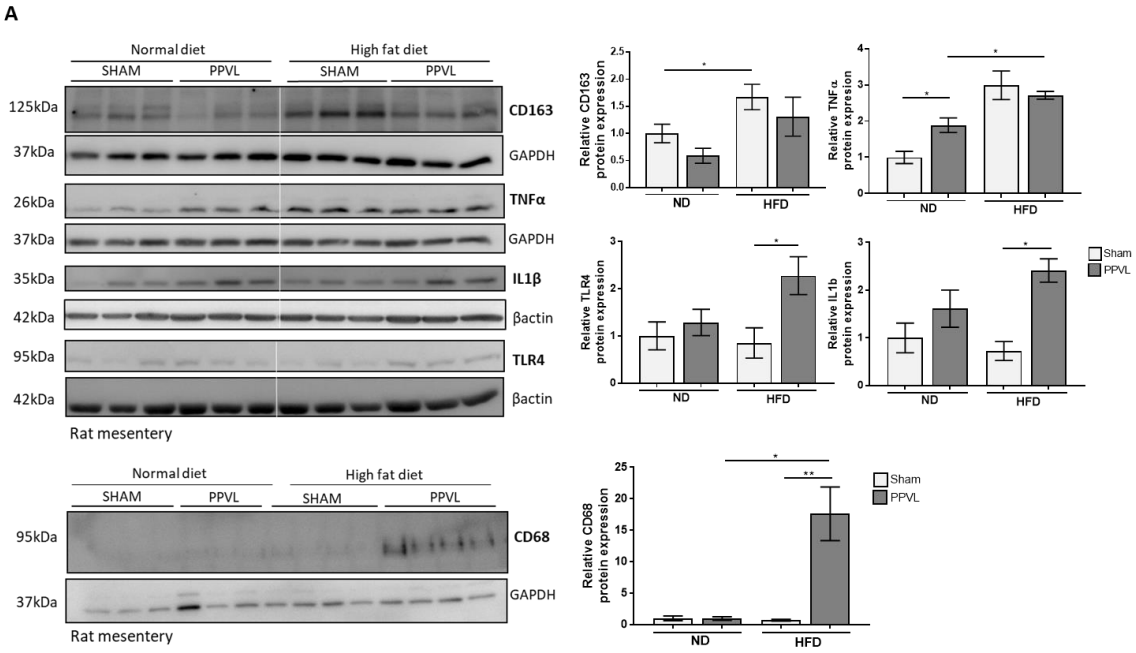


**Figure 5. Increased expression of proinflammatory proteins in the mesentery of rats fed with HFD after a PPVL surgery. (A)** Western blotting of CD163, TNFα, IL1b, TLR4 and CD68 in ND vs HFD fed rats after Sham or PPVL surgery. Densitometric quantification of protein expression relative to loading control b-actin or GAPDH is also shown. *p<0.05. Results are expressed as mean ± SEM.

Based on the marked increased of CD68 by western blot, we wanted to follow up the study of the mesenteric inflammation. We performed an IHC of CD68 on the rat mesentery depot to study the macrophage distribution. Correlating with the immunoblotting result, HFD-PPVL rats presented a significant increase in CD68 expression compared with their controls **(Figure 6A,B).** We next dissected the expression of CD68 in different mesenteric areas where macrophages could be acting. We found an important increase of CD68 expression in the outside layer (serous) of the mesentery, which is in contact with the peritoneal cavity and therefore with adjacent important organs **(Figure 6C).** Overall, these results suggest an aggravated inflammatory state of the adipose tissue in the portal hypertensive rats fed with HFD.

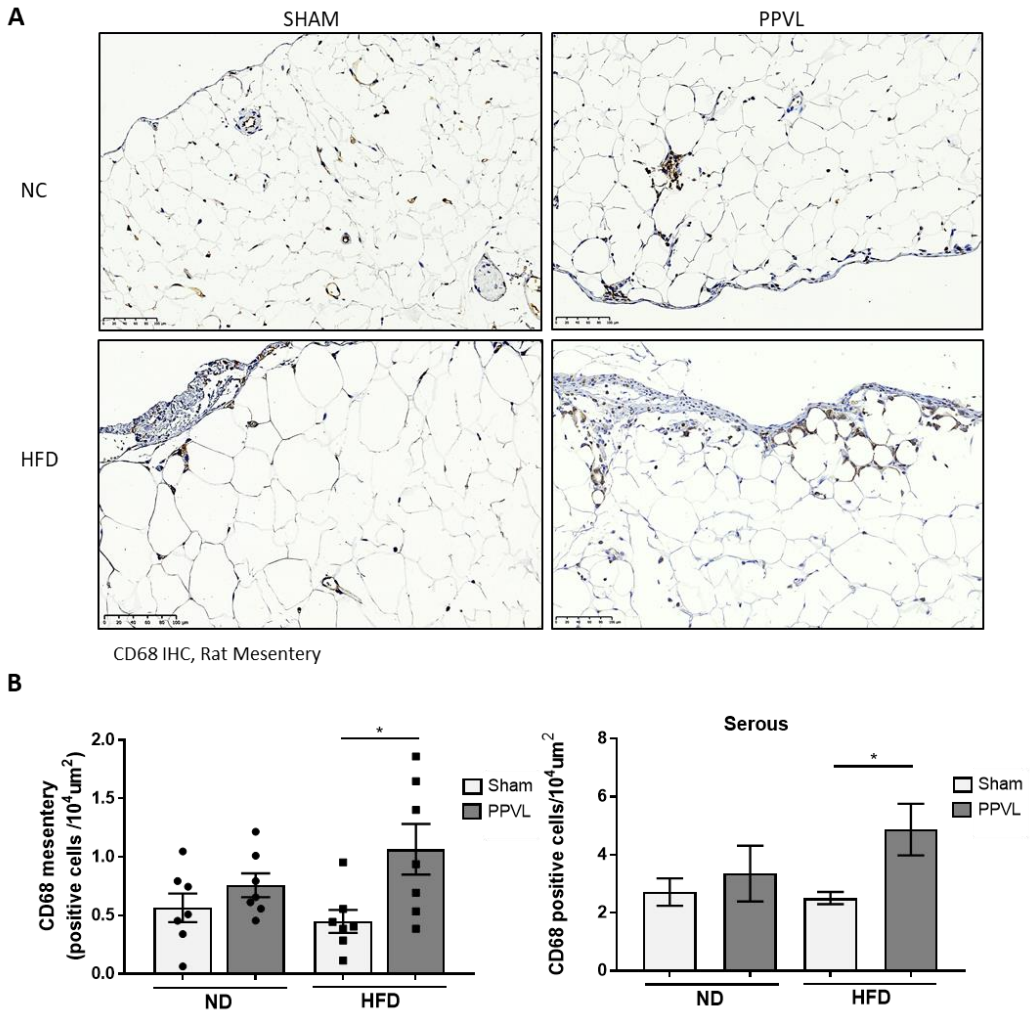


**Figure 6. Mesenteric inflammation in HFD PPVL rats focalizes in the serous layer of the mesentery. (A)** Representative immunostainings for the macrophage marker CD68 in paraffin-embedded mesenteric sections of ND/HFD fed rats after 1 week of SHAM/PPVL surgery. **(B)** Quantification of CD68+ cells in all the mesenteric section followed by a quantification specifically of the serous layer. *p<0.05 versus HFD Sham. Results are expressed as mean ± SEM. Scale bars =250 µm (A).

Mesentery has been recognized as a complex organ which, apart from being a white adipose tissue depot, constitute one of the most important microvascular networks during chronic liver disease. Thus, we next sought to determine if angiogenesis in the mesenteric vascular bed, as a result of a PPVL insult, was altered by a previous high fat diet. CD31 endothelial cell marker expression was increased in NC PPVL rats as expected

but this increase was not exacerbated by a HFD. On the contrary, CD31 positive vessels were reduced in portal hypertensive rats fed with high fat diet **(Figure 7A,B)**. In the same line, the vasculogenic protein VEGF and its receptor implicated in angiogenesis, VEGFR2, were increased in PPVL groups, independently of the diet **(Figure 7C).** This result could suggest an impairment on the new vessel formation exerted by hypertrophic adipocytes.

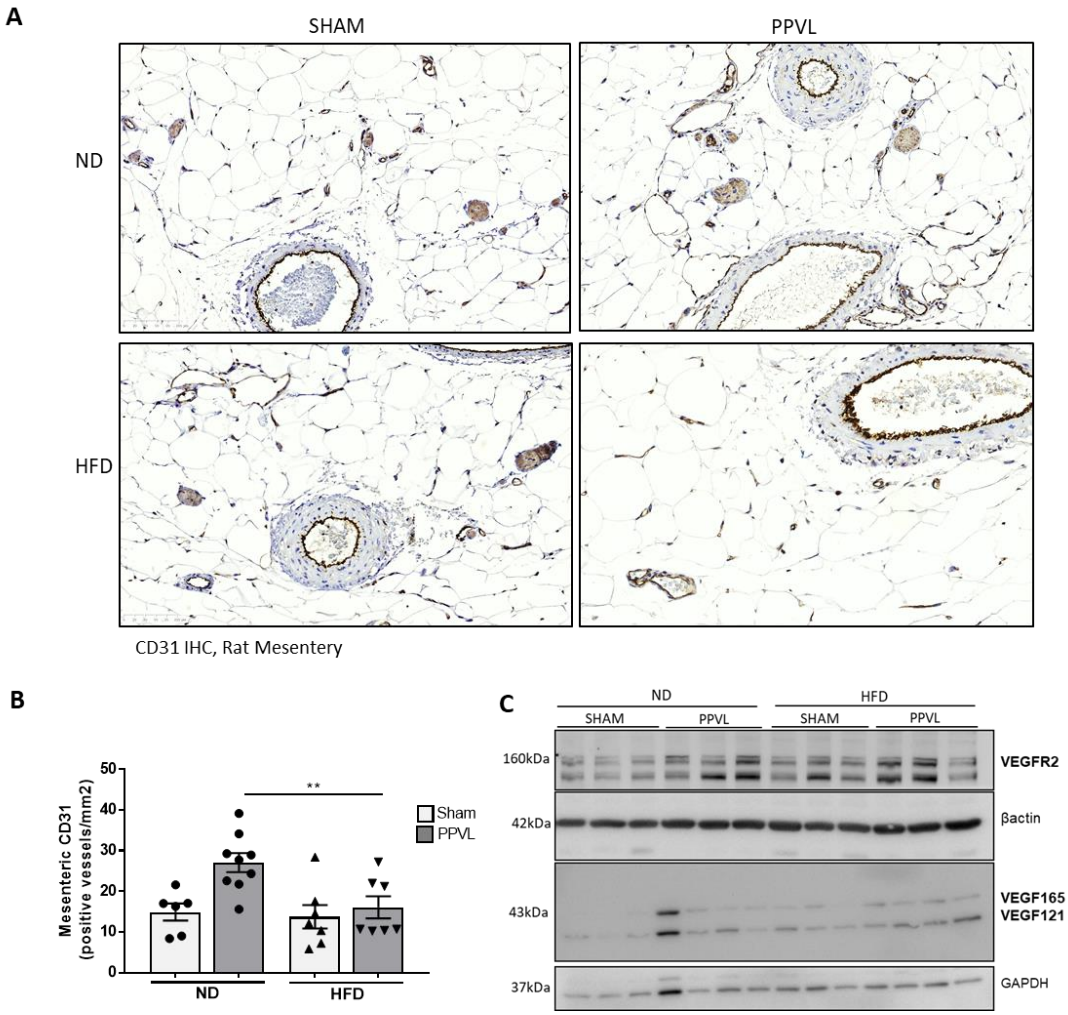


**Figure 7. Neovessel formation does not increase for the effect of a PPVL in the mesentery of HFD fed rats. (A)** Representative immunostainings for the endothelial marker CD31 in paraffin-embedded ND/HFD fed rats after 1 week of SHAM/PPVL surgery. **(B)** Quantification of CD31+ vessels in ND Sham (n=6), ND PPVL (n=9), HFD Sham (n=7), HFD PPVL (n=7). Results are expressed as mean ± SEM. **p<0.005 versus ND PPVL. **(C)** Western Blotting of VEGF and VEGR2 markers of pathological angiogenesis. Scale bars =100 µm (A)

Even though knowing that the portal vein ligation mimics the extrahepatic liver disease effect without affecting directly the liver, we next wondered if these extrahepatic effects produced by both diet and portal vein ligation could impact eventually the liver and aggravate the outcome of the disease. We analysed the state of the liver and we found a significant increase of the portal inflammatory infiltrate in the portal hypertensive rats independent of diet **(Figure 8B).** Transaminases, however, were significantly increased in the PPVL rats when fed with a HFD, suggesting an increased liver damage **(Figure 8C,D).** Sirius-red did not show signs of fibrosis in any group (Data not shown).

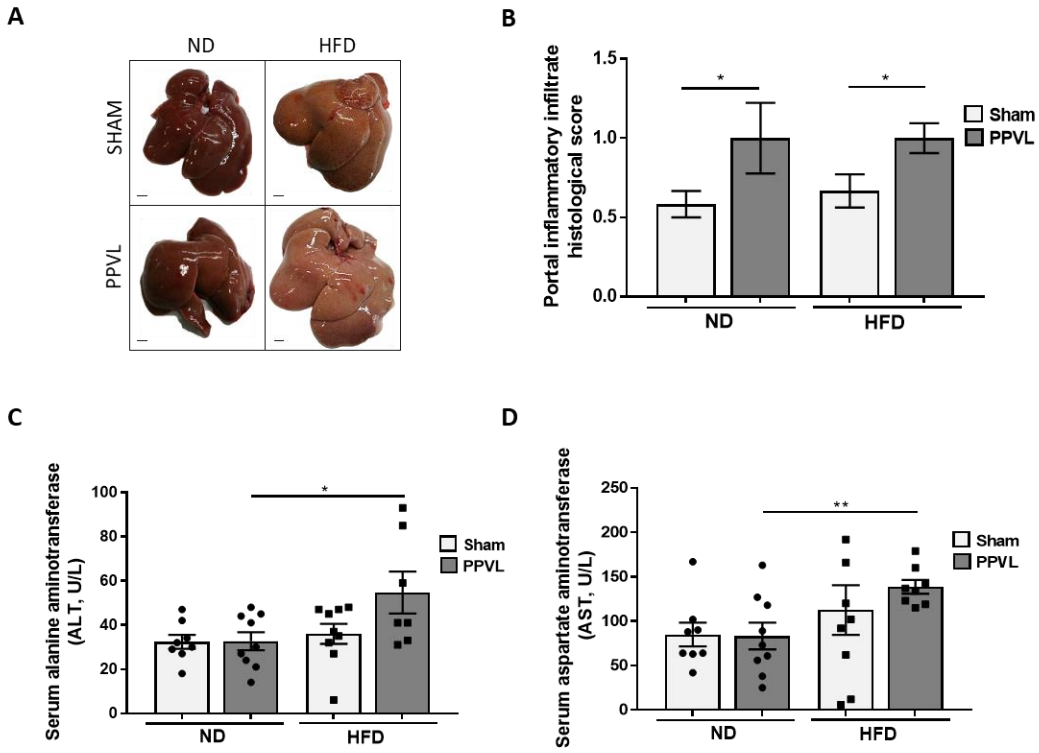


**Figure 8. HFD PPVL rats exhibited increased liver damage. (A)** Macroscopic photographs of representative livers. **(B)** Semiquantitative portal inflammatory infiltrate. **(C and D)** Transaminase levels. All results are expressed as mean ± SEM. **p<0.005, *p<0.05 versus ND PPVL.

Since the liver represents also an important fat depot during obesity, we next measured the metabolic state of the liver after both insults, to see if the increased liver damage correlated with greater fat accumulation. High fat diet fed rats exhibited increased steatosis as expected in a NAFLD model **(Figure 9A)** as well as increased liver triglycerides and cholesterol even thought, any of them was exacerbated by the PPVL insult. All

together, these results suggest that the aggravated extrahepatic state due to a high fat diet could eventually affect the liver when there is a previous damage.

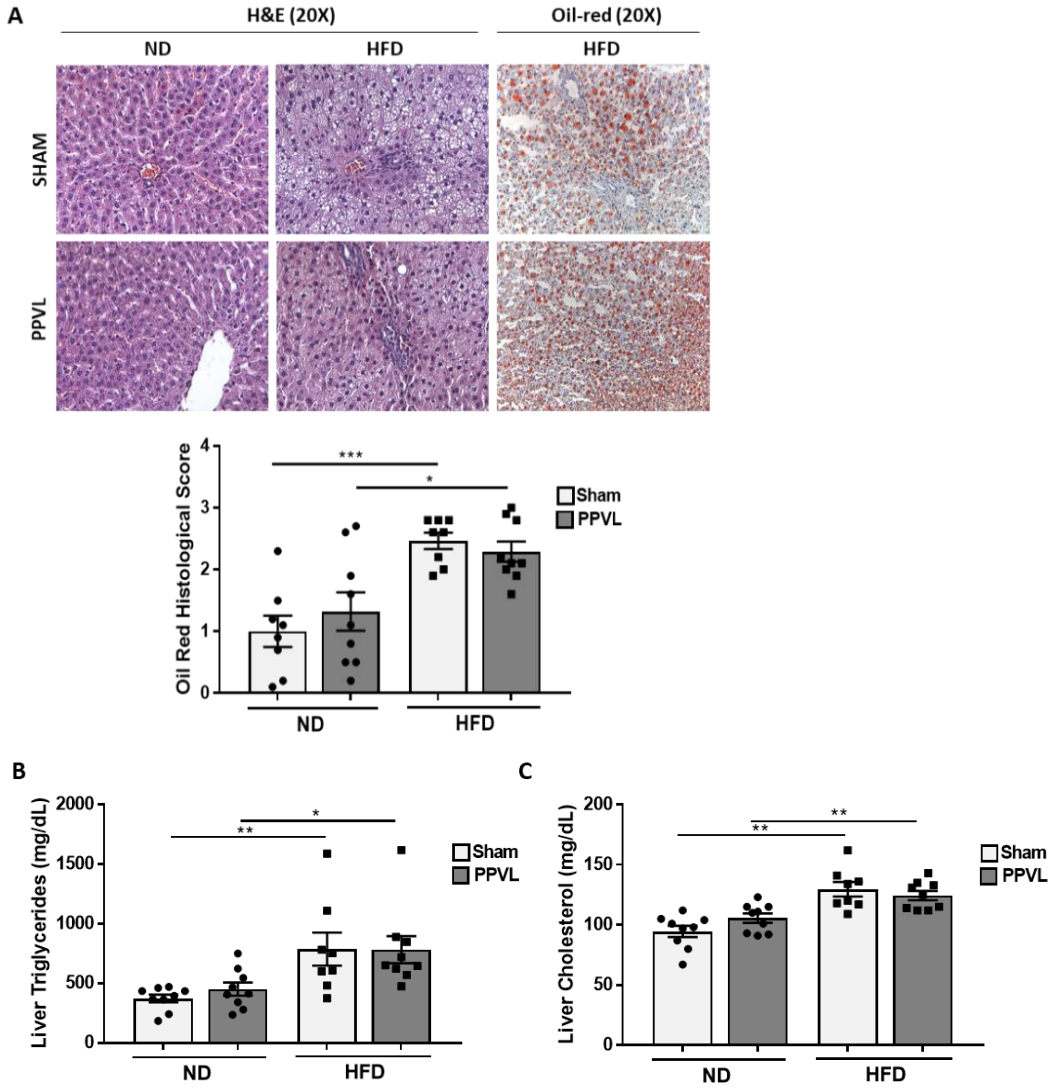


**Figure 9. Liver lipid metabolism in HFD fed rats is not increased by a PPVL insult. (A)** Representative images of haematoxylin and eosin (H&E) and oil red staining. Oil red staining semiquantification is also shown. ***p<0.0005 versus ND Sham **(B and C)** Liver triglyceride and Liver cholesterol levels in ND Sham (n=9), ND PPVL (n=9), HFD Sham (n=8) and HFD PPVL (n=)9 group. All results are expressed as mean ± SEM. **p<0.005 * p<0.05 versus ND PPVL.

## 5.3 CPEB4 is overexpressed in pathologic adipose tissue

In order to find the causality of the aggravated state of the extrahepatic adipose tissue in HFD fed animals with liver disease, we focused on the protein CPEB4. Previous published evidence linked CPEB4 with important lipid functions[148] as well as with cirrhosis and pathological angiogenesis[149]. Furthermore, CPEB family of proteins have been bioinformatically predicted to regulate up to 20% of the whole human mRNAs. Based on these data, we hypothesize that CPEB4 could be regulating the translation of important mRNAs involved in adipose tissue expansion and inflammation. To further underscore the importance of CPEB4 in obesity driven NAFLD, we investigated first, if CPEB4 is regulated during obesity through measurement of its expression in visceral adipose tissue. We found CPEB4 overexpressed in the epididymal adipose tissue of the obese portal hypertensive rats **(Figure 10A).** Moreover, in a previous milder model we developed on the laboratory with a HFD of 45% fat for 16 weeks, we were already able to see in mesenteric tissue, how CPEB4 was clearly overexpressed compared to normal diet fed rats **(Figure 10B).**

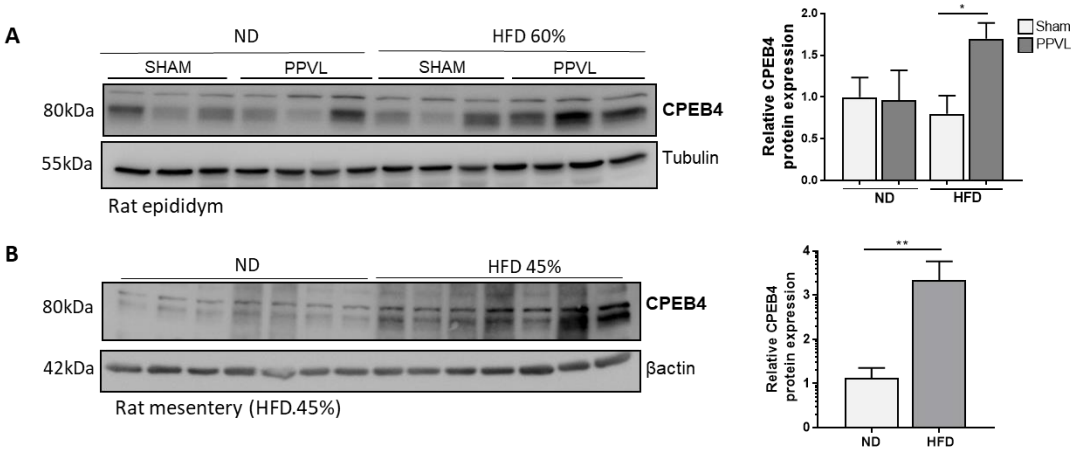


**Figure 10. CPEB4 protein expression increases in pathologic rat white adipose tissue. (A)** Western Blotting of CPEB4 in rat epididymal adipose tissue after 16 weeks of ND or HFD (60% Kcal derived from lipids) plus a PPVL or Sham operation for one week. **(B)** Western blotting of CPEB4 in mesenteric adipose tissue of rats fed with normal diet or HFD (45% Kcal derived from lipids) for 16 weeks.

We next generate a NAFLD model in mice to have the genetic tool to further on be able to generate KO models. Supporting the CPEB4 increased expression seen in rat's adipose tissue, mice fed with HFD for 16 weeks expressed also increased CPEB4 expression in the epididymal adipose tissue **(Figure 11B)** compared to low fat diet (LFD) fed mice. Of note, this increase was exacerbated due to the PPVL **(Figure 11A).**

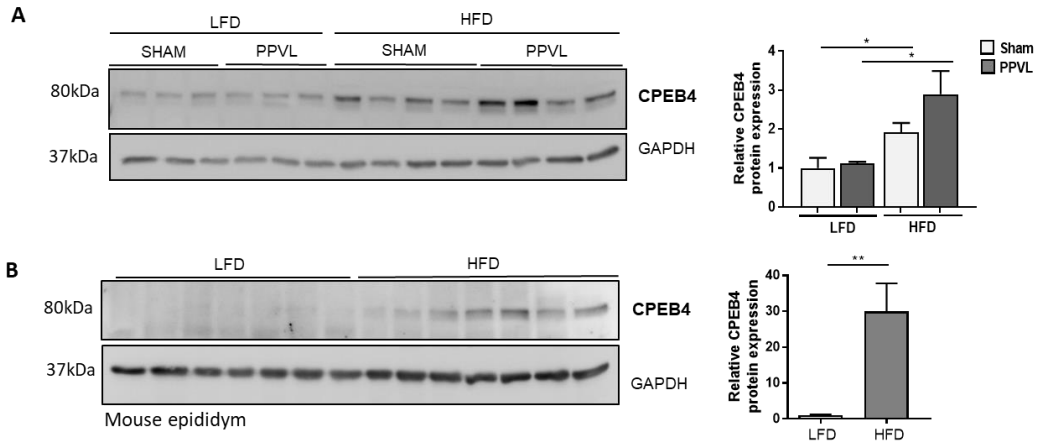


**Figure 11. CPEB4 protein expression increases in pathologic mouse adipose tissue. (A)** Western blotting of CPEB4 expression in epididym of mice fed with LFD or HFD for 16 weeks and under Sham or PPVL operation for 7 days. **(B)** Western blotting of CPEB4 expression in epididym of mice fed with LFD compared to a HFD.

To further validate the clinical impact of our results, we measured CPEB4 levels in omental adipose tissue of obese and obese NAFLD patients compared to lean controls. Interestingly, obese subjects showed increased protein levels of CPEB4 in visceral adipose tissue **(Figure 12B)**. CPEB4 mRNA levels did not change between Lean and Obese patients nor even in NASH patients **(Figure 12A)** indicating a possible CPEB4 regulation through a post-translational mechanism in this scenario. All together, these results strongly suggest that CPEB4 could be participating in a process involved with obesity such as the adipose tissue expansion characteristic of obesity.

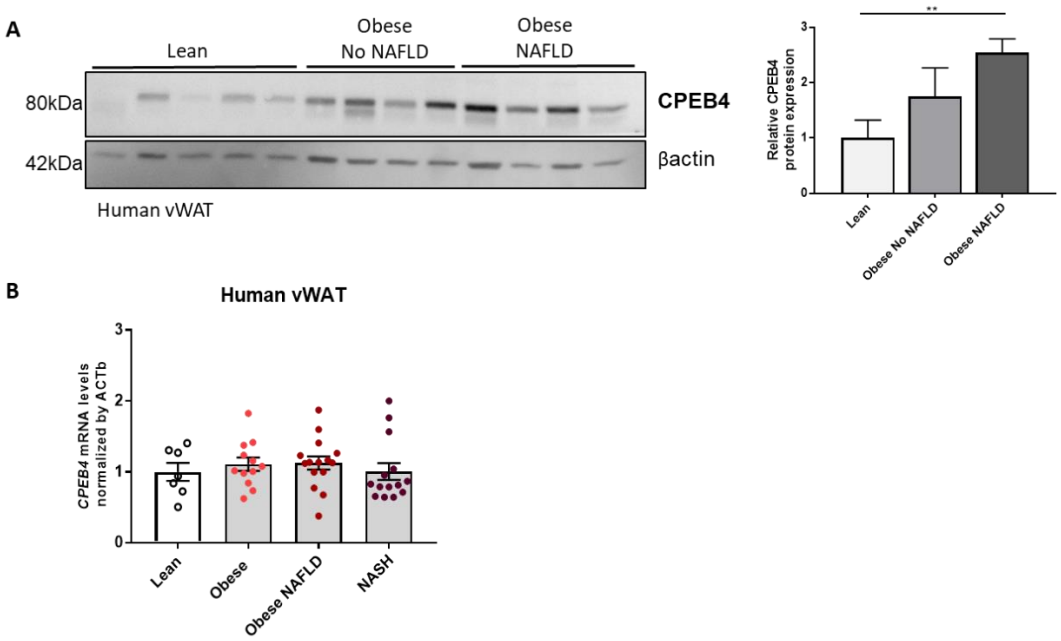


**Figure 12. CPEB4 protein expression increases in obese human with and without NAFLD pathology. (A)** Western blotting of CPEB4 expression in omental adipose tissue of lean, obese and obese NAFLD patients. **(B)** mRNA expression of CPEB4 in omental adipose tissue of Lean (n=7), Obese without NAFLD (n=12), Obese with NAFLD (n=13) and NASH (n=14) patients**.**

### 5.3.1 CPEB4 promotes adiposity

In order to elucidate the CPEB4 role in adipose tissue during NAFLD development, we used first, a global loss-of-function genetic mouse model (CPEB4$^{KO}$). CPEB4$^{KO}$ mice as well as their control wild type (WT) mice at 6 weeks of age were fed with a HFD for 16 weeks to generate a NAFLD model **(Figure 13A).** Consistent with the literature, WT mice with high fat diet feeding resulted in a marked body weight gain**.** Interestingly, CPEB4$^{KO}$ mice gained less body weight than their controls WT **(Figure 13B,C).** This finding brought us to investigate the behaviour of the principal extrahepatic target organs affected by a high fat diet.

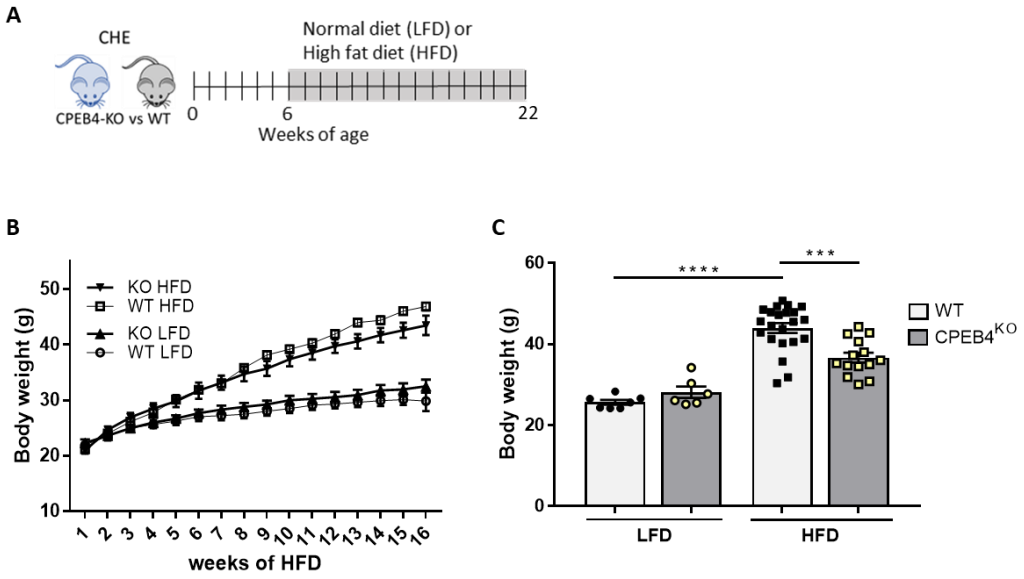


**Figure 13. CPEB4 ablation results in reduced body weight in mice under high fat diet exposure for 16 weeks. (A)** Schematic representation of the NAFLD model protocol used in mice. **(B and C)** Body weight profile and endpoint weight of WT and CPEB4$^{KO}$ mice fed with LFD (n=6-7/genotype) or HFD (n=12-20/genotype). Statistical analysis was performed by t- test. Data are expressed as mean ± SEM. ***P<0.001

To ascertain whether the resistance of CPEB4$^{KO}$ mice to gain body weight in response to HFD feeding reflected a specific decrease in visceral adiposity, we measured the weight of fat depots. Total body weight decrease in the HFD fed animals lacking CPEB4 was correlated with a weight decrease of the white adipose tissue depots **(Figure 14A).** In accordance, when dissecting the individual visceral adipose tissue (mesenteric, epididymal and retroperitoneal), we found a comparable weight reduction in the three of them in HFD-fed CPEB4$^{KO}$ mice compared with WT mice on the same diet **(Figure 14C)**. In addition, serum triglycerides after HFD feeding did also decrease when CPEB4 was ablated **(Figure 14B).**

Remarkably, genetic ablation of CPEB4 in LFD fed mice, in which CPEB4 expression in WAT is low, had no effect on adipose tissue weight, relative to WT littermates on the same diet. These results suggest that CPEB4 plays a crucial role in the dysregulation of the adipose tissue homeostasis due to a high fat diet feeding.

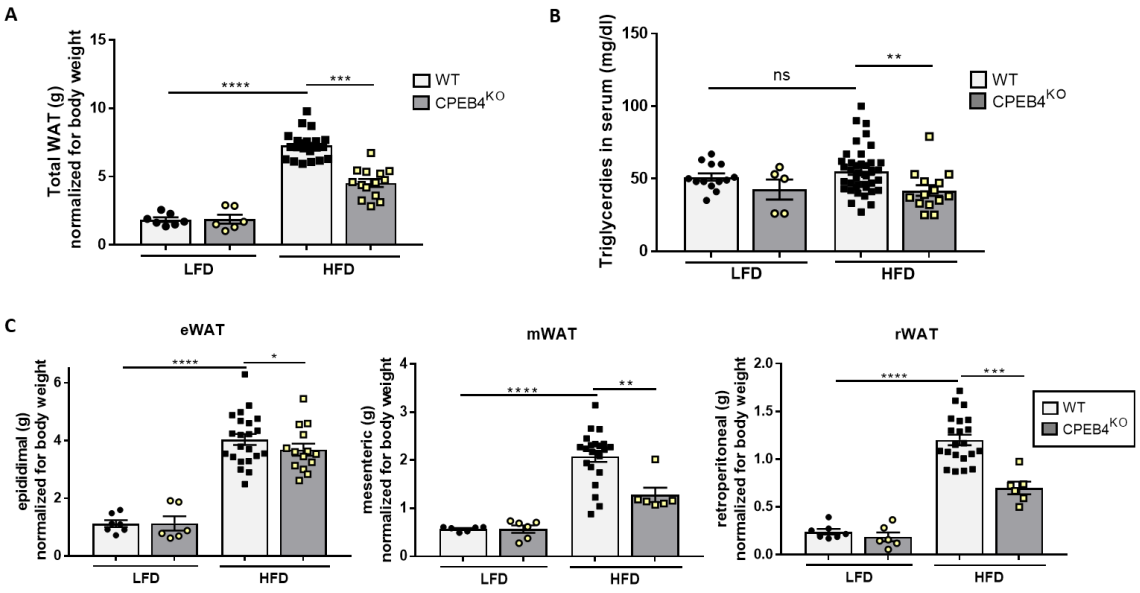


**Figure 14. CPEB4 ablation resulted in reduced white adipose fat pad weight in mice fed with high fat diet for 16 weeks. (A)** Total WAT weight derived from epididymal (eWAT), mesenteric (mWAT) and retroperitoneal (rWAT) adipose tissues from WT or CPEB4$^{KO}$ fed with LFD or HFD. **(B)** Serum triglycerides (LFD n=6/ genotype) (HFD n=12-20/genotype). **(C)** epididymal, mesenteric and retroperitoneal individual weights. All results are expressed as mean ± SEM

The observation that CPEB4$^{KO}$ mice had reduced susceptibility to obesity prompted us to examine whether white adipocytes might rely on CPEB4 dependent reprogramming to fuel cell hypertrophy during excessive intake of fat calories. To do so, we focused on the epididymal WAT. Adipocyte size quantification revealed the presence of smaller adipocytes in the CPEB4$^{KO}$ mice fed with HFD compared with the WT **(Figure 15C,D)**. Correlating, the majority of adipocytes in the CPEB4$^{KO}$ HFD group were found to have around 5000 µm$^2$ of area while in the WT HFD were bigger, with an area of more than 6000 µm$^2$. Interestingly, epididymal hypertrophy reduction was accompanied by a decrease adipose tissue proliferation as showed the PCNA levels **(Figure 15B).** No cellular changes in the normal adipose tissue architecture, including changes in adipocyte size and proliferation were observed in CPEB4$^{KO}$ mice compared to ET when both were fed on LFD.

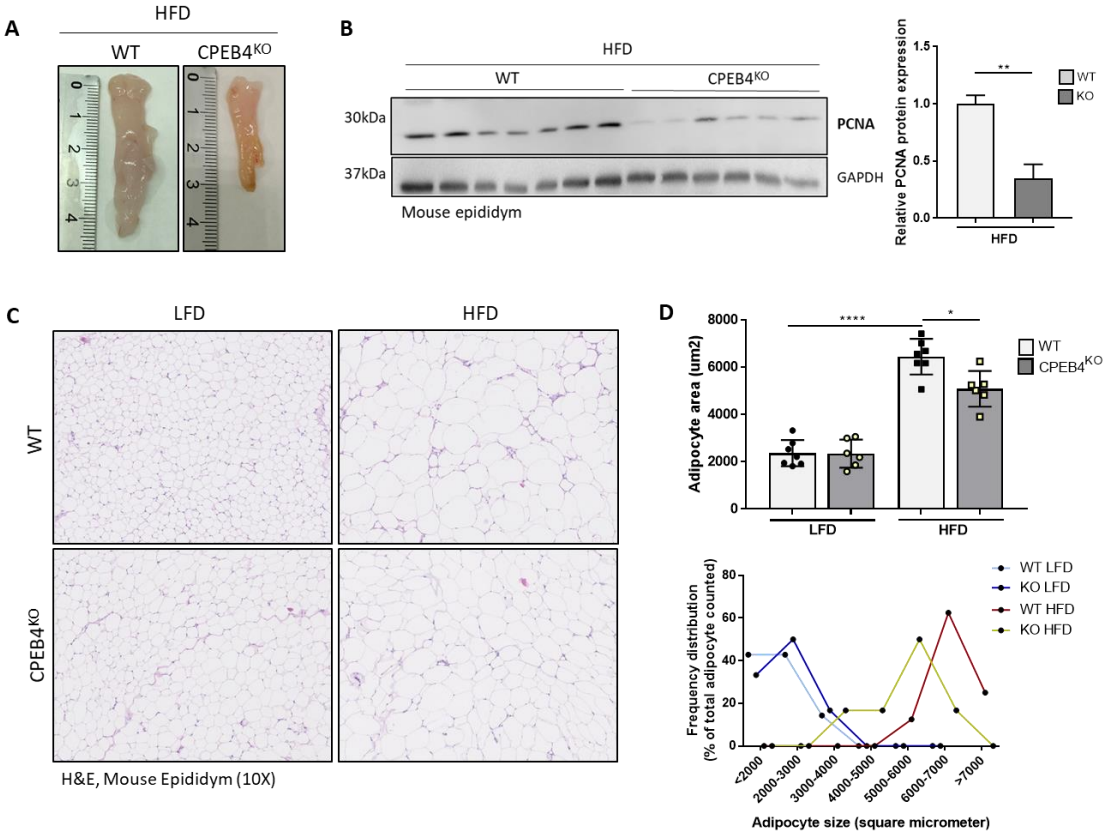


**Figure 15. CPEB4$^{KO}$mice exhibit less hypertrophy and hyperplasia of the white adipose tissue when fed with a high fat diet. (A)** Macroscopic photographs of representative epididymal fat depots of WT or CPEB4$^{KO}$ mice fed with LFD or HFD for 16 weeks. **(B)** Western blotting of the proliferative marker PCNA in WT versus CPEB4$^{KO}$ mice fed with HFD. **(C)** Representative images of haematoxylin and eosin staining in paraffin embedded epididymal mouse sections. **(D)** Adipocyte area and number quantification in WT LFD (n=7), CPEB4$^{KO}$ LFD (n=6) compared to WT HFD (n=7) and CPEB4$^{KO}$ HFD (n=6). All results are expressed as mean ± SEM.

### 5.3.2 CPEB4 deficiency attenuates angiogenesis and adipose tissue inflammation on diet induced obesity

During obesity, white adipose tissue is hypervascularized and the adipose vasculature displays phenotypic and functional plasticity to coordinate with metabolic demands of adipocytes. Thus, adipose tissue microcirculation is heavily impacted by adipose tissue expansion, where angiogenesis is necessary to counter hypoxia arising as a result of tissue expansion[155,55]. In support of this notion, we found that HFD fed mice presented a marked increased angiogenesis. Interestingly in this context, we have demonstrated how adipose tissue from CPEB4$^{KO}$ mice under HFD present less vasculature than its WT control, as indicated by the marker Isolectin B4 (IB4) **(Figure 16 A,B)**. Moreover, we found the pro-angiogenic factor VEGFA protein expression to be significantly reduced in two of its isoforms in CPEB4$^{KO}$ compared to WT littermates under HFD **(Figure 1C).**

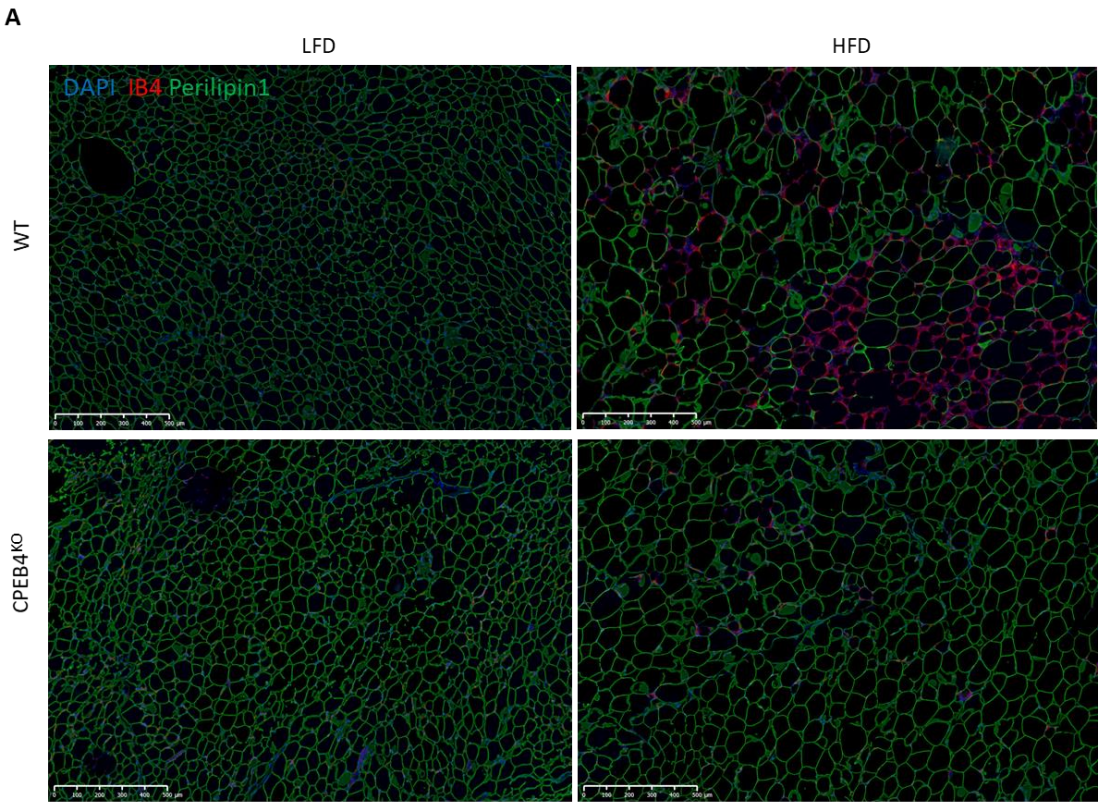

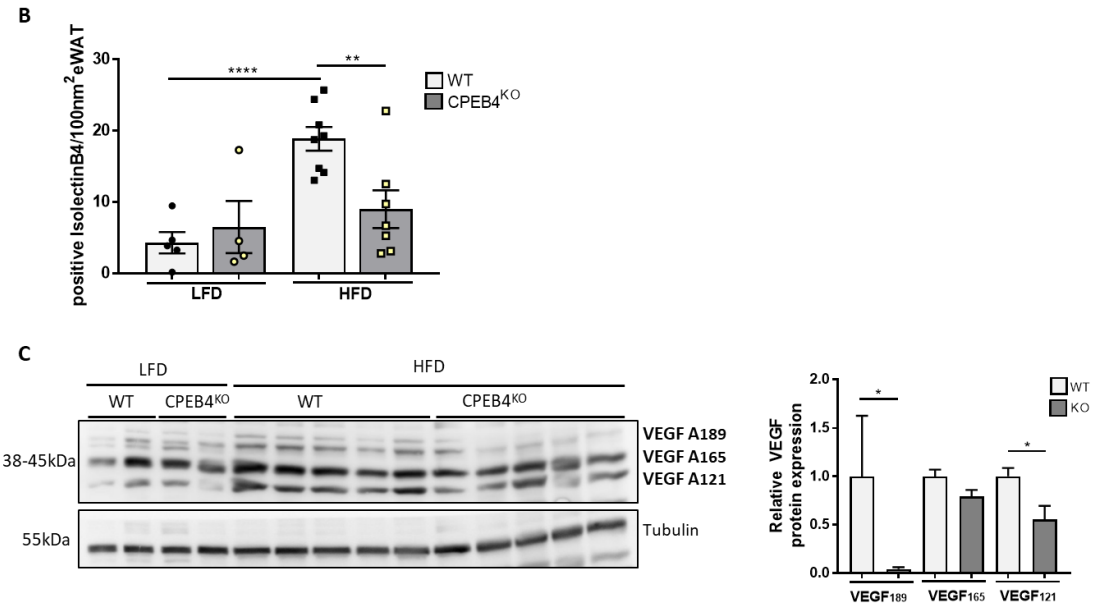


**Figure 16. CPEB4$^{KO}$mice exhibit less angiogenic signal than WT mice when fed with a high fat diet. (A)** Representative images from immunofluorescence double stained eWAT tissue slides with perilipin 1 and Isolectin B4 of WT or CPEB4$^{KO}$ mice fed with LFD or HFD for 16 weeks. **(B)** Isolectin positive signal quantification of WT LFD (n=5), CPEB4$^{KO}$ LFD (n=4) compared to WT HFD (n=8) and CPEB4$^{KO}$ HFD (n=6). **(C)** Immunoblotting of VEGFA isoforms in epididymal adipose tissue. All results are expressed as mean ± SEM, *p<0.05 Representative images of IB4 or CD31 immunofluorescence and its quantification in the specified tissues (n=3-4/genotype). Scale bar 500 µm.

Since an excess of adipose tissue represents also a great source of inflammation, we wonder how the lack of CPEB4 affects the inflammatory state of the adipose tissue. We first demonstrated that WT mice displayed the expected inflammatory state within abdominal fat depots following prolonged HFD feeding, relative to LFD fed mice. Interestingly, CPEB4 depletion robustly improved this inflammatory phenotype as measured by CD68, TNFα and CD206 protein levels **(Figure 17A)**. Consistent with this observation, we found that ablation of CPEB4 strongly reduced the formation of crown-like structures (CLS, adipose tissue arranged around dead adipocytes) measured by CD68$^{+}$ immunohistochemistry **(Figure 17B-C)**. This result correlates also with a decrease in the macrophage chemoattractant protein-1 in CPEB4$^{KO}$ mice fed with HFD **(Figure 17D),** master regulator in the macrophage recruitment. All together, these results suggest an important role of CPEB4 in the adipose inflammation process.

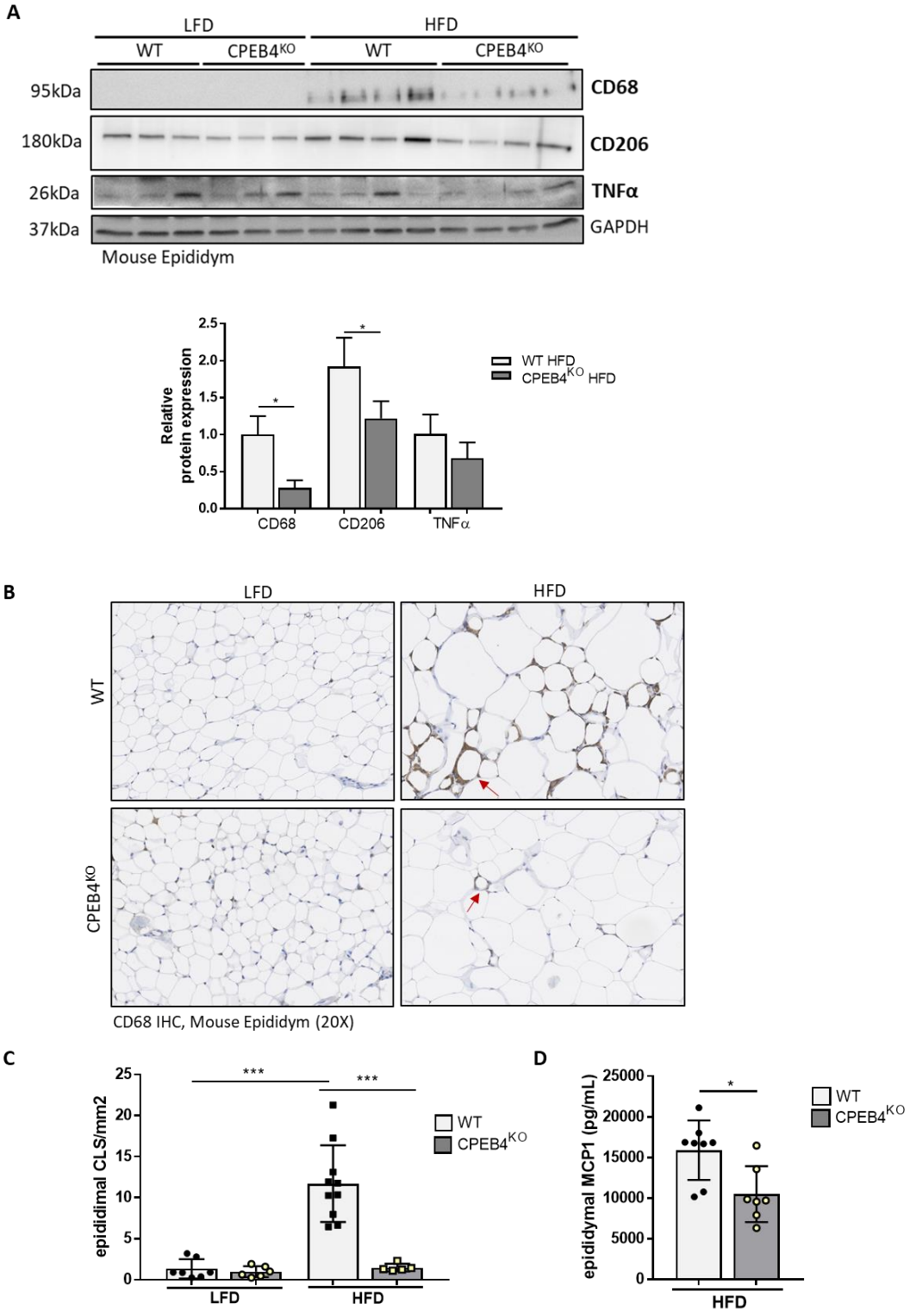
A
LFD
HFD
WT
CPEB4KO
WT
CPEB4KO
95kDa
CD68
180kDa
CD206
26kDa
TNFα
37kDa
GAPDH
Mouse Epididym
Relative protein expression
2.5
2.0
1.5
1.0
0.5
0.0
*
*
CD68
CD206
TNFα
WT HFD
CPEB4KO HFD
B
LFD
HFD
WT
CPEB4KO
CD68 IHC, Mouse Epididym (20X)
C
epididimal CLS/mm2
25
20
15
10
5
0
***
***
LFD
HFD
WT
CPEB4KO
D
epididymal MCP1 (pg/mL)
25000
20000
15000
10000
5000
0
*
HFD
WT
CPEB4KO

**Figure 17. CPEB4$^{KO}$mice present less adipose tissue inflammation. (A)** Western Blotting of the macrophage and proinflammatory markers CD68, CD206 and TNFα in mouse epididymal adipose tissue. Protein expression quantification normalized by GAPDH is also shown. **(B)** Representative immunostainings for the macrophage marker CD68 in paraffin-embedded WT/CPEB4$^{KO}$ mice fed with LFD or HFD for 16 weeks. **(C)** Crown-like structures quantification based on CD68 immunostaining in WT LFD (n=7), CPEB4$^{KO}$ LFD (n=6), WT HFD (n=10), CPEB4$^{KO}$ HFD (n=5) *p<0.0001. **(D)** MCP1 ELISA levels in epididymal adipose tissue of WT HFD (n=8) versus CPEB4$^{KO}$ HFD mice (n=7). *p<0.05. All results are expressed as mean ± SEM.

To investigate mechanisms that might account for the reduced inflammation in the WAT of CPEB4$^{KO}$ mice, we defined changes in the macrophage adipose tissue population (ATM) in greater detail. To this end, we isolated the epididymal stromal vascular fraction of WT or CPEB4$^{KO}$ mice fed with HFD for 16 weeks and further performed flow cytometry analysis to characterize ATM populations. Consistent with the previous results, ablation of CPEB4 did modify the percentage of F4/80high$^{+}$CD11b$^{+}$ total adipose tissue macrophage population. Indeed, WT HFD fed mice showed increased ATM compared with the CPEB4$^{KO}$ with a clear cluster of population with high positive F4/80 expression. **(Figure 18A)**.

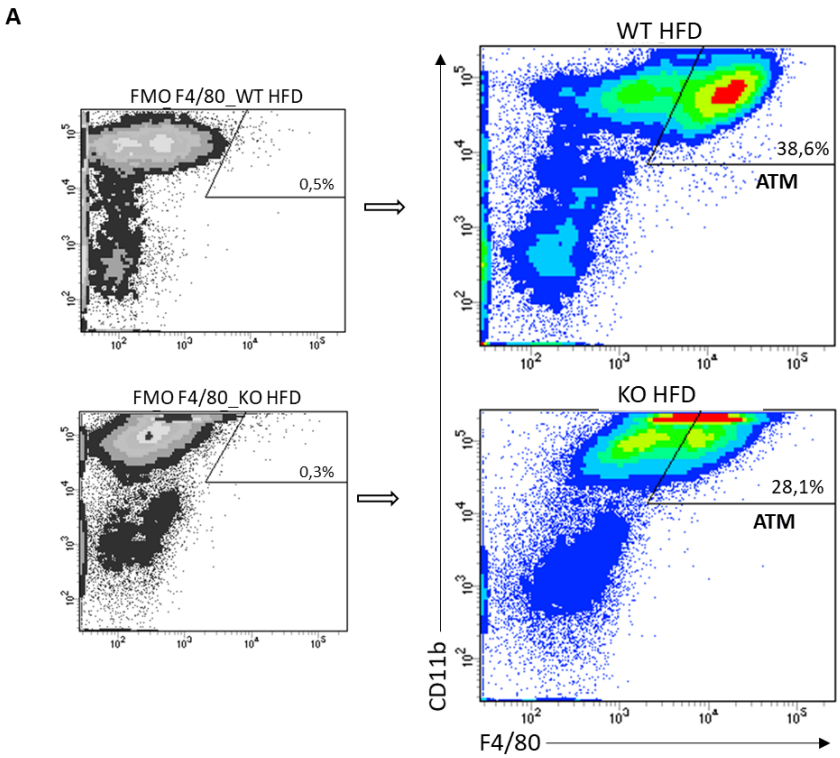

**Figure 18. CPEB4$^{KO}$ mice present less eWAT ATM than WT mice under high fat diet. (A)** Representative flow cytometry plots (right) showing frequencies of F4/80+CD11b+ macrophages (ATM) among stromal vascular cells isolated from eWAT of HFD-fed WT or CPEB4$^{KO}$ mice. Gates are made using Fluorescent minus one (FMO) controls of F4/80 marker (left).

We next performed further subfractionation of the purified ATM population (F4/80high$^{+}$ CD11b$^{+}$) using CD206 and CD11c markers, focusing on the metabolic macrophage population (Mme). Consistently with the previous observations, ablation of CPEB4 in obesity setting altered the activation status of the ATM. We found that the Mme proinflammatory population (F4/80$^{+}$CD11b$^{+}$CD206$^{+}$CD11c$^{+}$) was higher in the WT than in the CPEB4$^{KO}$ mice fed with HFD **(Figure 19A).** On the contrary, the strictly resolutive macrophage population M2 (F4/80$^{+}$CD11b$^{+}$CD206$^{+}$CD11c$^{-}$) was higher in the CPEB4$^{KO}$ compared to WT fed with HFD, consistent with the observation that CPEB4 deletion prevents the generation of low-grade inflammation in response to high-fat feeding. Moreover, TLR4, known to be the receptor through Mme macrophages, mediates their inflammatory responses to fatty acids was also decreased in the CPEB4$^{KO}$ mice fed with HFD compared to WT mice **(Figure 19B).**

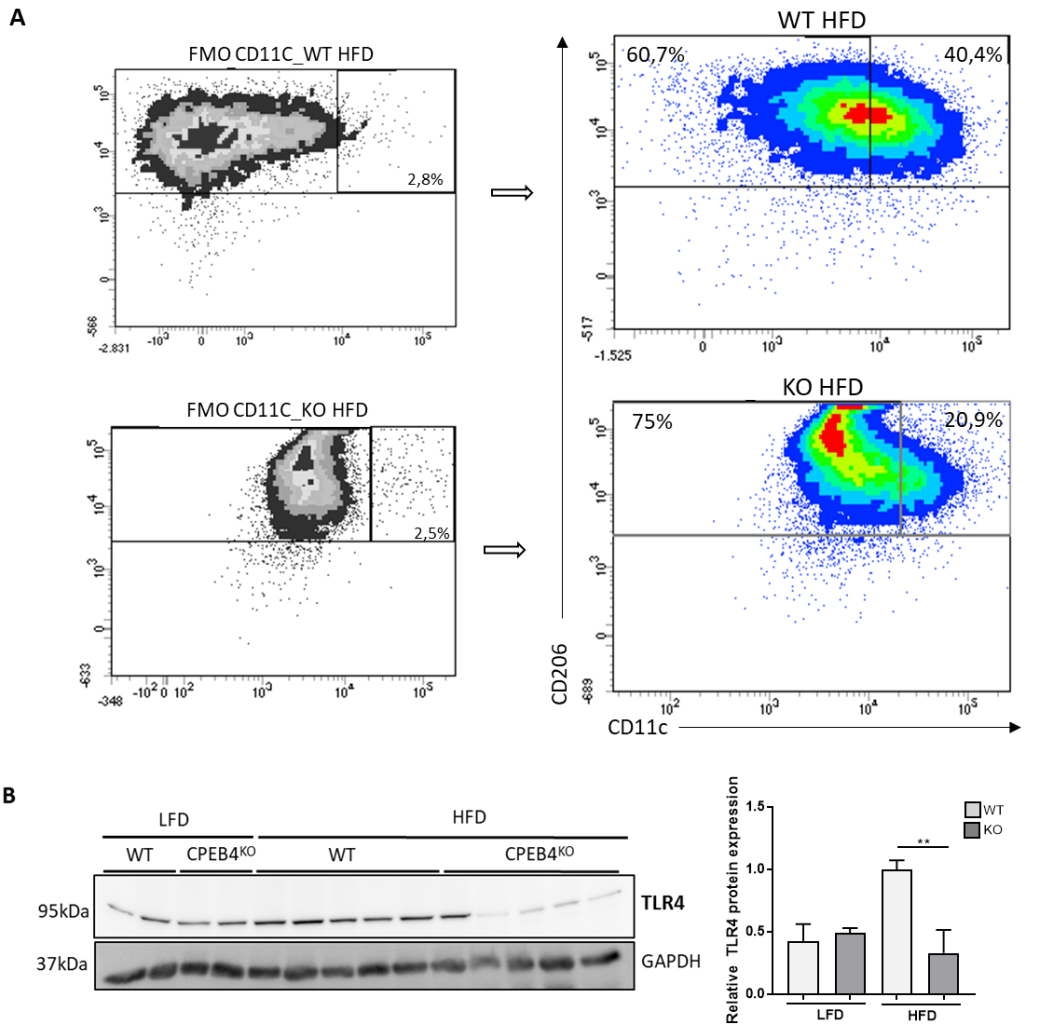


**Figure 19. Metabolic macrophage subpopulation content is higher in the eWAT of the WT than the CPEB4$^{KO}$ mice during diet induced obesity. (A)** Representative flow cytometry plots showing (left) FMO controls of CD11c marker to gate the (right) Mme population (CD206$^{+}$CD11c$^{+}$) among the F4/80$^{+}$hiCD11b$^{+}$ cells of the WT and CPEB4$^{KO}$ phenotype fed with HFD. **(B)** Western Blotting of the macrophage TLR4 marker in mouse epididymal adipose tissue. **p<0.01

These results suggest that CPEB4 ablation may dampen inflammation by inducing a phenotypic switching on alternative activation of macrophages towards an anti-inflammatory phenotype, which in turn reduces pathological inflammation induced by high-fat diet and contributes to maintenance of tissue homeostasis.

### 5.3.3 CPEB4 deficiency does not exhibit increased WAT lipolysis in basal conditions

During obesity, high levels of saturated fatty acids (SFAs) contribute to adipose tissue inflammation and dysfunction. We wonder if the decreased adiposity and inflammatory state observed on the absence of CPEB4 could be partly due to an increase in the lipolytic activity of the adipose tissue and consequently an increase of circulating fatty acids.

Although lipolysis is used to mobilize stored energy during fasting or exercise in fat adipocytes, we explored if CPEB4 could be perturbing lipolysis even in basal conditions.

To molecularly verify it, whole eWAT depots were subjected to immunoblotting. Hormone-sensitive lipase (HSL), a key enzyme of the lipolytic pathway, is activated trough phosphorylation at Serine residues. Decreased protein levels of the active HSL forms were observed in the CPEBKO HFD fed group (Figure 16A). It is also known how under basal conditions adipocytes lipid droplets are coated by the specialized protein called perilipin. In accordance with the pHSL decrease, Perilipin1 was increased in the CPEB4KO group compared with WT HFD, protecting the lipid droplet from lipolysis **(Figure 20A).**

As a result of the lipolytic route activation, fatty acids and glycerol are released in the circulation. Nevertheless, in non-fasted conditions circulating NEFAs come not only from lipolysis of stored TG in adipocytes but also from the hydrolysis of circulating TG. Serum NEFA levels in CPEB4$^{KO}$ fed with HFD did not show a significant decreased compared with the WT **(Figure 20B).**

All together, these results support the idea that limited white adipose tissue differentiation and adipogenic capacity, rather than an increased lipolysis, are the main contributors to the decreased visceral adiposity observed in the CPEB4$^{KO}$ mice under HFD feeding.

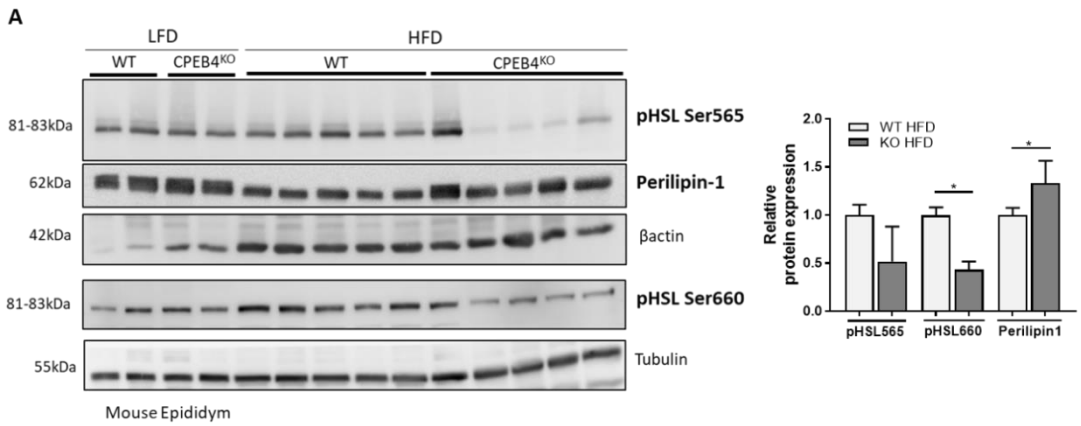

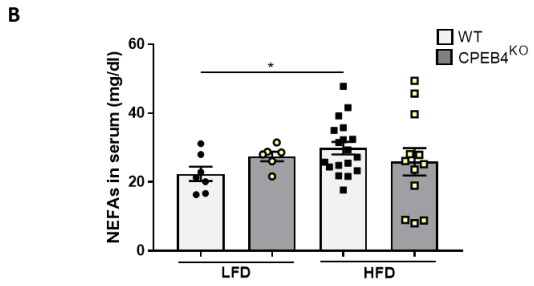


**Figure 20. CPEB4$^{KO}$ mice show decreased lipolysis in fed conditions. (A)** Immunoblot analysis (left) and quantification (right) of eWAT using the indicated antibodies. **(B)** Serum NEFA levels (n=6-17/genotype/nutritional status) *p<0.05.

We next aimed to see if the CPEB4$^{KO}$ adipose tissue improvements were also taking place in the liver since its capacity to storage fat. CPEB4KO mice exhibited complete loss of CPEB4 protein also in the liver **(Figure 21A)**. In contrast to the observed in white adipose tissue, the amount of CPEB4 in liver was not increased by high-fat diet feeding for 16 weeks **(Figure 21A)**. Regarding liver weight, it didn't display differences at this stage comparing genotypes within the same diet group **(Figure 21B).** Transaminases increased as expected by the HFD feeding without showing differences for the presence or absence of CPEB4 **(Figure 21C)**. Histological comparison failed to reveal any difference in the degree of hepatosteatosis compared HFD-fed WT mice**.** CPEB4$^{KO}$ mice exhibited the same amount of lipid droplets **(Figure 21D)** as well as triglycerides in the liver **(Figure 21E)** comparing genotypes under the same diet**.** Liver fibrosis determined by Sirius red staining revealed also no apparent signs of fibrosis after HFD of CPEB4$^{KO}$ compared to WT mice (data not shown). These results state the importance of targeting CPEB4 in the extrahepatic territory and suggest independent dual roles of CPEB4 in the modulation of adiposity and fatty liver.

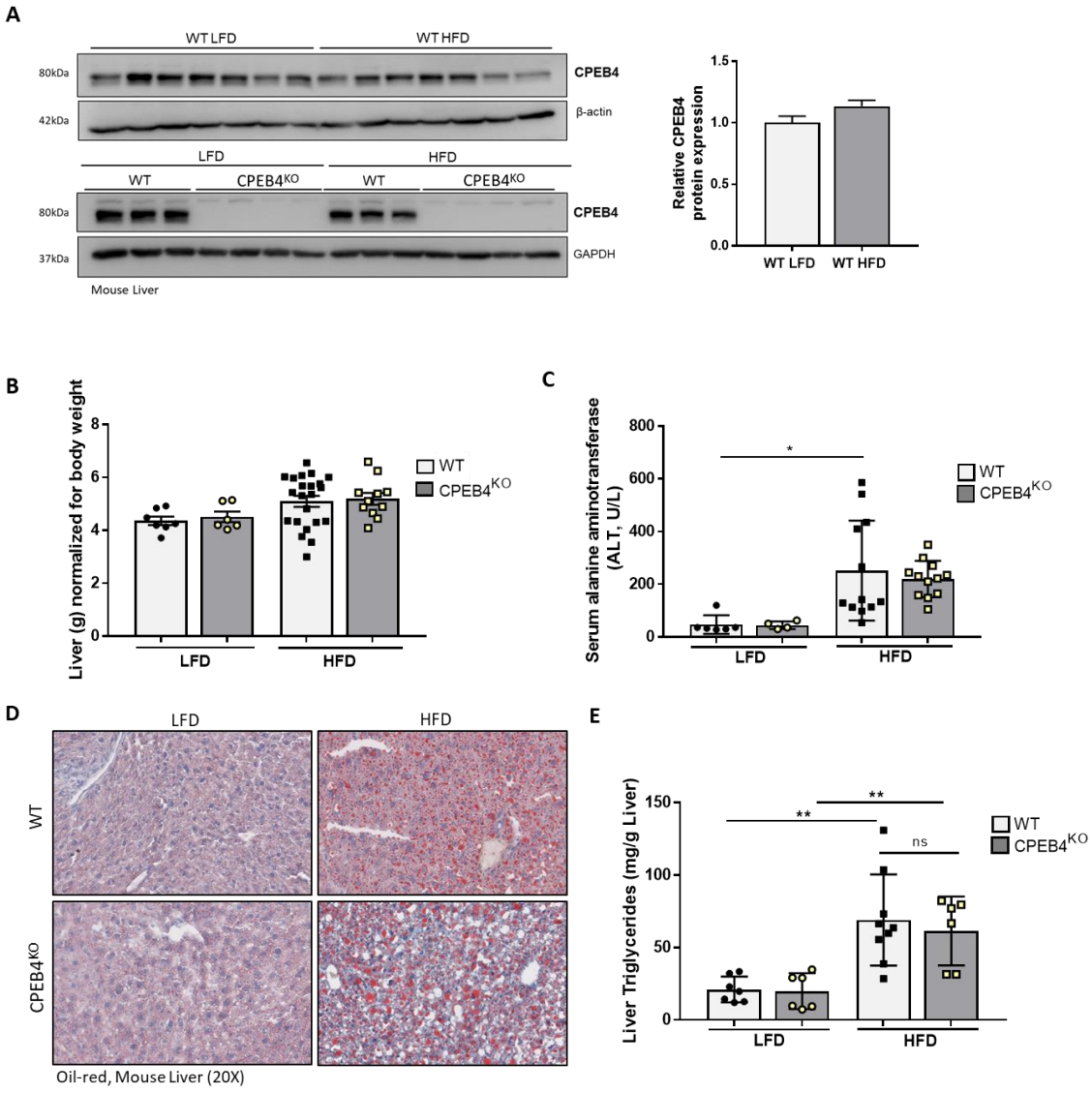


**Figure 21. Liver state after total ablation of CPEB4 in mice fed with LFD or HFD for 16 weeks. (A)** Immunoblotting and quantification of CPEB4 protein expression in mouse liver tissue of WT or CPEB4$^{KO}$, fed with LFD or HFD. **(B)** Liver weight normalized by body weight in WT LFD (n=7), CPEB4$^{KO}$ LFD (n=6), WT HFD (n=22) and CPEB4$^{KO}$ HFD (n=12). **(C)** ALT in livers from WT and CPEB4$^{KO}$ mice fed ND or HFD (n=6 for ND fed mice, n=12 for HFD fed mice). **(D)** Representative Oil-red staining in liver sections of the same animals. **(E)** Liver triglyceride content normalized with liver weight from WT and CPEB4$^{KO}$ mice fed with ND (n=7 and 6, respectively) or HFD (n=9 and 6, respectively). **p<0.005. All results are expressed as mean ± SEM.

## 5.4 CPEB4 is responsible for the adipocyte reprograming in a pathologic context.

### 5.4.1 CPEB4 regulates adipogenesis in murine white adipose tissue

Given that the predominant cell type present in adipose tissue are mature adipocytes we examined the specific role of CPEB4 in this cell type. CPEB4 mRNA and protein levels progressively increased over the course of adipocyte 3T3-L1 differentiation **(Figure 22A,B)**. We then isolated undifferentiated primary preadipocytes from epididymal WAT of 4 month old male mice. We chemically induced preadipocytes to differentiate into mature adipocytes and extracted mRNA. In line with the increased expression of CPEB4 in mature 3T3-L1 adipocyte-like cells, mature primary adipocytes showed also increased levels of CPEB4 compared to their own preadipocytes **(Figure 22C,D).** These results indicate that CPEB4 could be important during the adipogenic process.

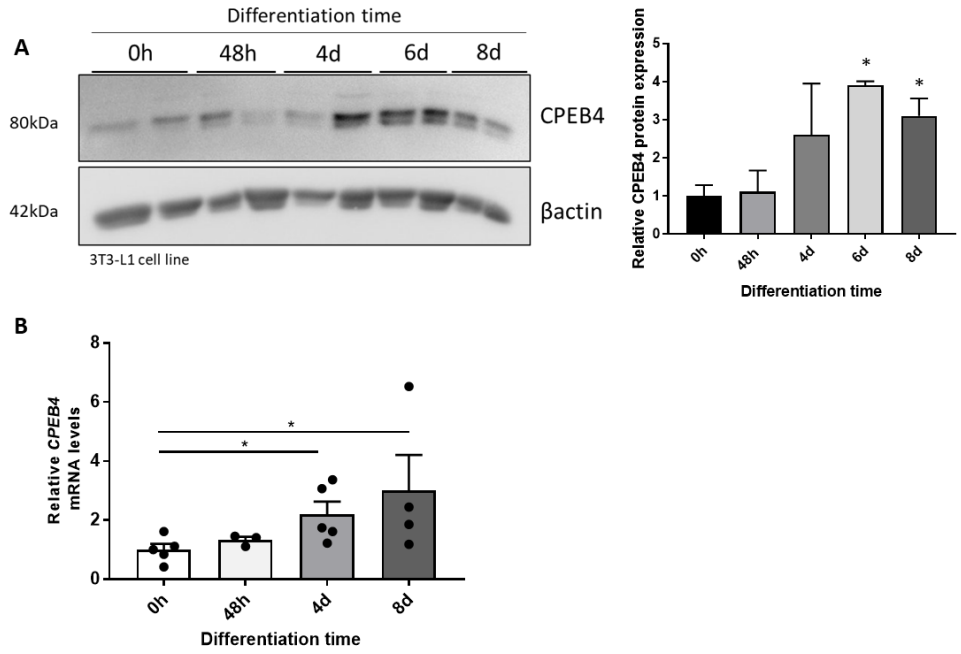

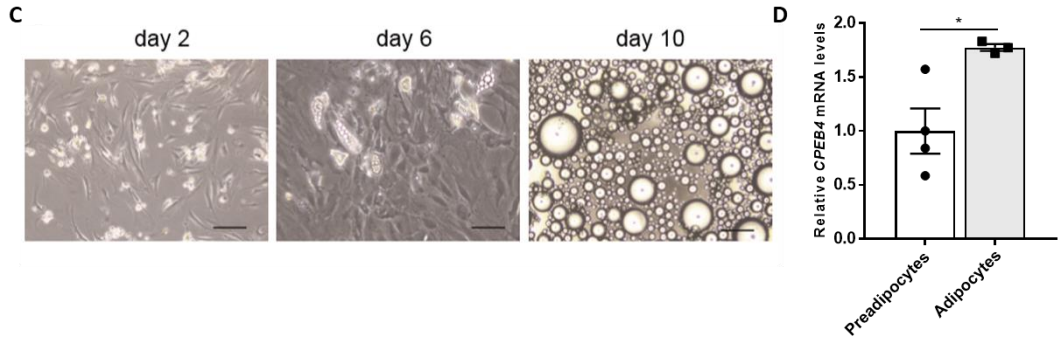


**Figure 22. CPEB4 expression increases during adipogenesis. (A)** Immunoblotting and quantification of CPEB4 protein expression during 3T3-L1 differentiation. **(B)** CPEB4 mRNA levels during 3T3-L1 differentiation. *p<0.05 **(C)** Phase contrast micrographs of adipocytes. Scale bar 100µm. **(D)** CPEB4 mRNA levels on mice epididymal adipocytes compared with isolated preadipocytes. *p<0.05**.** All results are expressed as mean ± SEM.

To functionally test for intrinsically altered white adipocyte differentiation potential after CPEB4 depletion, we conducted loss-of-function studies in vitro. We silenced CPEB4 expression in 3T3-L1 cells using short hairpin RNAs (shRNAs). We transfected 3T3-L1 cells with recombinant lentiviruses expressing IPTG inducible shRNAs against CPEB4 (shCPEB4), and compared with 3T3-L1 cells expressing a control scramble shRNAs (shSCR). Differentiated 3T3-L1 adipocytes, efficiently CPEB4 silenced, showed reduced levels of the adipogenic marker Perilipin1 **(Figure 23A).** Knowing that the adipocyte maturity depends on a first instance in its capacity of accumulate lipids and enlarge lipid droplet size, we assessed fat accumulation in these cells using an Oil-Red Oro staining. 3T3-L1 shCPEB4 failed in accumulating mature lipid droplets compared to controls 3T3-L1 shSCR cells **(Figure 23B).**

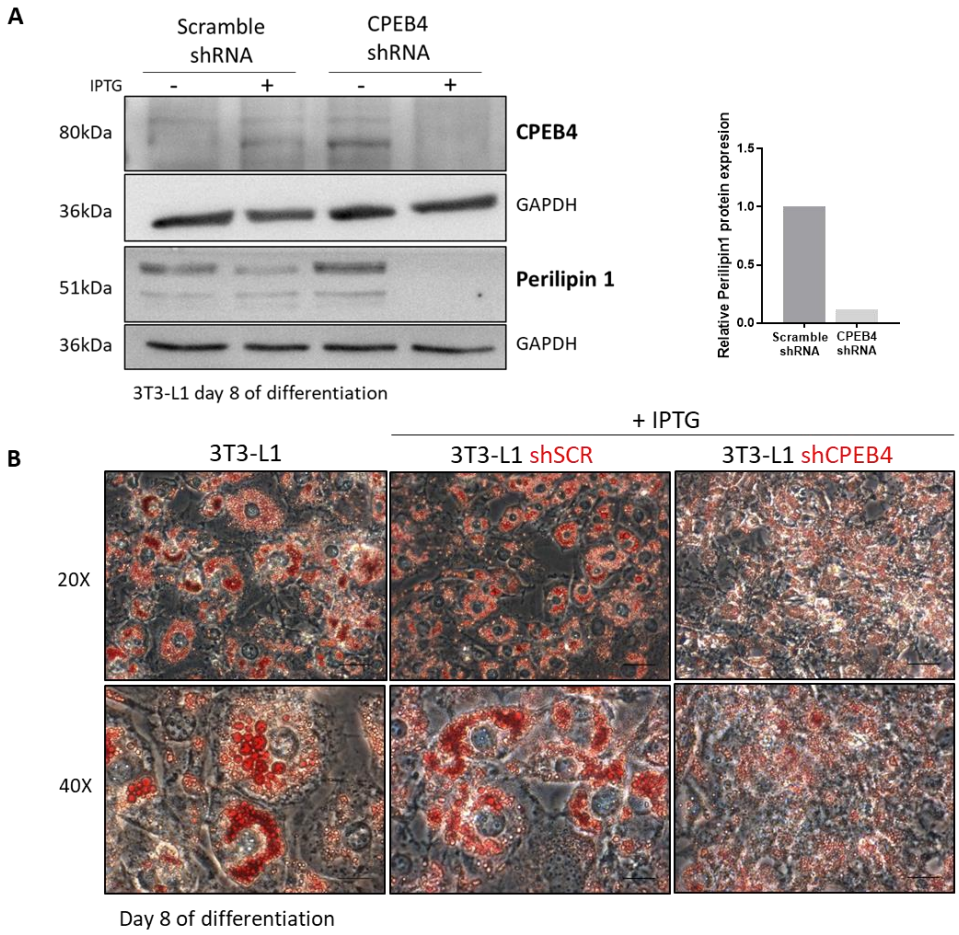


**Figure 23. 3T3-L1 adipocytes are uncapable to accumulate mature lipid droplets. (A)** CPEB4 immunoblotting in differentiated 3T3-L1 adipocytes, transfected with scramble or CPEB4 shRNA with or without IPTG. **(B)** Representative image of ORO staining in 3T3-L1 adipocytes at day 8 of differentiation.

Consistently, CPEB4 deficiency also greatly decreased genes encoding adipose markers. PPARγ and C/EBPα expression significantly decrease both at mRNA and protein level during differentiation **(Figure 24A-B).** In addition, CPEB4 deficient adipocytes showed decreased expression of the glucose transporter type 4 (GLUT4) **(Figure 24C-D).** All together, these data indicate that CPEB4 enhances the adipogenic programme in preadipocytes.

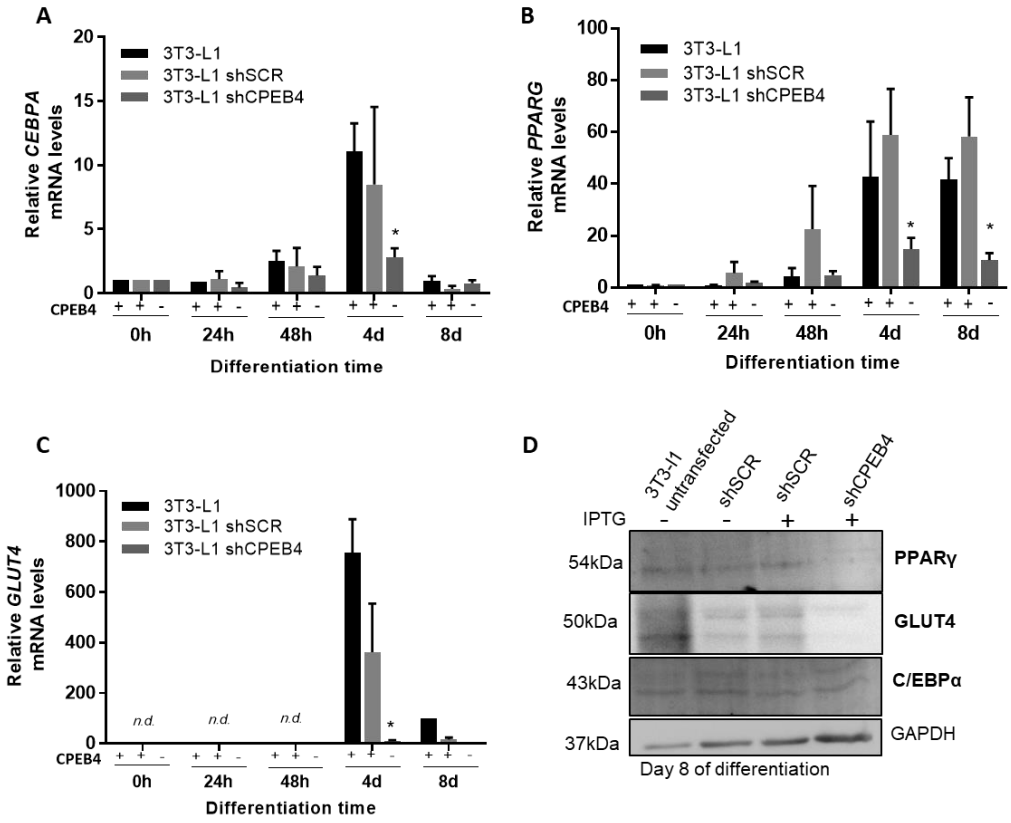


**Figure 24. Adipogenic transcription factors expression decrease in CPEB4 knockdown adipocytes. (A-C)** C/EBPα, PPARγ and GLUT4 mRNA expression during adipocyte differentiation. **(D)** PPARγ, GLUT4 and C/EBPα protein levels in mature adipocytes transfected with scramble or CPEB4 shRNA. *n* = 3 independent experiments. *p<0.05. All results are expressed as mean ± SEM.

### 5.4.2 CPEB4 favours the migration and inflammatory infiltration in visceral adipose tissue

We next used the knockdown of CPEB4 in mouse 3T3-L1 preadipocytes to further decipher the causal relationship between adipocyte CPEB4 expression and macrophage activation in obesity. CPEB4-depleted preadipocytes were induced to differentiate into mature adipocytes for 10 days, and then exposed to free fatty acids (palmitic, oleic and linoleic acids, which are abundant in obese WAT) for up to 24 hours, to mimic the in vivo context of high-fat diet feeding and WAT inflammation. We harvested cell-free conditioned medium from these mature adipocytes post stimulation and used it to treat primary mouse bone marrow-derived macrophages (BMDM) isolated from wild-type mice and placed in functional scratch migration assays with Ibidi silicone inserts. As controls, macrophages were incubated with conditioned media from 3T3-L1 adipocytes transfected with scramble shRNAs with or without IPTG, transfected with CPEB4 shRNA without IPTG, or left untransfected **(Figure 25A).** This in vitro system models the pathophysiology of obesity-related WAT inflammation where most of the WAT macrophages are derived from bone marrow. Interestingly, the migratory properties of macrophages were significantly impaired when exposed to conditioned media from CPEB4KD adipocytes **(Figure 25B),** which is consistent with a role for CPEB4 inducing the production of adipocyte-derived factors which paracrinely promote macrophage migration during obesity.

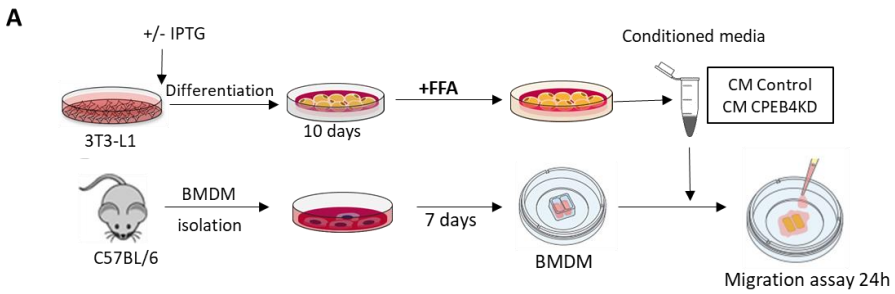

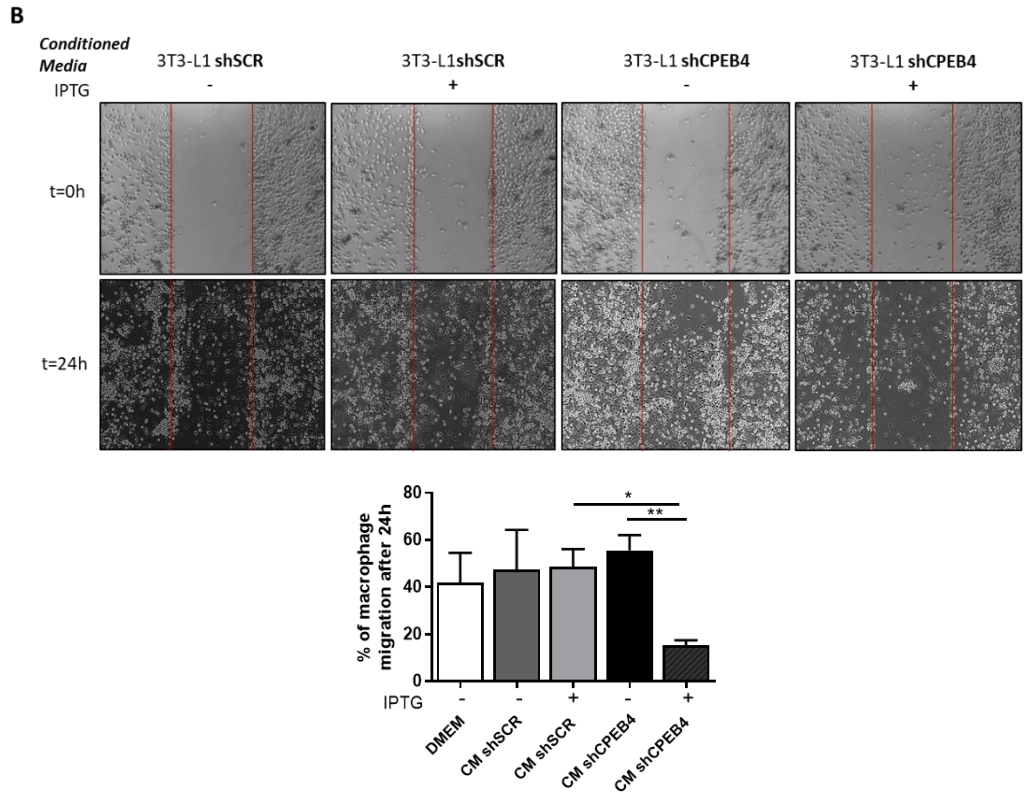


**Figure 25. CPEB4 knockdown in 3T3-l1 adipocytes decrease macrophage migration in a scratch protocol. (A)** Schematic representation of the migration protocol. **(B)** BMDM migration assay using conditioned media from 3T3-l1 cells transfected with scramble or CPEB4 shRNA for 24h. *n* = 3 independent experiments. **p<0.005. All results are expressed as mean ± SEM.

To further define the role of CPEB4 regulating the crosstalk between adipocytes and macrophages, we analyzed the ability of macrophages to directionally respond to chemoattractants released by adipocytes. For this purpose, we designed cell migration transwell assays where conditioned medium from adipocytes was placed in the lower part of a chamber and bone marrow-derived macrophages were seeded in the upper chamber **(Figure 26A)**. We found that conditioned medium from wild-type adipocytes (either untransfected or transfected with scramble shRNA) resulted in marked increase in macrophage migration, which was even greater than the migration elicited by the potent chemotactic factor MCP-1. This migratory ability was severely reduced in macrophages treated with conditioned medium from adipocytes lacking CPEB4 (i.e., transfected with CPEB4 shRNA) **(Figure 26B)**, indicating that the CPEB4-dependent release of factor(s) from adipocytes was the trigger for the macrophage migration.

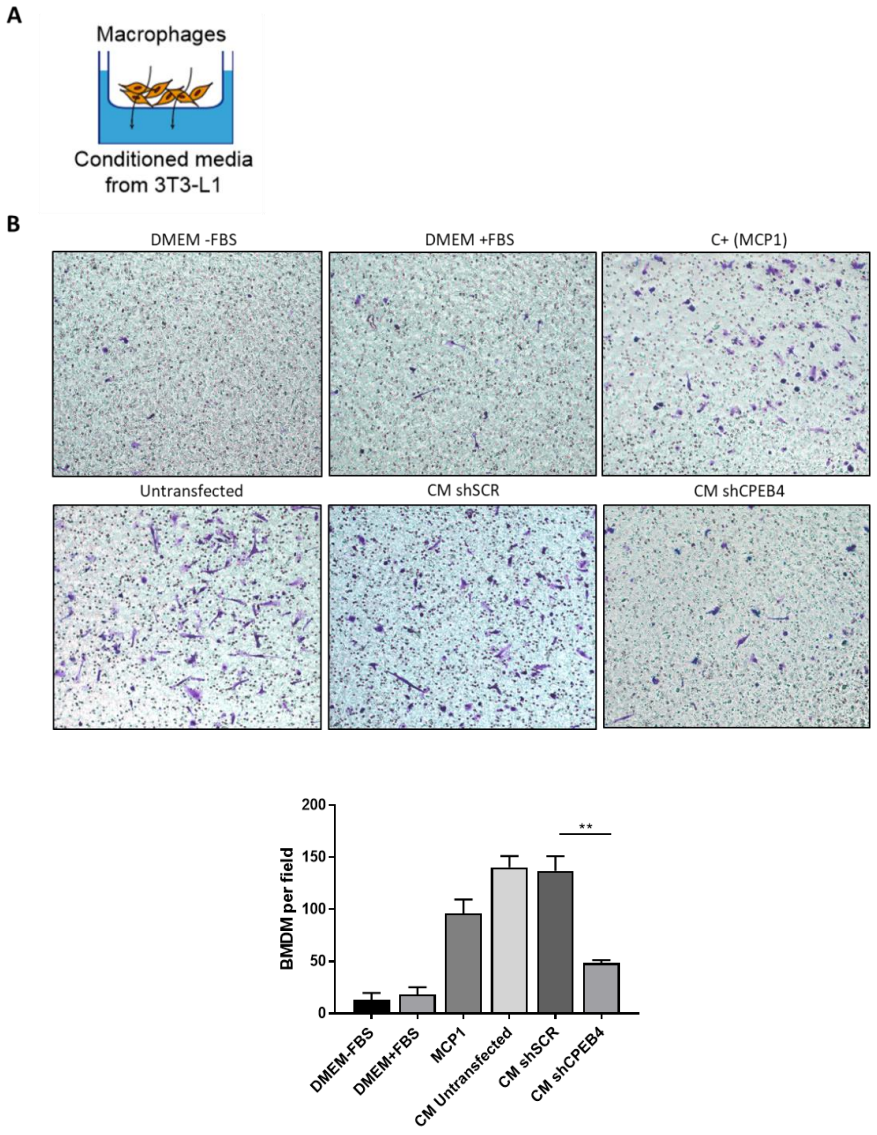


**Figure 26**. **CPEB4 knockdown in 3T3-l1 adipocytes decrease macrophage migration in a transwel protocol. (A)** Schematic representation of the migration transwell protocol. **(B)** Transwell cell migration assay showing that migration of macrophages is inhibited by conditioned media derived from CPEB4 shRNA-transfected adipocytes, compared with macrophages exposed to conditioned media from scramble shRNA-transfected or untransfected adipocytes. **p<0.005 Images taken at 20x.

Interestingly, the supernatant from macrophages treated during 24 hours with conditioned media from FFA-treated CPEB4shRNA-transfected 3T3-L1 adipocytes exhibited increased protein expression of the potent anti-inflammatory cytokine IL10 **(Figure 27B)**, which is characteristically secreted by macrophages with an anti-inflammatory profile, compared with macrophages treated with conditioned media from FFA-treated wild-type adipocytes. These results collectively suggest that differentiated obese adipocytes, which express high levels of CPEB4, generate and release factors that drive at least part of the migratory and inflammatory phenotype of adipose macrophages, in a critical process that is CPEB4 dependent since adipocytes lacking CPEB4 do not have this capacity.

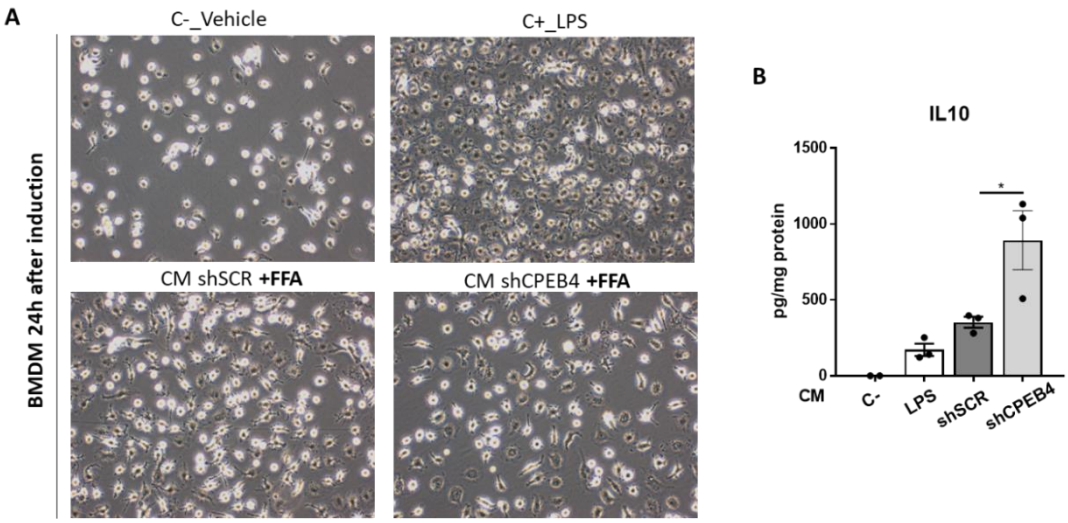


**Figure 27**. **Macrophage response to adipocyte conditioned media in the presence or absence of CPEB4 (A)** Phase contrast micrographs of isolated BMDM treated for 24h with conditioned media or controls. **(B)** Concentration of the anti-inflammatory cytokine Il10 in macrophages exposed to the conditioned media from shSCR or shCPEB4 transfected adipocytes treated for 24h with FFA. *p<0.05, *n* = 3 independent experiments**.**

To address whether this reduced macrophage migratory capacity induced by CPEB4 silencing in adipocytes was mediated by a direct effect of CPEB4 on mature adipocytes and not by the observed effect of CPEB4 on adipogenesis, and differentiation, we generated mice with tamoxifen-inducible CPEB4 deletion ($CPEB4^{IKO}$). We isolated and cultured stromal vascular fraction preadipocytes from epididymal WAT of these mice.

Mouse primary preadipocytes were subjected to differentiation and then stimulation with free fatty acids. Differentiated, mature adipocytes were then exposed to tamoxifen (1 µM, from seeding to differentiation day 10) to induce depletion of CPEB4. Control adipocytes retaining CPEB4 expression were exposed to vehicle. Adipocyte-conditioned medium was collected and used to treat bone marrow-derived macrophages obtained from wild-type mice and measure their migration **(Figure 28A)**. Notably, macrophages exposed to conditioned medium derived from CPEB4$^{IKO}$ adipocytes exhibited less migration capability than did macrophages exposed to conditioned medium derived from control wild-type adipocytes **(Figure 28B)**, strongly indicating that this effect was a CPEB4-mediated cell autonomous effect on the already mature adipocyte and suggesting that this function is largely linked to the anti-inflammatory properties of CPEB4-depleted adipocytes rather than a defect in differentiation itself.

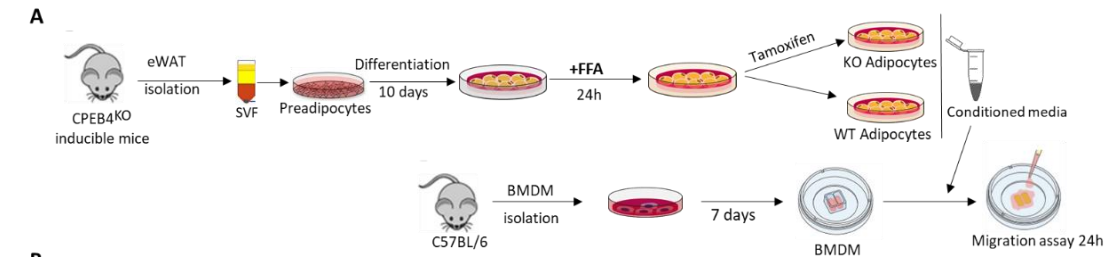


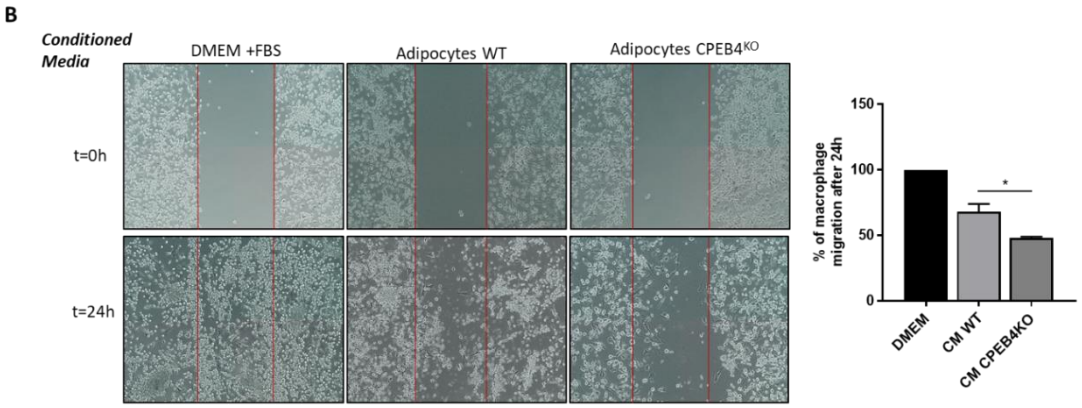


**Figure 28. CPEB4 knockdown in primary adipocytes decrease macrophage migration. (A)** Schematic representation of the migration protocol. **(B)** BMDM migration assay using conditioned media from primary adipocytes isolated from inducible CPEB4KO mice for 24h. *n* = 3 independent experiments. *p<0.05. All results are expressed as mean ± SEM.

So far, we have seen not only CPEB4 expression to be essential for the adipose tissue angiogenesis and inflammation but also that the effect seem to be adipocyte specific in our model. Since macrophages play also a crucial role in the obesity-driven inflammation of the adipose tissue, we wanted to discard the possibility of the phenotypic changes in the CPEB4$^{KO}$ mice coming not only from an adipocyte specific effect but also from an effect over the macrophage. To explore it, we used a specific myeloid CPEB4$^{KO}$ model (CPEB4MKO) fed with HFD for 15 weeks. After this period, we found that mice lacking CPEB4 exclusively in myeloid cells, when placed on a HFD, showed no difference in body weight gain nor in growth of visceral WAT compared to WT in the same diet **(Figure 29A,B)**.

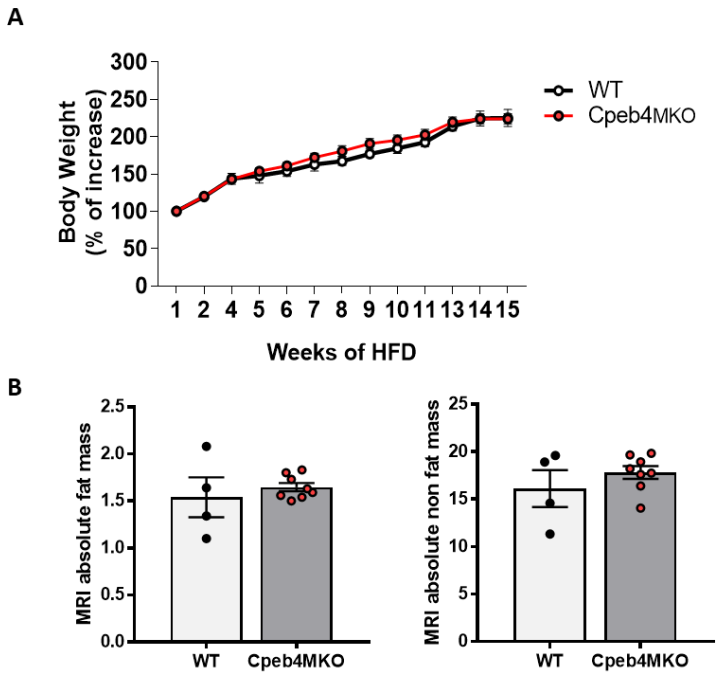


**Figure 29. Myeloid specific CPEB4 knockdown does not alter the fat accumulation under a HFD.** **(A)** Body weight profile of WT and CPEB4MKO mice fed with HFD for 16 weeks (n=6-10/genotype). **(B)** Absolute fat and lean mass measured with magnetic resonance imaging (MRI). Statistical analysis was performed by t- test.

The histological evaluation of the eWAT by a pathologist showed a tendency in the CPEB4MKO mice to have a slightly more severe inflammatory infiltration. **(Figure 30A,B).** These findings rule out the possibility that the effects observed in the whole-body CPEB4$^{KO}$ mice on HFD were attributed to deletion of CPEB4 in macrophages.

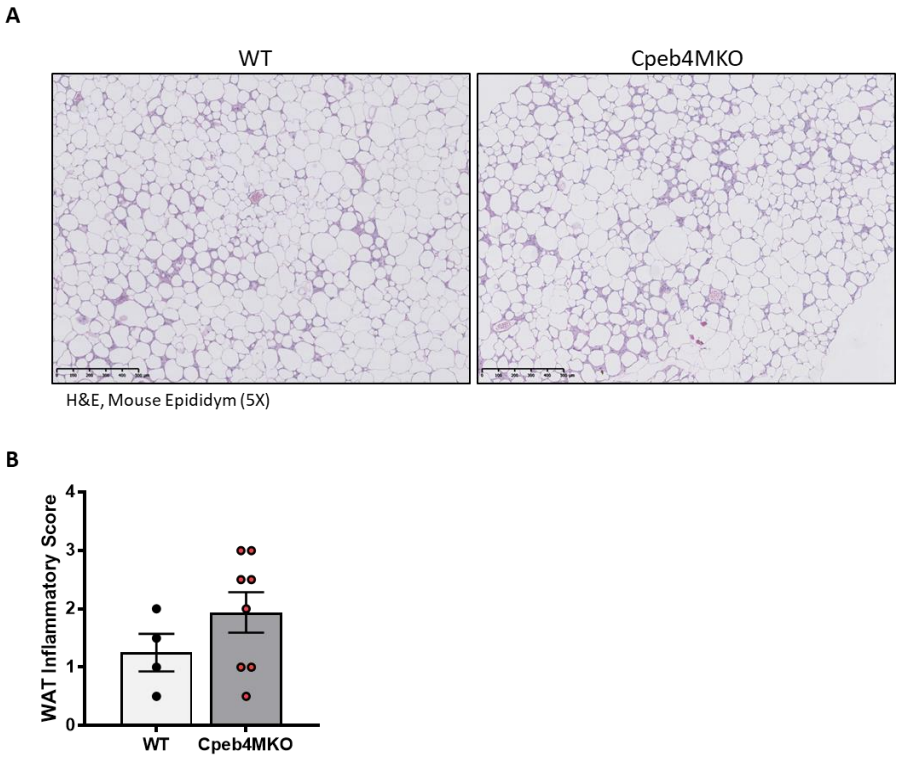


**Figure 30. Myeloid specific CPEB4 knockdown does not show significantly more WAT inflammatory infiltrate. (A)** Representative images of haematoxylin and eosin staining in paraffin embedded epididymal mouse sections. **(B)** Histological score of WAT inflammatory infiltrate in the epididymal WAT.

# DISCUSSION

# 6 Discussion

## 6.1 The obesity epidemic and liver disease

Obesity is a growing epidemic worldwide and a major risk factor to suffer chronic liver disease. One of the earliest manifestations of obesity is non-alcoholic fatty liver disease (NAFLD), which may progress to non-alcoholic steatohepatitis (NASH), fibrosis/cirrhosis, and eventually liver cancer[1-4]. Obesity is in fact per se a risk factor for progression in the natural history of chronic liver disease.

Understanding the cellular and molecular mechanisms underlying the interaction between obesity and chronic liver disease is essential to identify new and more efficient therapeutic targets to treat patients in the first stages of the disease and prevent the development of overt pathology. Most studies in this regard have been focused on obesity-related disturbances taking place within the liver. However, the implications of obesity on extrahepatic abdominal organs are of major relevance to get the whole picture of the disease. This is particularly important in the context of liver injury since pathologic processes occurring outside this organ play a major role in disease progression and aggravation. These processes would coexist with the typical obesity-abdominal alterations, acting in a parallel or sequential and somehow synergic way to cause the full spectrum of the disease phenotype.

Filling this knowledge gap was the aim of this PhD Thesis.

## 6.2 Obesity aggravates extrahepatic manifestations of chronic liver disease

To determine the impact of obesity on chronic liver disease, we used an animal model of high-fat diet feeding plus partial portal vein ligation. The use of this model with two hits is convenient and ideal because: (a) it develops all the abdominal manifestations of obesity resembling human disease; (b) it closely reproduces the extrahepatic alterations found in humans with chronic liver disease; (c) it mimics the pathogenesis of human liver steatosis; and (d) it shows a high homogeneity and reproducibility.

We aimed to treat the complexity of the disease studying the implication of the extrahepatic territory in the CLDs development. In the first part of this work, we showed how obesity exacerbates the extrahepatic complications associated to liver disease affecting the adipose tissue depots. In line with previous reports[156,157] we show the effect

of a HFD in the development of NAFLD increasing the adipose depot weight. It must be stressed here that the increase compared with normal diet fed rats was not as pronounced as expecting, thus creating a mild model with a low grade chronic inflammation. We tried to address how portal hypertension in an already stablished obese subject could affect the visceral adipose tissue and eventually the liver state. We show here how obese animals with the extrahepatic manifestations of liver disease due to the PPVL surgery present the most enlarged adipocytes in its epididymal and mesenteric white depots. All obese rats presented enlarged adipocytes compared to lean rats, as highly reported[158,159], but interestingly, although without significant differences in adiposity, the portal hypertensive group showed the biggest adipocytes. Highly enlarged adipocytes have been described as a feature of a more pathologic adipose tissue [160,161,162]. Thus, if obesity can aggravate the extrahepatic manifestations of chronic liver disease, it is tempting to speculate that it could also highly aggravate the liver disease phenotype in a more severe scenario such as liver failure.

Indeed, many proinflammatory markers in the mesenteric adipose tissue were upregulated in NAFLD rats. Within the inflammatory response that occurs during obesity, adipose tissue macrophages (ATM) are considered responsible for the adipose tissue remodelling [163,67]. In our study, CD163 macrophage marker, commonly associated with a resolutive inflammatory response was decreased in obese PPVL rats compared to the Sham group. In concordance, the proinflammatory macrophage marker CD68 was overexpressed in the mesentery of this same obese-PPVL group. This observation further reinforces the idea of a more proinflammatory adipose tissue in obese animals with a liver disease pathology.

Whereas macrophages in lean mice and humans make up around 5% of the cells in adipose tissue, during obesity they constitute up to 50% of all adipose tissue cells [164,165] with the consequences this implies. As well as increasing in number, adipose tissue macrophages (ATMs) change their localisation during obesity [67]. We were able to evidence this observation in our model by measuring CD68 expression in different mesenteric regions. We show how in obese portal hypertensive rats, CD68 expression converges mainly in the serous layer of the mesentery. Considering the serous layer as the outer layer of the mesentery which is in contact with the abdominal and peritoneal cavity and so with important internal organs, this result points toward a more proinflammatory state in the abdominal region which could compromise the health-span [166,167].

The portal hypertensive model PPVL, largely described by our group and others, mimics the extrahepatic manifestations of the liver disease and so results in alterations in the

splanchnic territory rather than the liver [168,169]. Nevertheless, with the obese component in the scene, exacerbating the extrahepatic inflammation, is there an affection in the liver? We propose that the increased inflammation in abdominal adipose tissues, which through the portal flux reach the liver, could increase the amount of proinflammatory cytokines arriving at the liver. Indeed, although not finding differences in liver lipid metabolism, we report here an increased transaminase levels in the liver of obese animals with a portal hypertension of only 7 days. This result suggests the profound command of the extrahepatic adipose tissue over other metabolic organs as the liver.

Our next approach was to study if the angiogenesis results altered when there is a previous obese pathology. Knowing that tissue growth is dependent on its vasculature [170,171], we expected in the HFD PPVL animals a worsen angiogenic state with more pathologic vasculature due to the need of the adipose tissue to expand and the harmful that obesity per se exhibits in our model. Instead, we show how in an obese established rat model the induction of portal hypertension does not correlate with an increase number of vessels in the mesentery. Our result goes in line with several publications supporting the idea that the synergy between adipose tissue expansion and vascularization appears to be lost during obesity [155,172,173]. Sung et al. demonstrate that improving vascular network in adipose tissue protects obese mice against metabolic complications even at later stages of disease [174]. Thus, it is likely that impaired vascularization in our model may contribute to metabolic perturbations as a result of the stress and inflammatory responses. All together these observations could explain, at least in part, the decreased vessel number observed in our PPVL model with a more inflamed adipose tissue. Nevertheless, more research should be done in the mechanistic behind the adipose tissue vasculature.

## 6.3 CPEB4 as a key factor in the adipose tissue homeostasis disruption

Several recent studies have unveiled important CPEB4 functions in health and disease. CPEB4 has been reported to regulate the lipid metabolism in hepatic steatosis in a hepatocyte specific way[148]. Moreover, numerous works unveil a role for CPEB4 in other chronic liver diseases. In previous results of our group we were able to demonstrate that CPEB4 protein expression is upregulated in the cirrhotic liver of human patients and animal models of liver fibrosis and cirrhosis. We also found that CPEB4 specifically regulates the pro-vasculogenic and pro angiogenic responses in cirrhotic livers and extrahepatic organs (mesenteric vascular bed, portosystemic collateral circulation)[149,150]. As a proangiogenic, CPEB4 is able to promote VEGF mRNA translation regulation, targeting specifically the pathologic angiogenesis. Regarding its pro-vasculogenic

response, CPEB4 has been demonstrated to regulate the transient-ampliying cells responsible to generate new vessels. More recently, we demonstrated that CPEB4 induces a metabolic reprogramming in hepatic stellate cells that is essential to promote liver fibrosis[151].

All these results pointed us to study the possibility of CPEB4 being also involved in the extrahepatic manifestations of liver disease in a context of obesity. In this work we found for the first time an overexpression of CPEB4 in adipose tissue of obese animals. Not only that, but obese animals presenting also a portal hypertensive pathology showed even higher levels of CPEB4 in their white adipose tissues suggesting an overall link of CPEB4 in the obese-liver disease relationship. Moreover, we further supported the relevance of this finding demonstrating how this CPEB4 increase in pathologic adipose tissue happens also in human obese patients. Both obese patients with or without a NAFLD pathology overexpressed CPEB4 suggesting a specific role of CPEB4 in pathologic adipose tissue.

Knowing as well that CPEB4 expression is critical in response to a challenge, these observations brought us to hypothesize a possible implication of CPEB4 in the adipose tissue altered metabolism and therefore contributing to the adverse effects of obesity in liver disease. To test this hypothesis, we generated CPEB4 knockout mice and treat these animals and their wild-type littermates with high-fat diet or normal diet for 16 weeks. Consistent with our hypothesis, we observed how adult mice with CPEB4 deletion display decreased adiposity in a NAFLD model of 16 weeks of high fat diet challenge. This reduction in the final white depot weight was the cause of the final body weight observed in the $CPEB4^{KO}$ mice compared to WT mice.

## 6.4 Lack of CPEB4 ameliorates adipose tissue response to HFD

Several mechanisms have been reported in the literature in order to explain adiposity alterations. Generally, they occur through changes in cell size or/and number [175,176]. Excluding alterations in food intake, the reduction of adiposity in the CPEB4 depleted mice under a HFD exposure is likely due to a marked reduction in fat cell mass and in a decreased proliferation of white adipose tissue. Beside, we analysed if the main function of the adipose tissue was altered by the lack of CPEB4. Although an increased lipolytic potential could explain partially the decreased adiposity of the $CPEB4^{KO}$ mice, we report here how under HFD conditions and without a fasting stimuli, $CPEB4^{KO}$ mice exhibit a decreased lipolytic activity, ruling out its implication in the phenotype.

Not surprisingly, approaches that reduce adipose tissue depots attenuate proinflammatory adipokine levels and reduce the severity of their resultant pathologies [177,178]. In this line, we report here both a decrease in the angiogenic response as well as a decreased expression of the well-established proinflammatory markers in the CPEB4$^{KO}$ fed with a HFD. Interestingly, most of these markers are macrophage-related. It is known that 90% of ATM are localized to dead adipocytes during chronic inflammation, forming crown like structures [179,180,67]. Here, we report a remarkably decrease in the epididymal CLS of the CPEB4$^{KO}$ mice compared to the WT. This decrease was accompanied by a decrease in the monocyte recruiting factor, MCP-1. Moreover, in line with other studies[181,182] we show how the percentage of CD11c$^{+}$CD206$^{+}$ ATMs with mixed M1/M2 phenotype, increase in obese animals. Phenotypically, macrophages exist along a spectrum, the poles of which have been designated classically as M1 and M2. This CD11c+/CD206+ mixed population has been recently described as metabolic macrophages (Mme), and correlate with the BMI and ROS production[66,183], consequently associated with a more proinflamatory phenotype[184]. Interestingly, lack of CPEB4 was able to reduce the metabolic macrophage population. CPEB4$^{KO}$ mice exhibited a higher percentage of resident macrophages compared to proinflammatory ones, which express anti-inflammatory molecules, regulate adipocyte lipid metabolism and act as efferocytes to clear apoptotic cells and resolve inflammation. Moreover, Mme macrophages mediate their inflammatory responses to fatty acids through TLR4 expression[185]. In the same line we report a decrease of TLR4 expression in CPEB4$^{KO}$ Mice. We are able to demonstrate how in our model in the absence of CPEB4 during a high fat diet exposure the proinflammatory response is strongly reduced, specifically in terms of macrophages. These results raise a key question: is this CPEB4 effect direct or indirect on macrophages?

In the last years, mRNA regulation by deadenylation has been described as a key element to regulate the intensity and duration of the inflammatory responses[186]. Indeed, CPEB4 was found to participate in inflammation resolution by promoting the expression of negative feedback inhibitors of the inflammatory pathway[187]. Thus, it would be logical to expect an increase in the proinflammatory macrophage response on the CPEB4 absence. Indeed, the specific myeloid CPEB4$^{KO}$ model challenged with a HFD for 15 weeks showed a tendency to have a slightly more severe inflammatory infiltration than its WT. Thus, we believe the CPEB4 effect on the inflammatory response in our model results from an indirect effect on macrophages. Altogheter, these observations could explain, in part, the differential phenotype observed upon CPEB4 deletion in our study.

## 6.5 CPEB4, the good and the bad

One of the most complex features of CPEB4 represent its capacity to fluctuate during the development of the disease. *Maillo et al* [148] showed how during an acute stress CPEB4 acts beneficiously for the liver; hepatocyte CPEB4 levels increase to restore celular homeostasis, and its depletion exacerbates hepatosteatosis. Nevertheless, when the stress is more persistent and long-lasting over time such as 16 weeks of HFD, the CPEB4 protein in the liver remains at low levels, even below normal **(Figure 21A)** and CPEB4 depletion does not modify steatosis. But, does it stay at low levels during all the disease progression? Findings from our group demonstrate that CPEB4 protein expression is increased in the fibrotic and cirrhotic liver of human patients and animal models, where it plays a pathological role mediating angiogenesis and fibrogenesis. Ongoing research of our group indicates how in chronic stress scenarios CPEB4 is highly expressed and its depletion would be beneficial.

To add a further degree of complexity, it's known that CPEB4 differential expression not only fluctuate depending on the disease stage but also depending on the cell type where it is expressed. Recent published data provides new insights into the role of CPEB4 mediating the fibrotic process in hepatic stellate cells through glycolisis[151]. CPEB4 depletion in this scenario is able to reduce fibrogenesis in the liver.

Altogheter, these results lead us to speculate a detrimental cell-specific role for CPEB4 in the extrahepatic adipose tissue and specifically on the adipocyte cell type during HFD-induced obesity.

## 6.6 Adipogenesis is orchestrated by CPEB4

Adipogenesis is mostly defined as the process by which preadipocytes get differentiated into adipocytes. It is reflected by both the appearance of various specific mRNA and protein markers and triglyceride accumulation. Adipogenesis takes place principally in the childhood and remains constant through adulthood, since during normal homeostasis there is not much requirement for adipose tissue expansion. In normal conditions only 10% of human adipocyte renewed every year[188], although in rodent adipose tissue turnover is way higher, 0.6% adipocytes renewed every day [189].

Nevertheless, in response to a long term obesogenic environment, is adipogenesis present? Many studies suggest that while fat tissue expansion in adulthood is initially achieved by hypertrophy, a long term high fat diet stimulates fat tissue hyperplasia[190,

[191,192]. On the contrary, several studies with contrasting results claim that the pool of fat cells remains constant [188,193]. To add another layer of complexity, other recent data suggests that overnutrition induces hypertrophy or hyperplasia depending on the location of the adipose tissue affected [194]. Thus, although the debate is still open, what it is evident is that under a HFD, adipocytes need to expand, and if it happens through recruiting new adipocytes from the resident pool of progenitors, hyperplasia represents an increase in adipogenesis.

Our results show that in the absence of CPEB4, adipocytes are uncapable of accumulate lipids to form big lipid droplets characteristic of a mature adipocyte. Moreover, the master transcription factors positively regulating adipogenesis showed also reduced expression in CPEB4 deficient adipocyte cell lines during its differentiation. These results indicate a role of CPEB4 regulating adipogenesis during obesity.

## 6.7 The strong connection of CPEB4 in the adipocyte-macrophage crosstalk

As stated before, the obtained results point towards a role of CPEB4 modulating the pathological inflammation induced by an obesogenic exposure. In this regard and besides the role of CPEB4 in adipogenesis, we have also underscored a key role of this protein regulating the essential crosstalk between the adipocyte and the macrophage. As stated before, adipose tissue macrophages (ATMs) are key players in the regulation of AT homeostasis and consequently in obesity-related metabolic disorders. Through migration assays, we have found how CPEB4 levels in inflamed adipocytes regulate the macrophage infiltration in the adipose tissue. Additionally, we have found this results to be independent of the CPEB4 adipogenic function described before. Cross-talk between fat cells and their environment is typically mediated in three ways: nutritional mechanisms, neural pathways, and via the elaboration of adipokines, being this last one the main contributor [45]. Since all the validated targets described in previous works are secreted proteins, it is tempting to speculate the role of CPEB4 regulating the adipocyte secretory system.

In conclusion in this study, we believe we have deepened our understanding in the pathophysiology mechanisms involved in the first NAFLD stages where obesity is crucial. These results suggest a previously unappreciated role for CPEB4 in the adipose tissue regulation during obesity, thereby turning it into a potential therapeutic target, where its specific inhibition could help to resolve the obesity-induced inflammation and to a bigger extend, the metabolic syndrome.

## 6.8 Limitations of the study and future perspectives

As George Bernard Shaw state once, “Science never solves a problem without creating 10 more”. Therefore, I would like to discuss how I would address the future of this project trying to unveil the new paths that we have opened during these years.

Regarding the first part of this study, results obtained in the mild NAFLD model pointed towards an effect of the adipose tissue in the exacerbation of the extrahepatic manifestations of liver disease. In this line, we believe the use of a more severe disease model such as NASH or cirrhosis, could positively complement the results observed in the mild model presented here.

On the second part of this project, the precise molecular mechanism underlying the phenotype observed upon CPEB4 deletion is still incompletely understood. HFD is largely described to change the host microbiome, producing a disruption in the intestinal barrier and thus, affecting several systemic organs. In this regard, an omission in the project is the participation of the gut in the whole observed phenotype after CPEB4 deletion. The aim of this thesis in a first instance was to study the role of CPEB4 in all the components of the gut-liver axis, as it is undoubtable important in the development of NAFLD. Although for a matter of time the intestine is still an ongoing focus of research, preliminary results pointed towards CPEB4 participating in the leakiness of the gut barrier during its disruption by a high fat diet. We are currently planning to confirm this result and assess in detail the mechanisms behind, using our total CPEB4 KO model. Indeed, if the absence of CPEB4 would be able to maintain the intestinal barrier integrity against a HFD insult, this result would support the healthier inflammatory state of the adipose tissue.

On the other side, to fully understand the specific CPEB4 adipocyte function, one of the major limitations of this project has been the lack of an in vivo specific adipocyte CPEB4 KO. Since the time limitation left, after discovering the potential role of CPEB4 in the adipocyte cell type, we decided to use an in-vitro approach to assess its functions and mechanisms on this cellular type. Thus, we strongly think, in order to bring the finding one step closer to the clinics, it is needed to demonstrate the cell specific CPEB4 KO effect in vivo. The results derived from the cell specific KO analysis will likely confirm our observations in vitro. However, if the specific KO phenotype does not follow the observations seen in the full body KO phenotype, it will point towards a global contribution effect of CPEB4 rather than a cell autonomous CPEB4 function on the adipocyte.

We also believe, in order to better understand CPEB4 dynamics in an obese context, it is necessary to investigate the mechanism behind the CPEB4 regulation of adipogenesis. Although the obtained results point towards CPEB4 controlling terminal adipogenesis in a pathologic context, to study the CPEB4 contribution on early-stage adipocyte differentiation, it would be necessary to use a mesenchymal stem cells approach, since 3T3-L1 are already committed to an adipocyte lineage.

Finally, and since CPEB paralogs have been demonstrated to be able to lead compensatory mechanisms by the CPEB4 absence, it would be interesting to explore how the other CPEB paralogs contribute in the adipose tissue response to an obesogenic insult. Although CPEB4 represents the CPEB isoform whose expression levels behave more similarly comparing in vivo and in vitro adipocytes and, since its expression increases during adipocyte differentiation **(Supplementary Figure)**, we still cannot exclude the involvement of CPEB1, CPEB2 or CPEB3 on the system specially in the CPEB4 absence.

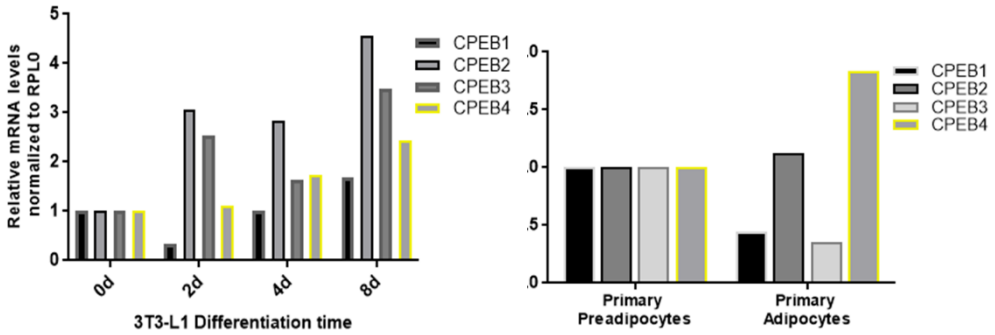


**Supplementary Figure.** CPEB4 paralog follows a similar expression pattern in 3T3-L1 differentiation and primary adipocytes differentiation. Expression levels of CPEB paralogs in adipocytes during (A) adipocyte differentiation of 3T3-L1 cells and (B) on primary mice isolated preadipocytes and adipocytes.

Regarding experimental settings, there is no doubt that the major challenge of this thesis was to obtain a non-degraded and pure immunoprecipitated RNA from fat adipocytes to further on sequence it (ongoing work). Working with adipose tissue has been a constant challenge during all this thesis. Without time limitations and with the experience gained, we think it would be useful to perform the RNA-seq experiment in primary adipocytes and compare it with the in vivo data, since in vitro adipocyte could display specific features that may be different in tissue-resident adipocytes in vivo. Therefore, our present data support that the anti-adipogenic and anti-inflammatory phenotype of the full CPEB4$^{KO}$ mice on HFD is mostly driven by the absence of CPEB4 in the adipocyte.

# CONCLUSIONS

# 7 Conclusions

The present study provides new insights into the contribution of the extrahepatic territory in the NAFLD development.

Moreover, in this study we have found CPEB4 to be biological relevant in the adipose tissue during the obesity process. We describe a new CPEB4 role and we propose that CPEB4 function is required in vivo and in vitro for the adipose tissue expansion that takes place during obesity.

The main conclusions of this work are the following:

1. The pathogenesis and severity of liver disease is exacerbated during obesity, not only because of excessive accumulation of fat within the liver (steatosis), but also due to the presence of an enlarged and proinflammatory extrahepatic visceral adipose tissue which contributes to further increase the risk of progression and aggravation of the disease.

3. CPEB4 is overexpressed in pathologic adipose tissue, both in humans and rodents. During obesity and obesity related diseases, CPEB4 protein expression increases in WAT and plays a major role orchestrating and contributing to the complex phenotype of the obese visceral adipose tissue.

4. CPEB4 promotes adiposity by regulating adipocyte differentiation and proliferation in visceral adipose tissue. The knockdown of CPEB4 in adult mice exposed to a HFD limits the adipose tissue accumulation as well as improves all the associated adipose tissue state.

5. The leaner phenotype of $CPEB4^{KO}$ mice is not a consequence of an increased lipolysis but the incapability of the adipocyte to accumulate fat

6. CPEB4 promotes adipose tissue inflammation by regulating the crosstalk between adipocytes and adipose tissue macrophages.

7. CPEB4 is responsible for the adipocyte posttranscriptional reprogramming in a pathologic context.

8. Depletion of CPEB4 is beneficial to counteract the deleterious effects of obesity, by reducing adipogenesis and the proinflammatory state of the obese white adipose tissue.

# BIBLIOGRAPHY

# 8 Bibliography


1. Andrew M.Moon Amit G.Singal Elliot B.Tapper. Contemporary Epidemiology of Chronic Liver Disease and Cirrhosis. *Clin. Gastroenterol. Hepatol.* (2019).

2. Bosch, J., Groszmann, R. J. & Shah, V. Evolution in the understanding of the pathophysiological basis of portal hypertension. *J. Hepatol.* **62**, 1–22 (2015).

3. Ishibashi, H., Nakamura, M., Komori, A., Migita, K. & Shimoda, S. Liver architecture, cell function, and disease. *Semin. Immunopathol.* **31**, 399–409 (2009).

4. Bilzer, M., Roggel, F. & Gerbes, A. L. Role of Kupffer cells in host defense and liver disease. *Liver Int.* **26**, 1175–1186 (2006).

5. Toosi, A. E. rfan. K. Liver Fibrosis: Causes and Methods of Assessment, A Review. *Rom. J. Intern. Med.* **53**, 304–314 (2015).

6. Parola, M. & Pinzani, M. Liver fibrosis: Pathophysiology, pathogenetic targets and clinical issues. *Mol. Aspects Med.* **65**, 37–55 (2019).

7. Fernández, M. *et al.* Angiogenesis in liver disease. *J. Hepatol.* **50**, 604–620 (2009).

8. Groszmann, R. J. & Abraldes, J. G. Portal Hypertension. **39**, 125–130 (2005).

9. Fernandez, M., Vizzutti, F., Garcia-Pagan, J. C., Rodes, J. & Bosch, J. Anti-VEGF Receptor-2 Monoclonal Antibody Prevents Portal-Systemic Collateral Vessel Formation in Portal Hypertensive Mice. *Gastroenterology* **126**, 886–894 (2004).

10. Peter Carmeliet, R. K. J. Molecular mechanisms and clinical applications of angiogenesis. *Nature* **473**, 298–307 (2011).

11. Iredale, J. P. Models of liver fibrosis: exploring the dynamic nature of inflammation and repair in a solid organ. **117**, 539–548 (2007).

12. Gracia-Sancho, J., Maeso-Díaz, R., Fernández-Iglesias, A., Navarro-Zornoza, M. & Bosch, J. New cellular and molecular targets for the treatment of portal hypertension. *Hepatol. Int.* **9**, 183–191 (2015).

13. L.Friedman, S. Liver fibrosis – from bench to bedside. *J. Hepatol.* **38**, (2003).

14. Blei, A. T. Portal hypertension and its complications. *Curr. Opin. Gastroenterol.* **23**, 275–282 (2007).

15. Dahai Zhang, Teruo Utsumi, Hui-Chun Huan1, Lili Gao, P. S., Chuhan Chung, Kazunori Shibao, Kohji Okamoto, Koji Yamaguchi, R. J. & Groszmann, Levente Jozsef, Zhengrong Hao, William C. Sessa, and Y. I. Reticulon 4B (Nogo-B) Is a

Novel Regulator of Hepatic Fibrosis. *Hepatology* **27**, 1–19 (2014).

16. Ma, L. *et al.* MicroRNA-214 promotes hepatic stellate cell activation and liver fibrosis by suppressing Sufu expression article. *Cell Death Dis.* **9**, 1–13 (2018).

17. Sua, Y. & C., rez and W. microRNAs as novel regulators of angiogenesis. *Circ Res.* **104**, 442–454 (2009).

18. Bolognesi, M., Di Pascoli, M., Verardo, A. & Gatta, A. Splanchnic vasodilation and hyperdynamic circulatory syndrome in cirrhosis. *World J. Gastroenterol.* **20**, 2555–2563 (2014).

19. Groszmann, R. J. Reassessing Portal Venous Pressure Measurements. *Gastroenterology* **86**, 1611–1614 (1984).

20. Calvin Coffei, J. and O. P. The mesentery:structure, function, and role in disease. *Lancet* **1**, 238–247 (2016).

21. Sanyal, A. J., Bosch, J., Blei, A. & Arroyo, V. Portal Hypertension and Its Complications. *Gastroenterology* **134**, 1715–1728 (2008).

22. Mejias, M. *et al.* Beneficial effects of sorafenib on splanchnic, intrahepatic, and portocollateral circulations in portal hypertensive and cirrhotic rats. *Hepatology* **49**, 1245–1256 (2009).

23. Fernandez, M. Molecular pathophysiology of portal hypertension. *Hepatology* **61**, 1406–1415 (2015).

24. Singh, M. & Benencia, F. Inflammatory processes in obesity: focus on endothelial dysfunction and the role of adipokines as inflammatory mediators. *Int. Rev. Immunol.* **38**, 157–171 (2019).

25. World Health Organization. Obesity and overweight. (2018). Available at: https://www.who.int/news-room/fact-sheets/detail/obesity-and-overweight.

26. Ng, M., Fleming, T. & Robinson, M. Global, regional, and national prevalence of overweight and obesity in children and adults during 19802013: A systematic analysis for the Global Burden of Disease Study 2013 (The Lancet (2014) 384 (766-81)). *Lancet* **384**, 746 (2014).

27. Xia, Q. & Grant, S. F. A. The genetics of human obesity: Genetics of human obesity. *Ann. N. Y. Acad. Sci.* **1281**, 178–190 (2013).

28. Burton, P. R. *et al.* Genome-wide association study of 14,000 cases of seven common diseases and 3,000 shared controls. *Nature* **447**, 661–678 (2007).

29. Zeggini, E. *et al.* Multiple type 2 diabetes susceptibility genes following genome-wide association scan in UK samples. *Science (80-. ).* **316**, 1336–1341 (2007).

30. Locke, A. E. *et al.* Genetic studies of body mass index yield new insights for obesity biology. *Nature* **518**, 197–206 (2015).

31. Willer, C. J. *et al.* Six new loci associated with body mass index highlight a neuronal influence on body weight regulation. *Nat. Genet.* **41**, 25 (2009).

32. RW, C. Therapeutic options in the management of obesity. *N. Z. Med. J.* **126**, 66–81 (2013).

33. Motycka, C. A., Onge, E. S. & Miller, S. A. Treatment options for obesity and potential therapies on the horizon. *P T* **36**, 282–301 (2011).

34. Schulz, T. J. *et al.* Identification of inducible brown adipocyte progenitors residing in skeletal muscle and white fat. *Proc. Natl. Acad. Sci. U. S. A.* **108**, 143–148 (2011).

35. Coelho, M., Oliveira, T. & Fernandes, R. Biochemistry of adipose tissue: An endocrine organ. *Arch. Med. Sci.* **9**, 191–200 (2013).

36. DOLE, V. P. A relation between non-esterified fatty acids in plasma and the metabolism of glucose. *J. Clin. Invest.* **35**, 150–154 (1956).

37. J.M, F. Molecular mapping of the mouse ob mutation. *Genomics* **11**, 1054–1062 (1991).

38. Yiying Zhang, Ricardo Proenca, Margherita Maffei, Marisa Barone, L. L. & J. M. F. Positional cloning of the mouse obese gene and its human homolgue. *Nature* 425–432 (1994).

39. CM, R. Adipocyte-derived hormones, cytokines, and mediators. *Endocrine.* **29**, 81–90 (2006).

40. Ahima, R. S. & Flier, J. S. Leptin. *Annu. Rev. Physiol.* **62**, 413–37 (2000).

41. Bełtowski, J. Adiponectin and resistin - New hormones of white adipose tissue. *Med. Sci. Monit.* **9**, 55–62 (2003).

42. Gastaldelli, A., Gaggini, M. & Defronzo, R. A. Role of Adipose Tissue Insulin Resistance in the Natural History of Type 2 Diabetes : Results From the San Antonio Metabolism Study. **66**, 815–822 (2017).

43. Mark M. Yore, Ismail Syed, P. M. M.-V. *et al.* Discovery of a class of endogenous mammalian lipids with antidiabetic and anti-inflammatory effects. *Cell* **159**, 318–332 (204AD).

44. Smith, U., Kahn, B. B., Israel, B. & Medical, D. Adipose tissue regulates insulin sensitivity: role of adipogenesis, de novo lipogenesis and novel lipids. *J Intern Med.* **280**, 465–475 (2017).

45. Rosen, E. D. & Spiegelman, B. M. What we talk about when we talk about fat. *Cell* **156**, 20–44 (2014).

46. Kamstra, J. H. *et al.* Transcriptional and epigenetic mechanisms underlying enhanced in vitro adipocyte differentiation by the brominated flame retardant bde-47. *Environ. Sci. Technol.* **48**, 4110–4119 (2014).

47. Lefterova, M. I., Haakonsson, A. K., Lazar, M. A. & Mandrup, S. PPARγ and the global map of adipogenesis and beyond. *Trends Endocrinol. Metab.* **25**, 293–302 (2014).

48. Rosen, E., Eguchi, J. & Xu, Z. Transcriptional targets in adipocyte biology. *Expert Opin. Ther. Targets* **13**, 975–986 (2009).

49. Ross, S. E. *et al.* Inhibition of adipogenesis by Wnt signaling. *Science (80-. ).* **289**, 950–953 (2000).

50. Halberg, N. *et al.* Hypoxia-Inducible Factor 1 Induces Fibrosis and Insulin Resistance in White Adipose Tissue. *Mol. Cell. Biol.* **29**, 4467–4483 (2009).

51. Skurk, T., Alberti-Huber, C., Herder, C. & Hauner, H. Relationship between adipocyte size and adipokine expression and secretion. *J. Clin. Endocrinol. Metab.* **92**, 1023–1033 (2007).

52. Lemoine, A. Y., Ledoux, S. & Larger, E. Adipose tissue angiogenesis in obesity. *Thromb. Haemost.* **110**, 661–669 (2013).

53. Cao, Y. Obesity Protects Cancer from Drugs Targeting Blood Vessels. *Cell Metab.* **27**, 1163–1165 (2018).

54. Cai, X. *et al.* Angiogenesis in a 3D model containing adipose tissue stem cells and endothelial cells is mediated by canonical Wnt signaling. *Bone Res.* **5**, 1–13 (2017).

55. Nijhawans, P., Behl, T. & Bhardwaj, S. Angiogenesis in obesity. *Biomed. Pharmacother.* **126**, 110103 (2020).

56. Ghaben, A. L. & Scherer, P. E. Adipogenesis and metabolic health. *Nat. Rev. Mol. Cell Biol.* **20**, 242–258 (2019).

57. Li, M., Qian, M. & Xu, J. Vascular Endothelial Regulation of Obesity-Associated Insulin Resistance. *Front. Cardiovasc. Med.* **4**, 1–9 (2017).

58. Sikaris, K. A. The clinical biochemistry of obesity. *Clin. Biochem. Rev.* **25**, 165–81 (2004).

59. Schipper, H. S. *et al.* Natural killer T cells in adipose tissue prevent insulin resistance. *J. Clin. Invest.* **122**, 3343–3354 (2012).

60. Ellulu, M. S., Patimah, I., Khaza'ai, H., Rahmat, A. & Abed, Y. Obesity & inflammation: The linking mechanism & the complications. *Arch. Med. Sci.* **13**, 851–863 (2017).

61. Makki, K., Froguel, P. & Wolowczuk, I. Adipose Tissue in Obesity-Related Inflammation and Insulin Resistance: Cells, Cytokines, and Chemokines. *ISRN Inflamm.* **2013**, 1–12 (2013).

62. Jung, U. J. & Choi, M. S. Obesity and its metabolic complications: The role of adipokines and the relationship between obesity, inflammation, insulin resistance, dyslipidemia and nonalcoholic fatty liver disease. *Int. J. Mol. Sci.* **15**, 6184–6223 (2014).

63. Mills, C. D., Kincaid, K., Alt, J. M., Heilman, M. J. & Hill, A. M. M-1/M-2 Macrophages and the Th1/Th2 Paradigm. *J. Immunol.* **164**, 6166–6173 (2000).

64. Murray, P. J., Allen, J. E., Fisher, E. A. & Lawrence, T. Macrophage ac1. Murray, P. J., Allen, J. E., Fisher, E. A. & Lawrence, T. Macrophage activation and polarization nomenclature and experimental guidelines. 41, 14–20 (2015).tivation and polarization nomenclature and experimental guidelines. **41**, 14–20 (2015).

65. Coats, B. R. *et al.* Metabolically Activated Adipose Tissue Macrophages Perform Detrimental and Beneficial Functions during Diet-Induced Obesity. *Cell Rep.* **20**, 3149–3161 (2017).

66. Kratz, M. *et al.* Metabolic dysfunction drives a mechanistically distinct proinflammatory phenotype in adipose tissue macrophages. *Cell Metab.* **20**, 614–625 (2014).

67. Boutens, L. & Stienstra, R. Adipose tissue macrophages: going off track during obesity. *Diabetologia* **59**, 879–894 (2016).

68. Ahima, R. S. & Flier, J. S. Adipose tissue as an endocrine organ. *Trends Endocrinol. Metab.* **11**, 327–332 (2000).

69. Laclaustra, M., Corella, D. & Ordovas, J. M. Metabolic syndrome pathophysiology: The role of adipose tissue. *Nutr. Metab. Cardiovasc. Dis.* **17**, 125–139 (2007).

70. Matsuzawa, Y. The metabolic syndrome and adipocytokines. *Expert Rev. Clin. Immunol.* **3**, 39–46 (2007).

71. VAGUE, J. The Degree of Masculine Differentiation of Obesities: A FACTOR DETERMINING PREDISPOSITION TO DIABETES, ATHEROSCLEROSIS, GOUT, AND URIC CALCULOUS DISEASE. *Am. J. Clin. Nutr.* **Volume 4**, Pages 20–34

72. Reaven, G. M. Role of insulin resistance in human disease. *Diabetes* **37**, 1595–

1607 (1988).

73. Lonardo, A. *et al.* Nonalcoholic fatty liver disease: Evolving paradigms. *World J. Gastroenterol.* **23**, 6571–6592 (2017).

74. Lonardo, A., Ballestri, S., Marchesini, G., Angulo, P. & Loria, P. Nonalcoholic fatty liver disease: A precursor of the metabolic syndrome. *Dig. Liver Dis.* **47**, 181–190 (2015).

75. Yang, K. C. *et al.* Association of Non-alcoholic Fatty Liver Disease with Metabolic Syndrome Independently of Central Obesity and Insulin Resistance. *Sci. Rep.* **6**, 1–10 (2016).

76. Younossi, Z. M. *et al.* Global epidemiology of nonalcoholic fatty liver disease—Meta-analytic assessment of prevalence, incidence, and outcomes. *Hepatology* **64**, 73–84 (2016).

77. Pydyn, N., Miękus, K., Jura, J. & Kotlinowski, J. New therapeutic strategies in nonalcoholic fatty liver disease: a focus on promising drugs for nonalcoholic steatohepatitis. *Pharmacol. Reports* **72**, 1–12 (2020).

78. Elisa Fabbrini, Shelby Sullivan, and S. K. Obesity and Nonalcoholic Fatty Liver Disease: Biochemical, Metabolic and Clinical Implications. *Hepatology* (2010). doi:10.1097/IAE.0000000000002105

79. Tessari, P., Coracina, A., Cosma, A. & Tiengo, A. Hepatic lipid metabolism and non-alcoholic fatty liver disease. *Nutr. Metab. Cardiovasc. Dis.* **19**, 291–302 (2009).

80. Pardina, E. *et al.* Increased Expression and Activity of Hepatic Lipase in the Liver of Morbidly Obese Adult Patients in Relation to Lipid Content. *Obes. Surg.* **19**, 894–904 (2009).

81. Westerbacka, J. *et al.* Genes involved in fatty acid partitioning and binding, inflammation are overexpressed in the human fatty liver of insulin-resistant subjects. *Diabetes* **56**, 2759–65 (2007).

82. Kohjima, M. *et al.* Re-evaluation of fatty acid metabolism-related gene expression in nonalcoholic fatty liver disease. *Intern. J. Mol. Med.* 351–358 (2007).

83. Nguyen, P. *et al.* Liver lipid metabolism. *J. Anim. Physiol. Anim. Nutr. (Berl).* **92**, 272–283 (2008).

84. Geisler, C. E. & Renquist, B. J. Hepatic lipid accumulation: Cause and consequence of dysregulated glucoregulatory hormones. *J. Endocrinol.* **234**, R1–R21 (2017).

85. Ginsberg, H. N., Zhang, Y. L. & Hernandez-Ono, A. Regulation of plasma triglycerides in insulin resistance and diabetes. *Arch. Med. Res.* **36**, 232–240 (2005).

86. Titchenell, P. M., Lazar, M. A. & Birnbaum, M. J. Unraveling the Regulation of Hepatic Metabolism by Insulin. *Trends Endocrinol. Metab.* **28**, 497–505 (2017).

87. Mullins, G. R. *et al.* Catecholamine-induced lipolysis causes mTOR complex dissociation and inhibits glucose uptake in adipocytes. *Proc. Natl. Acad. Sci. U. S. A.* **111**, 17450–17455 (2014).

88. Qaid, M. M. & Abdelrahman, M. M. Role of insulin and other related hormones in energy metabolism. *Cogent Food Agric.* **2**, 1–18 (2016).

89. Usselman, C. W. N. S. S. J. R. B. 乳鼠心肌提取 HHS Public Access. *Physiol. Behav.* **176**, 139–148 (2017).

90. Gastaldelli, A. & Cusi, K. From NASH to diabetes and from diabetes to NASH: Mechanisms and treatment options. *JHEP Reports* **1**, 312–328 (2019).

91. Tana, C. *et al.* Cardiovascular risk in non-alcoholic fatty liver disease: Mechanisms and therapeutic implications. *Int. J. Environ. Res. Public Health* **16**, 1–19 (2019).

92. Rosato, V. *et al.* NAFLD and extra-hepatic comorbidities: Current evidence on a multi-organ metabolic syndrome. *Int. J. Environ. Res. Public Health* **16**, (2019).

93. R.K.Rao. Endotoxemia and Gut Barrier Dysfunction in Alcoholic Liver Disease. *Hepatology* **50**, (2009).

94. Geurts, L., Neyrinck, A. M., Delzenne, N. M., Knauf, C. & Cani, P. D. Gut microbiota controls adipose tissue expansion, gut barrier and glucose metabolism: Novel insights into molecular targets and interventions using prebiotics. *Benef. Microbes* **5**, 3–17 (2014).

95. Rohr, M. W., Narasimhulu, C. A., Rudeski-Rohr, T. A. & Parthasarathy, S. Negative Effects of a High-Fat Diet on Intestinal Permeability: A Review. *Adv. Nutr.* 1–15 (2019). doi:10.1093/advances/nmz061

96. Park, M.-Y., Kim, M. Y., Seo, Y. R., Kim, J.-S. & Sung, M.-K. High-fat Diet Accelerates Intestinal Tumorigenesis Through Disrupting Intestinal Cell Membrane Integrity. *J. Cancer Prev.* **21**, 95–103 (2016).

97. Cani, P. D. *et al.* Selective increases of bifidobacteria in gut microflora improve high-fat-diet-induced diabetes in mice through a mechanism associated with endotoxaemia. *Diabetologia* **50**, 2374–2383 (2007).

98. Turnbaugh, P. J., Ridaura, V. K., Faith, J. J., Rey, F. E. & Gordon, J. I.

Metagenomic Analysis in Humanized Gnotobiotic Mice. *Sci. Transl. Med.* **1**, 1–19 (2009).

99. Wong, V. W. S. *et al.* Molecular Characterization of the Fecal Microbiota in Patients with Nonalcoholic Steatohepatitis - A Longitudinal Study. *PLoS One* **8**, 1–11 (2013).

100. Campo, L., Eiseler, S., Apfel, T. & Pyrsopoulos, N. Fatty Liver Disease and Gut Microbiota: A Comprehensive Update. *J. Clin. Transl. Hepatol.* **7**, 1–5 (2019).

101. Le Roy, T. *et al.* Intestinal microbiota determines development of non-alcoholic fatty liver disease in mice. *Gut* **62**, 1787–1794 (2013).

102. Caligiuri, A., Gentilini, A. & Marra, F. Molecular pathogenesis of NASH. *Int. J. Mol. Sci.* **17**, (2016).

103. Day, C. P. & James, O. F. W. Steatohepatitis: A tale of two 'Hits'? *Gastroenterology* **114**, 842–845 (1998).

104. Tilg, H. & Moschen, A. R. Evolution of inflammation in nonalcoholic fatty liver disease: The multiple parallel hits hypothesis. *Hepatology* **52**, 1836–1846 (2010).

105. Lebeaupin, C. *et al.* Endoplasmic reticulum stress signalling and the pathogenesis of non-alcoholic fatty liver disease. *J. Hepatol.* **69**, 927–947 (2018).

106. Boursier, J. *et al.* The severity of NAFLD is associated with gut dysbiosis and shift in the metabolic function of the gut microbiota. *Hepatology* **63**, 764–775 (2017).

107. Arab, J. P., Arrese, M. & Trauner, M. Recent Insights into the Pathogenesis of Nonalcoholic Fatty Liver Disease. *Annu. Rev. Pathol. Mech. Dis.* **13**, 321–350 (2018).

108. FH, C. On Protein Synthesis. *F.K. Sanders (ed.). Symp. Soc. Exp. Biol. Number XII Biol. Replication Macromol. Cambridge Univ. Press. pp. 138–163.* (1958).

109. CRICK, F. Central Dogma of Molecular Biology. *Nature* 561–563 (1970).

110. Jackson, R. J. Alternative mechanisms of initiating translation of mammalian mRNAs. *Biochem. Soc. Trans.* **33**, 1231–1241 (2005).

111. Fernández-Miranda, G. & Méndez, R. The CPEB-family of proteins, translational control in senescence and cancer. *Ageing Res. Rev.* **11**, 460–472 (2012).

112. Kahvejian, A., Svitkin, Y. V., Sukarieh, R., M'Boutchou, M. N. & Sonenberg, N. Mammalian poly(A)-binding protein is a eukaryotic translation initiation factor, which acts via multiple mechanisms. *Genes Dev.* **19**, 104–113 (2005).

113. Shatsky, I. N., Terenin, I. M., Smirnova, V. V. & Andreev, D. E. Cap-Independent

Translation: What's in a Name? *Trends Biochem. Sci.* **43**, 882–895 (2018).

114. Nürenberg, E. & Tampé, R. Tying up loose ends: Ribosome recycling in eukaryotes and archaea. *Trends Biochem. Sci.* **38**, 64–74 (2013).

115. Kaul, G., Pattan, G. & Rafeequi, T. Eukaryotic elongation factor-2 (eEF2): Its regulation and peptide chain elongation. *Cell Biochem. Funct.* **29**, 227–234 (2011).

116. Simsek D, Tiu GC, Flynn RA, Byeon GW, Leppek K, Xu AF, Chang HY, B. M. The Mammalian Ribo-interactome Reveals Ribosome Functional Diversity and Heterogeneity. *Cell* (2017). doi:10.1016/j.cell.2017.05.022.The

117. Zhen Shi, Kotaro Fujii, Kyle M. Kovary, Naomi R. Genuth, Hannes L. Röst, Mary N. Teruel, and Maria Barna, Zhen Shi, Kotaro Fujii, Kyle M. Kovary, Naomi R. Genuth, Hannes L. Röst, Mary N. Teruel, and M. B. Heterogeneous ribosomes preferentially translate distinct subpools of mRNAs genome-wide. *Mol Cell* (2017). doi:10.1016/j.physbeh.2017.03.040

118. Pique, M., Lopez, J. M., Foissac, S., Guig, R. & Mendez, R. A Combinatorial Code for CPE-Mediated Translational Control. *Cell* **132**, 434–448 (2008).

119. Belloc, E., Piqué, M. & Méndez, R. Sequential waves of polyadenylation and deadenylation define a translation circuit that drives meiotic progression. *Biochem. Soc. Trans.* **36**, 665–670 (2008).

120. Novoa, I., Gallego, J., Ferreira, P. G. & Mendez, R. Mitotic cell-cycle progression is regulated by CPEB1 and CPEB4-dependent translational control. *Nat. Cell Biol.* **12**, 447–456 (2010).

121. Merkel, D. J. *et al.* The C-terminal region of cytoplasmic polyadenylation element binding protein is a ZZ domain with potential for protein-protein interactions. *J. Mol. Biol.* **425**, 2015–2026 (2013).

122. Hake, L. E., Mendez, R. & Richter, J. D. Specificity of RNA Binding by CPEB: Requirement for RNA Recognition Motifs and a Novel Zinc Finger. *Mol. Cell. Biol.* **18**, 685–693 (1998).

123. Charlesworth, A., Meijer, H. A. & De Moor, C. H. Specificity factors in cytoplasmic polyadenylation. *Wiley Interdiscip. Rev. RNA* **4**, 437–461 (2013).

124. Eckmann, C. R., Rammelt, C. & Wahle, E. Control of poly(A) tail length. *Wiley Interdiscip. Rev. RNA* **2**, 348–361 (2011).

125. Mendez, R., Hake, L., Andresson, T. et al. Phosphorylation of CPE binding factor by Eg2 regulates translation of c-mos mRNA. *Nature* 302–307 (2000).

126. Mendez, R., Murthy, K. G. K., Ryan, K., Manley, J. L. & Richter, J. D.

Phosphorylation of CPEB by Eg2 mediates the recruitment of CPSF into an active cytoplasmic polyadenylation complex. *Mol. Cell* **6**, 1253–1259 (2000).

127. Kim, J. H. & Richter, J. D. Opposing Polymerase-Deadenylase Activities Regulate Cytoplasmic Polyadenylation. *Mol. Cell* **24**, 173–183 (2006).

128. Bava, F. A. *et al.* CPEB1 coordinates alternative 3'-UTR formation with translational regulation. *Nature* **495**, 121–125 (2013).

129. Kurihara, Y. *et al.* CPEB2, A Novel Putative Translational Regulator in Mouse Haploid Germ Cells1. *Biol. Reprod.* **69**, 261–268 (2003).

130. Chen, H., Hsu, C. & Huang, Y. CPEB 2-dependent translation of long 3'- UTR Ucp1 mRNA promotes thermogenesis in brown adipose tissue . *EMBO J.* **37**, 1–15 (2018).

131. Lu, W. H., Yeh, N. H. & Huang, Y. S. CPEB2 Activates GRASP1 mRNA Translation and Promotes AMPA Receptor Surface Expression, Long-Term Potentiation, and Memory. *Cell Rep.* **21**, 1783–1794 (2017).

132. Tordjman, J. *et al.* Tumor suppressor role of cytoplasmic polyadenylation element binding protein 2 (CPEB2) in human mammary epithelial cells. *BMC Cancer* **19**, 1–16 (2019).

133. DeLigio, J. T., Lin, G., Chalfant, C. E. & Park, M. A. Splice variants of cytosolic polyadenylation element– binding protein 2 (CPEB2) differentially regulate pathways linked to cancer metastasis. *J. Biol. Chem.* **292**, 17909–17918 (2017).

134. Chen, P. J. & Huang, Y. S. CPEB2-eEF2 interaction impedes HIF-1α RNA translation. *EMBO J.* **31**, 959–971 (2012).

135. Hägele, S., Kühn, U., Böning, M. & Katschinski, D. M. Cytoplasmic polyadenylation-element-binding protein (CPEB)1 and 2 bind to the HIF-1α mRNA 3'-UTR and modulate HIF-1α protein expression. *Biochem. J.* **417**, 235–246 (2009).

136. Ford, L., Ling, E., Kandel, E. R. & Fioriti, L. CPEB3 inhibits translation of mRNA targets by localizing them to P bodies. *Proc. Natl. Acad. Sci. U. S. A.* **116**, 18078–18087 (2019).

137. Drisaldi, B. *et al.* SUMOylation Is an Inhibitory Constraint that Regulates the Prion-like Aggregation and Activity of CPEB3. *Cell Rep.* **11**, 1694–1702 (2015).

138. Pavlopoulos, E. *et al.* Neuralized1 Activates CPEB3: A Novel Function of Ubiquitination in Synaptic Plasticity and Memory Storage. *Cell* **147**, 1369–1383 (2012).

139. Fioriti, L. *et al.* The Persistence of Hippocampal-Based Memory Requires Protein

Synthesis Mediated by the Prion-like Protein CPEB3. *Neuron* **86**, 1433–1448 (2015).

140. Guillén-Boixet, J., Buzon, V., Salvatella, X. & Méndez, R. CPEB4 is regulated during cell cycle by ERK2/Cdk1-mediated phosphorylation and its assembly into liquid-like droplets. *Elife* **5**, 1–26 (2016).

141. Hu, W. & , Bingbing Yuan, and H. F. L. Cpeb4-mediated translational regulatory circuitry controls terminal erythroid differentiation. *Dev Cell* **29**, 660–672 (2014).

142. Burns, D. M., D'Ambrogio, A., Nottrott, S. & Richter, J. D. CPEB and two poly(A) polymerases control miR-122 stability and p53 mRNA translation. *Nature* **473**, 105–108 (2011).

143. Morgan, M., Iaconcig, A. & Muro, A. F. CPEB2, CPEB3 and CPEB4 are coordinately regulated by miRNAs recognizing conserved binding sites in paralog positions of their 3'-UTRs. *Nucleic Acids Res.* **38**, 7698–7710 (2010).

144. Giangarrà, V., Igea, A., Castellazzi, C. L., Bava, F. A. & Mendez, R. Global analysis of CPEBs reveals sequential and non-redundant functions in mitotic cell cycle. *PLoS One* **10**, 1–18 (2015).

145. Ortiz-Zapater, E. *et al.* Key contribution of CPEB4mediated translational control to cancer progression. *Nat. Med.* **18**, 83–90 (2012).

146. Pérez-Guijarro, E. *et al.* Lineage-specific roles of the cytoplasmic polyadenylation factor CPEB4 in the regulation of melanoma drivers. *Nat. Commun.* **7**, (2016).

147. Lu, R., Zhou, Z., Yu, W., Xia, Y. & Zhi, X. CPEB4 promotes cell migration and invasion via upregulating Vimentin expression in breast cancer. *Biochem. Biophys. Res. Commun.* **489**, 135–141 (2017).

148. Maillo, C. *et al.* Circadian- and UPR-dependent control of CPEB4 mediates a translational response to counteract hepatic steatosis under ER stress. *Nat. Cell Biol.* **19**, 94–105 (2017).

149. Calderone, V. *et al.* Sequential Functions of CPEB1 and CPEB4 Regulate Pathologic Expression of Vascular Endothelial Growth Factor and Angiogenesis in Chronic Liver Disease. *Gastroenterology* **150**, 982-997.e30 (2016).

150. Garcia-Pras, E. *et al.* Role and therapeutic potential of vascular stem/progenitor cells in pathological neovascularisation during chronic portal hypertension. *Gut* **66**, 1306–1320 (2017).

151. Activation, S. C. Gastroenterology CPEB4-Driven PFKFB3-Mediated Glycolytic Reprogramming is Essential for Hepatic.

152. Parras, A. *et al.* Autism-like phenotype and risk gene mRNA deadenylation by CPEB4 mis-splicing. *Nature* **560**, 441–446 (2018).

153. Kan, M.-C. *et al.* CPEB4 Is a Cell Survival Protein Retained in the Nucleus upon Ischemia or Endoplasmic Reticulum Calcium Depletion. *Mol. Cell. Biol.* **30**, 5658–5671 (2010).

154. Xia Zhang, Ricardo Goncalves, and D. M. M. The Isolation and Characterization of Murine Macrophages. (2008). doi:10.1002/0471142735.im1401s83.The

155. Clair Crewe, Yu Aaron An, and P. E. S. The ominous triad of adipose tissue dysfunction: inflammation, fibrosis, and impaired angiogenesis. *J. Clin. Invest.* **7**, (2017).

156. Keiran, N. *et al.* SUCNR1 controls an anti-inflammatory program in macrophages to regulate the metabolic response to obesity. *Nat. Immunol.* **20**, 581–592 (2019).

157. Velázquez, K. T. *et al.* Prolonged high-fat-diet feeding promotes non-alcoholic fatty liver disease and alters gut microbiota in mice. *World J. Hepatol.* **11**, 619–637 (2019).

158. Romero, M. *et al.* TP53INP2 regulates adiposity by activating β-catenin through autophagy-dependent sequestration of GSK3β. *Nat. Cell Biol.* **20**, 443–454 (2018).

159. Geoghegan, G. *et al.* Targeted deletion of Tcf7l2 in adipocytes promotes adipocyte hypertrophy and impaired glucose metabolism. *Mol. Metab.* **24**, 44–63 (2019).

160. Kim, J. I. *et al.* Lipid-Overloaded Enlarged Adipocytes Provoke Insulin Resistance Independent of Inflammation. *Mol. Cell. Biol.* **35**, 1686–1699 (2015).

161. Svensson, H. *et al.* Body fat mass and the proportion of very large adipocytes in pregnant women are associated with gestational insulin resistance. *Int. J. Obes.* 646–653 (2015). doi:10.1038/ijo.2015.232

162. Veilleux, A., Caron-Jobin, M., Noël, S., Laberge, P. Y. & Tchernof, A. Visceral adipocyte hypertrophy is associated with dyslipidemia independent of body composition and fat distribution in women. *Diabetes* **60**, 1504–1511 (2011).

163. Martinez-Santibañez, G. & Nien-Kai Lumeng, C. Macrophages and the Regulation of Adipose Tissue Remodeling. *Annu. Rev. Nutr.* **34**, 57–76 (2014).

164. Haase, J. *et al.* Local proliferation of macrophages in adipose tissue during obesity-induced inflammation. *Diabetologia* **57**, 562–571 (2014).

165. Weisberg, S. P. *et al.* Obesity is associated with macrophage accumulation in

adipose tissue Find the latest version : Obesity is associated with. *J Clin Invest.* **112**, 1796–1808 (2003).

166. Carlos A. Ordoñez, MDa and Juan Carlos Puyana, M. Management of Peritonitis in the Critically Ill Patient. *Changes* **29**, 997–1003 (2006).

167. Urbanavičius, V. *et al.* Comparison of changes in blood glucose, insulin resistance indices, and adipokine levels in diabetic and nondiabetic subjects with morbid obesity after laparoscopic adjustable gastric banding. *Med.* **49**, 9–14 (2013).

168. Königshofer, P., Brusilovskaya, K., Schwabl, P. & Reiberger, T. Animal models of portal hypertension. *Biochim. Biophys. Acta - Mol. Basis Dis.* **1865**, 1019–1030 (2019).

169. Gallego, J. *et al.* Therapeutic siRNA targeting endothelial KDR decreases portosystemic collateralization in portal hypertension. *Sci. Rep.* **7**, 1–16 (2017).

170. Bråkenhielm, E. *et al.* Angiogenesis inhibitor, TNP-470, prevents diet induced and genetic obesity in mice. *Circ. Res.* **94**, 1579–1588 (2004).

171. Persson, A. B. & Buschmann, I. R. Vascular Growth in Health and Disease. *Front. Mol. Neurosci.* **4**, 1–15 (2011).

172. Yilmaz, M. & Hotamisligil, G. S. Damned if you do, damned if you don't: The conundrum of adipose tissue vascularization. *Cell Metab.* **17**, 7–9 (2013).

173. Hosogai, N. *et al.* Adipose tissue hypoxia in obesity and its impact on adipocytokine dysregulation. *Diabetes* **56**, 901–911 (2007).

174. Sung, H. K. *et al.* Adipose vascular endothelial growth factor regulates metabolic homeostasis through angiogenesis. *Cell Metab.* **17**, 61–72 (2013).

175. Choe, S. S., Huh, J. Y., Hwang, I. J., Kim, J. I. & Kim, J. B. Adipose tissue remodeling: Its role in energy metabolism and metabolic disorders. *Front. Endocrinol. (Lausanne).* **7**, 1–16 (2016).

176. Longo, M. *et al.* Adipose tissue dysfunction as determinant of obesity-associated metabolic complications. *Int. J. Mol. Sci.* **20**, (2019).

177. Kusminski, C. M., Bickel, P. E. & Scherer, P. E. Targeting adipose tissue in the treatment of obesity-associated diabetes. *Nat. Rev. Drug Discov.* **15**, 639–660 (2016).

178. Mikirova, N. A., Casciari, J. J., Hunninghake, R. E. & Beezley, M. M. Effect of weight reduction on cardiovascular risk factors and cd34-positive cells in circulation. *Int. J. Med. Sci.* **8**, 445–452 (2011).

179. Cinti, S. *et al.* Adipocyte death defines macrophage localization and function in

adipose tissue of obese mice and humans. *J. Lipid Res.* **46**, 2347–2355 (2005).

180. Murano, I. *et al.* Dead adipocytes, detected as crown-like structures, are prevalent in visceral fat depots of genetically obese mice. *J. Lipid Res.* **49**, 1562–1568 (2008).

181. Wentworth, J. M. *et al.* Pro-inflammatory CD11c+CD206+ adipose tissue macrophages are associated with insulin resistance in human obesity. *Diabetes* **59**, 1648–1656 (2010).

182. Russo, L. & Lumeng, C. N. Properties and functions of adipose tissue macrophages in obesity. *Immunology* **155**, 407–417 (2018).

183. Lefere, S. & Tacke, F. Macrophages in obesity and non-alcoholic fatty liver disease: Crosstalk with metabolism. *JHEP Reports* **1**, 30–43 (2019).

184. Boutens, L. *et al.* Unique metabolic activation of adipose tissue macrophages in obesity promotes inflammatory responses. *Diabetologia* **61**, 942–953 (2018).

185. Nguyen, M. T. A. *et al.* A subpopulation of macrophages infiltrates hypertrophic adipose tissue and is activated by free fatty acids via toll-like receptors 2 and 4 and JNK-dependent pathways. *J. Biol. Chem.* **282**, 35279–35292 (2007).

186. Anderson, P. Post-transcriptional regulons coordinate the initiation and resolution of inflammation. *Nat. Rev. Immunol.* **10**, 24–35 (2010).

187. Navarro, C. S. CPEB4 function in macrophages. (University of Barcelona, 2018).

188. Spalding, K. L. *et al.* Dynamics of fat cell turnover in humans. *Nature* **453**, 783–787 (2008).

189. Rigamonti, A., Brennand, K., Lau, F. & Cowan, C. A. Rapid cellular turnover in adipose tissue. *PLoS One* **6**, (2011).

190. B. Gawronska-Kozak, J. Staszkiewicz, J. M. Gimble, and H. K.-B. Recruitment of fat cell precursors during long-term high fat diet in C57BL/6J mice is fat depot specific. *Obes. (Silver Spring)* **22**, 1091–1102 (2014).

191. Wang, Q. A., Tao, C., Gupta, R. K. & Scherer, P. E. Tracking adipogenesis during white adipose tissue development, expansion and regeneration. *Nat. Med.* **19**, 1338–1344 (2013).

192. Joe, A. W. B., Lin, Y., Even, Y., Vogl, A. W. & Rossi, F. M. V. Depot-specific differences in adipogenic progenitor abundance and proliferative response to high-fat diet. *Stem Cells* **27**, 2563–2570 (2009).

193. Salans, L. B., Horton, E. S. & Sims, E. A. Experimental obesity in man: cellular character of the adipose tissue. *J. Clin. Invest.* **50**, 1005–1011 (1971).

194. Tchoukalova, Y. D. *et al.* Sex- and depot-dependent differences in adipogenesis in normal weight humans. **18**, 1875–1880 (2011).